ADDIS ABABA UNIVERSITY INSTITUTE OF TECHNOLOGY (AAiT)

Characterizing and Understanding of the Hydrological System of Didesa Sub-Basin

Thesis
Submitted in Partial Fulfillment of the Requirements for the Degree of Master of Science in Hydraulic Engineering.

By
Timketa Adula

Advisor: Dr. Belete Berhanu

ADDIS ABABA UNIVERSITY
November, 2016

Abstract

Understanding hydrological characteristics of watersheds in Ethiopia highlands have significance importance for the water based development of the country. The Didesa sub basin, which is one of the major sub basins in Abay river basin, has not well studied as compare with the northern sub basins of Blue Nile (Tana sub basin). The study evaluated the quality of observed meteorological and hydrological data, established SWAT hydrological model, and developed different characterization parameters for different watersheds in the sub basin. The result indicated that the SWAT model developed for the sub basin evaluated and its performance certain with the statistical measures, coefficient of determination (R^2) and Nash coefficient (NS) with values ranging 0.62 to 0.8 and 0.6 to 0.8 respectively at daily time scale. The coefficient of determination R^2 and NS increases at monthly time scale and ranging 0.75 to 0.92 and 0.71 to 0.91 respectively. Sensitivity analysis is performed to identify parameters those were most sensitive for the sub basin. CN2, GWQMN, CH_K, ALPHA_BNK and LAT_TIME are the most sensitive parameters in the sub basin. The hydrological system of the sub basin is also characterized with its simulated stream flow at five major tributaries watersheds, dominate land use mosaic vegetation/crop lands followed by closed to open shrub land, soil Humic Nitosols and slope 0% to 36% as catchment attributes, and the peak flow for 2-10000 return period.

Acknowledgement

First and above all, I praise God, the almighty for providing me this opportunity and granting me the capability to proceed successfully.

I wish to express my gratitude to my thesis advisor Belete Berhanu (PhD), for his generous advice, inspiring guidance and encouragement throughout my research for this work. His expert advice from title selection up to final writes up of this thesis and especially for his patience and guidance during the writing process, the insightful discussion, for his support during the whole period of the study. His technical and editorial advice was essential to the completion of this dissertation and has taught me innumerable lessons and insights on the workings of academic research in general. This thesis could not have been completed without his generous and professional assistance. What I learn from him is not just how to write a thesis to graduation requirement but how to view this from world prospective.

I would like acknowledge Fesea Behulu (PhD), who is hydrologist at OWWDSE, providing me information about Didesa sub basin. Furthermore, his assistance in my final thesis by giving core idea of research thesis. I am extremely grateful for his assistance and suggestions throughout my thesis.

I would like to extend my sincere gratitude to Ethiopian Ministry of Water and Energy; and Ethiopian National Metrology Agency for their assistance in providing me the necessary data for the study.

I cannot finish without thanking my family. I warmly thank and appreciate my parents, my brothers and sisters for encouragement and spiritual support in all aspects of my life.

I would like to extend special thanks to my friends who are numerous to mention their name, especially Bikila Gudina, Dano Keranso, Ebisa Abiram for their encouragements and inspiring assistance in my thesis work.

Table of Contents

LIST OF FIGURES

List of Tables

Acronyms

SWAT - soil And Water Assessment Tool

UH - Unit Hydrograph

GOV - Goodness of Fit

ET – Evapotranspiration

FA – Frequency Analysis

OWWDSE – Oromia Water work Design and Supervision Enterprise

NRCS – Natural Resource Conservation service

SUH – Snyder Unit Hydrograph

1. INTRODUCTION

1.1. Background

Understandings of hydrological characteristics of watersheds in Ethiopia highlands have significance importance for the water based development of the country. It is a base to estimate watershed outflow in Ethiopia highlands with monsoonal climate where, rainfall-runoff relationship of the various landscapes units have complex hydrology (Sivapalan, 2005). Generally watershed variables attributed to the differences in hydrological response of rainfall are soil properties, geology, anthropogenic activities, relief size, local climate and vegetation cover (Black, 1997; Uhlenbrook, 2004; Sivapalan, 2005, Belete et al, 2015). Some watershed variables are more important in ways that are specific to different watersheds and scales. One way to advance the predictive power of watershed hydrology is to characterize watersheds based on the most influential variables (McDonnell et al., 2007), as this provides a basis for planning of land management issues for developing and securing water resources (Saxena et al.,2000). Moreover, characterization of watersheds with reference to hydrological response complements process-oriented modeling (Yadav et al., 2007). ,

Therefore, understanding of the hydrological characteristics of different watersheds as sources of stream flow is of considerable importance in the effective utilization of water resources, the need to improve and augment development and management activities of water resources, and to mitigate for negative impacts of climate change in the future. In line with this critical knowledge gap the flood occurrence in 2015 at Arjo Dedesa dam site initiate this hydrological characterizing and understanding studies at this particular watershed.

Didessa River, which is the largest tributary of the Blue Nile (Abbay) contributes roughly a quarter of the total flow of Blue Nile (Mamo, 2014) has total catchment area drained by the river is estimated to be about 28,000 km^2 originating from the mountain ranges of Gomma in South Western Ethiopia. Although the sub basin has comparatively sufficient hydrological and meteorological data series, its hydrological characteristics have not been well investigated as compared with northern side sub basins the Blue Nile River (Tana sub basin). In relation with its catchment situation, the occurrence of the 2015 flood incidence at the coffer dam site with below normal rainfall season, calling an urgent discussion and evaluation of the hydrological design of the coffer dam and the relief culvert (OWWDSE, 2016). It further invites detail hydrological study to characterize, to understand and to differentiate dominant hydrological processes and parameters, which govern the hydrological condition of the sub basin.

1.2. STATEMENT OF PROBLEM

Some indicative studies shows Didesa sub basin has differ hydrological characteristics than other Blue Nile sub basins. In addition to this event, the sub basin has not well studied as compare with the northern sub basins of Blue Nile such as (Tana sub basin). The output of this thesis may also contribute for the knowledge gap of the sub basin hydrological understanding. Therefore this study comes to board to fill the knowledge gap of the hydrological situation of the sub basin with finding scientific cause for the flood occurrence and to make sustainable the water resources development activity in the sub basin.

1.3. General Objective

The foremost objective of the study is to characterize the hydrological situation of Didesa Sub basin that possible elaborated with the following specific objectives.

1.3.1. Specific Objective:

- To determine the hydrological variables that characterizes the sub basin by using SWAT hydrologic model.
- To assess stream flow hydrograph of the sub basin
- To undertake frequency analysis of to fix extreme Floods with different return periods

1.4. Outline of the research

The thesis was divided in to seven chapters. Chapter one provides the brief introduction of the study, statement of the problem and objective of the research. Chapter two deals with brief explanation of literature review. Detail description of the study area, and Dataset and Data Sources for SWAT Model were included in chapter three and four respectively. The fourth chapter explains result and discussion part. Conclusions and recommendations are included in chapter five.

2. LITERATURE REVIEW

2.1. Watershed Hydrology

Beginning from the atmosphere water condenses to form drops of water. When they grow to as sufficient size, they fall as precipitation (rain, snow, hail etc.). Part of the precipitation intercepted by natural vegetative cover is redistributed to runoff or may evaporate directly back to the atmosphere. Precipitation also moves into the soil in one of the most important process of the hydrologic cycle- Infiltration. Percolation is the downward movement of water through the soil profile after infiltration and it may be saturated (flow governed by gravity potential) or unsaturated (flow governed by capillarity potential). The movement of water from the liquid phase to the vapor phase and then to the atmosphere, occurring from any wet surface referred to as evaporation, effectively reduces the moisture in the soil. There may also be interception of the downward movement of water causing redistribution or it may also indicate the amount of water lost through evaporative process following precipitation.

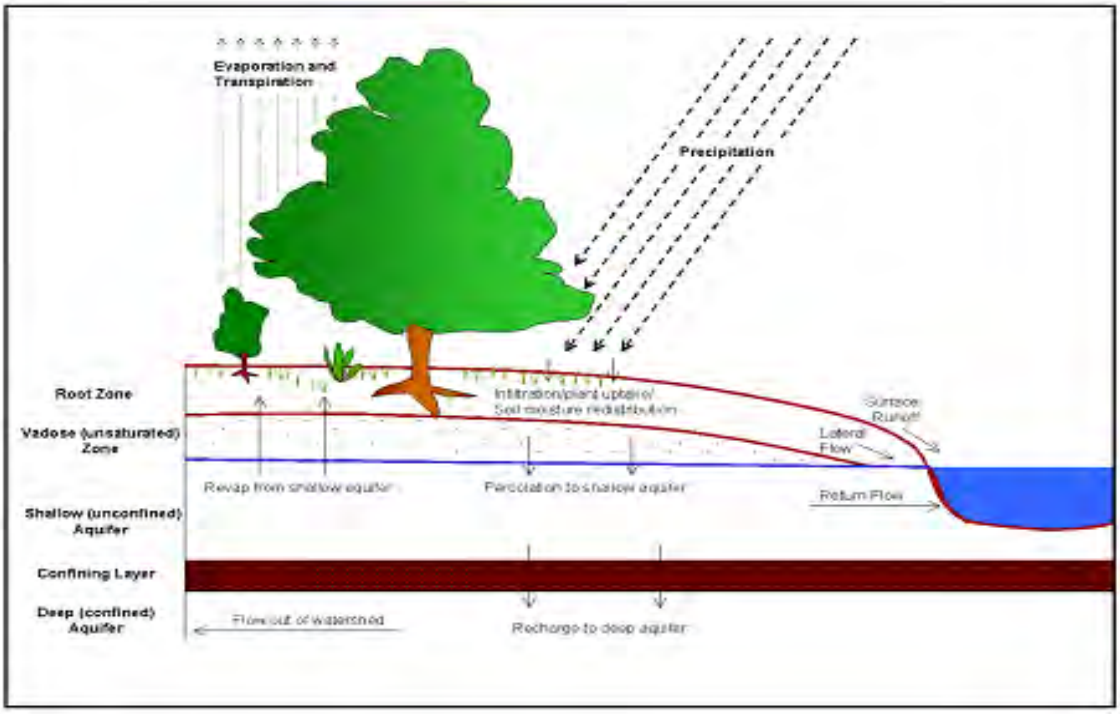

Figure 2-1: Schematic representation of the hydrologic cycle in SWAT (Neitsch et al. 2011)

Water also moves to the atmosphere through the stomata from the soil and roots via the plant's internal moisture supply system (transpiration). The combined evaporative processes are termed Evapotranspiration. When the water reaches the stream it is referred to as stream flow, discharge and it may have been supplied by surface runoff, subsurface flow, storm flow and base flow (Black, 1996).Several locations serve as storage in the hydrologic cycle, water could be stored in the aerated unsaturated portion of the soil mantle and beneath the water table under saturated conditions. Huge amount can also be stored on top of the soil while a considerable amount could also be stored in vegetation. Surface storage could be in form of ponds, puddles, lakes and wetlands of all types as well as in rivers and stream channels. During the period immediately following a runoff-producing event, the amount of water on the watershed naturally diminishes. As this occurs the source of water for the stream flow reduces in size, with the distant upper slopes drying out first and according to Black (1996) in the last stages of runoff, if allowed to continue long enough, only the channel will be contributing to stream flow. The amount of water precipitating in any given year in the hydrosphere is about 0.00046% of the total water on earth (Black, 1991). This is what makes up the part of the hydrologic cycle with which man most commonly interacts forming links between various storages and serving as the source of floods or drought. Watershed runoff exhibits different characteristics, which are dependent on the storage from which it is derived.

2.1.1. Hydrological processes

Forest vegetation directly affects the amount of water available for stream flow through the interception of rain and snow, the evaporation of intercepted water, and through transpiration. Altering forest vegetation can have an important influence on water balances at the site and watershed scale. In the hydrologic cycle (Figure 2-1), the forest canopy is the first surface that intercepts and stores precipitation, resulting in some amount (depending on canopy characteristics) returning to the atmosphere through sublimation and evaporation. Water also returns to the atmosphere through transpiration and by evaporation from the forest floor, soil surface, and open water bodies, such as lakes and wetlands. Forest vegetation reduces the rate at which snow melts and hence the rate of soil moisture recharge and downslope flow (Spittle house and Winkler 2002). A water balance equation is often used to express the contributions of these processes to stream flow. At the watershed scale, the water balance equation links stream flow (R), precipitation (P), evaporation (E), losses to regional groundwater (G), and changes in watershed storage (ΔS):

$R = P - E - G \pm \Delta S$

Where the variables are measured in water depth equivalent (millimeters) over time. The quantity G represents water that leaves the watershed as groundwater and thus does not contribute to stream flow. Watershed storage includes water stored as snow, surface water (lakes, ponds, and depression storage), glacier ice, soil moisture, and groundwater. As water flows through a watershed, it often moves between these storage compartments before discharging to a stream or being lost through evaporation and transpiration. For example, melt water draining from a snowpack and infiltrating the soil represents a loss of snowpack storage and a gain of soil moisture, but with no net effect on total watershed storage.

2.1.2. Why change in hydrological process?

In addition to climate change, land use change is one of the important human interventions altering the quality and quantity of both surface and ground water. The study of hydrological cycle and hydrological response of a catchment have become very complex due to complicated inter-relationship between various hydrological components such as precipitation, evaporation, transpiration, infiltration, and runoff. Both climate and land use change have adverse implications on the natural hydrologic system in terms of variation in the runoff regime, evapotranspiration (ET), subsurface flow, infiltration, etc., (Lørup, Refsgaard, & Mazvimavi, 1998; McColl & Aggett, 2007; Xu & Singh, 1998). The major factors contributing to land use change includes demographic changes, climatic variability, national resource conservation policies, and socio-economic factors (Elfert & Bormann, 2010; Mao & Cherkauer, 2009). According to Lin, Verburg, Chang, Chen, and Chen (2009), the factors that drive land-use change in any watershed include the altitude, slope, distance from the river, soil erosion coefficient, distance from major roads, distance from a built-up area, and population density. However, analyzing the land use and land cover change (LUCC) and identifying its driving factors is very complex (Niehoff, Fritsch, & Bronstert, 2002; Verburg, Schot, Dijst, & Veldkamp, 2004).

2.1.3. Role of model in explaining hydrological process

Hydrologic modeling plays a very important role in assessing the seasonal water availability, which is necessary to take decisions in water resources management. Both climate and land use and land cover change have great influence on the hydrological response of a watershed. (G.S. Dwarakish1and B.P. Ganasri1*, 2015)

The development of hydrologic models that consider spatio-temporal watershed characteristics helps in accurate prediction of dynamic water balance of a watershed (Costa, Botta, & Cardille, 2003; He & Hogue, 2012; Lørup et al., 1998). Therefore, hydrologic models have become increasingly important tools for the management of the water resources (Sarkar & Kumar, 2012; Shirke, Kawitkar, & Balan, 2012; Suliman, Jajarmizadeh, Harun, & Mat Darus, 2015). They are used for flow forecasting to support reservoir operation, flood mitigation, spillway design studies, and many other purposes (Sarkar & Kumar, 2012; Shirke et al., 2012). The basic approach in hydrologic modeling is that the model is used to calculate stream flow based on meteorological data and catchment characteristics, which are available in a basin or in its vicinity (Lørup et al., 1998; Ye, Zhang, Liu, Li, & Xu, 2013).

The better understanding of basin hydrology and the relationship between land use change and relative variation in ET, base flow, and surface runoff generation and associated water distribution is helpful to watershed planners and decision-makers (Tang et al., 2011; Thanapakpawin et al., 2006; Wang et al., 2012). A thorough understanding of the rainfall–runoff relationship is vital in modeling and designing urban drainage (Laouacheria & Mansouri, 2015).

Hydrological processes at the catchment scale are no longer stationary when the changes taking place in the catchment are highly variable in nature (Cornelissen, Diekkrüger, & Giertz, 2013; Mauser & Bach, 2009). Hydrologic models have become an indispensable tool for the study of hydrological processes and the impact of modern anthropogenic factors on the hydrologic system.

2.2. Hydrological System

Hydrologic system is a system of interrelated components, including the processes of precipitation, evaporation, transpiration, infiltration, groundwater flow, stream flow, etc., in addition to those structures and devices that are used to manage the system. Hydrologic system is subject to different kind of weather pattern and spatial complexity, and is dynamic and random in nature.

Hydrologic evaluations are required to determine the characteristics of the hydrologic system including the evaluation of the magnitude of various events and the frequency of certain magnitudes.

2.3. Hydrologic Characteristics

Hydrologic characteristics of watersheds reflect the volume of discharge hydrograph produced by a specific rainfall hyetograph (Karamouz,M.et al,2003). The following parameters, which are mainly used in rainfall-runoff simulation models (such as SWAT), show the timing of runoff and the depth and the discharge of the stream flow hydrograph which on the other hand required for preparing unit hydrograph that can reflect the property of watershed.

- Time of concentration(t_c): Time for a wave to propagate from the most distant point in the watershed to the outlet
- Lag time (t_p): Time from the center of mass of rainfall excess to the peak of the hydrograph.

A correct estimate of these parameters will insure the effectiveness of flood warning systems as a major component of an overall watershed management system. (Mohammed K. et al, 2003)

2.4. Hydrological Model

Why we need hydrologic models? Hydrology is principally concerned with the study of the motion of the earth's waters through the hydrologic cycle, and the transport of constituents such as sediment and pollutants in the water as it flows (Francisco Olivera, David R. Maidment and Randall J. Charbeneau, 1996). Hydrological modelling is very important for prediction of runoff and soil erosion, and is a major tool for research hydrologists and water resources engineers for planning and management of water resources. Hydrological models can be used to estimate river flows at ungauged sites, fill gaps in incomplete data series or predict future runoff and river flows. The need for hydrological models is increasing both in aspects of coverage and functionality. Also more and more researchers and practitioners require access to hydrological models and in particular model simulation results. Hence, hydrological models need to be more robust, transparent and defensible as they are increasingly relied on to make informed decisions on sharing and managing of limited water resources (Fu G, 2007). Distributed hydrological models consider the spatial non-uniformity of hydrological characteristics and processes in the river basin. These models are based on our understanding of the physics of the hydrological processes which control catchment response and use physically based equations to describe these processes. These models can be applied for the study of the effects of land use changes and human intervention on the catchment behavior.

Hydrological models are tools that describe the physical processes controlling the transformation of precipitation to stream flows. There are different hydrological models designed and applied to simulate the rainfall runoff relationship under different temporal and spatial dimensions. The focus of these models

is to establish a relationship between various hydrological components such as precipitation, Evapotranspiration, surface runoff, ground water flow and soil water movement (infiltration). Many of these hydrological models describe the canopy interception, evaporation, transpiration, snowmelt, interflow, overland flow, channel flow, unsaturated subsurface flow and saturated subsurface flow. These models range from simple unit hydrograph based models to more complex models that are based on the dynamic flow equations. Simulation programs implementing watershed hydrology and river water quality models are important tools for watershed management for both applied and operational research purposes.

A hydrological model represents the water cycle of a drainage basin and studies the response of this basin to climatic and physical conditions. Three different categories of hydrological models can be distinguished: physically process based, empirical and statistically based.

Physically process based models are described by mathematically formulated fundamental physical laws, where each basin is represented by a concept; a reservoir for instance. They are useful for inferring the distribution, magnitude, and past, present and future behavior of a process with limited observations. These equations can relate the changes of water properties into the those across the surface. These physical processes vary both temporally and spatially. They consider the spatial and temporal changes of different factors (CONWAY, 1997). Physically based distributed watershed models play also a major role in analyzing the impact of land management practices on water, sediment, and agricultural chemical yields in large complex watersheds.

Empirical models are a synthesis and a summary of field or experimental observations. Their fundamental parameters are not compulsory physically related. Empirical models are based on defining important factors through field observation, measurement, experiments and statistical methods**.** They are useful in predicting the hydrology or soil erosion, but are site specific and require long-term data (Elirehema, 2001). Empirical models are the result of several years of research data and numerically evaluate the effects of climate, soil properties, topography and crop management.

Statistically based models use many observations to estimate the behavior of watersheds and their interactions. They can be physically or empirically based. In addition to categorizing both soil erosion and hydrological models with respect to the way they are being synthesized, another distinction is the difference between distributed and global models. In global models, the watershed is one single entity and in distributed models, many units represent the variability of hydrological parameters on the surface. Spatial variability is handled by dividing a drainage basin into smaller geographical units, such as sub basins, land cover classes, elevation zones or a combination of them. The hydrological response units

(HRUs) represent areas where the modeling simplified and where the hydrological response is supposed to be homogeneous.

In recent years, distributed watershed models are increasingly used to study alternative management strategies in the areas of water resources allocation, flood control, impact of land use change and climate change, and finally environmental pollution control. Many of these models share a common base in their attempt to incorporate the heterogeneity of the watershed and spatial distribution of topography, vegetation, land use, soil characteristics, rainfall and evaporation. Some of the watershed models developed in the last two decades are CREAMS (Chemicals, Runoff, and Erosion from Agricultural Management Systems) (Knisel,, EPIC - Erosion Productivity Impact Calculator (Williams, 1995), AGNPS (Agricultural None Point Source model) (Young et al.,1987), SWAT (Soil and Water Assessment Tool) (Arnold et al., 1998) and HSPF (Hydrologic Simulation Program – Fortran) (Bicknell et al., 2001), ANSWERS (Areal Nonpoint Source Watershed Environmental Response Simulation) (Beasley and Huggins, 1982), EROSION-3D (SCHMIDT, 1995), EUROSEM (European Soil Erosion Model) (Morgan et. al., 1997), WEPP (Water Erosion Prediction Project) (Foster and Lane, 1987),HEC-HMS (Hydrological Modelling System) etc.

2.5. Software's used for this study

2.5.1. Arc SWAT Modeling

The Arc SWAT ArcGIS extension is a graphical user interface for the SWAT (Soil and Water Assessment Tool) model (Arnold et al., 1998). SWAT is a river basin, or watershed, scale model developed to predict the impact of land management practices on water, sediment, and agricultural chemical yields in large, complex watersheds with varying soils, land use, and management conditions over long periods of time. The model is physically based and computationally efficient, uses readily available inputs and enables users to study long-term impacts. SWAT can be used to simulate a single watershed or a system of multiple hydrologically connected watersheds. Each watershed is first divided into sub basins and then in hydrologic response units (HRUs) based on the land use and soil distributions.

SWAT model is a popular model for hydrological modeling. It enables the user to achieve a deeper insight into the water related processes of a specific catchment site. Its applicability on both large and small scale offers a huge range of opportunities. Further one can setup a model relatively easily, even though there is not a profound data base provided. SWAT was established for US conditions. Nevertheless there have been several successful simulations at Blue Nile, Ethiopia. As a further contribution to SWAT simulations in Ethiopia, in this study the SWAT model is applied to a sub basin of

Blue Nile Basin, namely Didessa sub basin. The work flow concerning SWAT model is summarized in the flowchart in figure 2-2. The steps are assigned to the working interfaces of ArcSWAT and SWAT-CUP. The available input data is gathered and overlaid followed by watershed delineation and HRU definition in ArcSWAT. Then the model is run resulting in the necessary files for calibration. Using those files there is a switch to SWAT-CUP, which provides an iterative procedure for parameter estimation. SWAT-CUP runs the model and examines different parameters within ranges previously assigned by the modeller. The resulting parameter ranges are validated. Finally they are applied to different model setups containing varying numbers of HRU

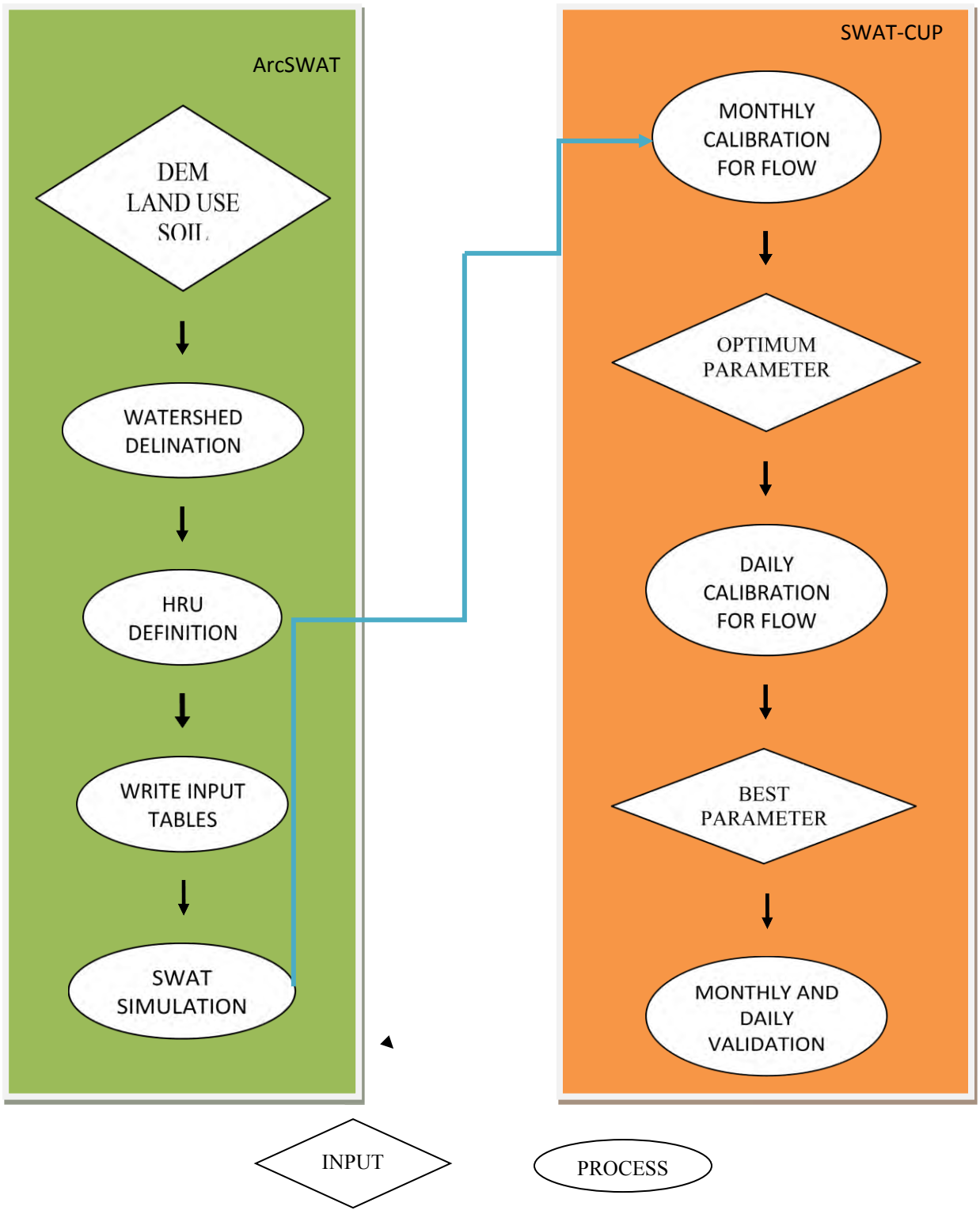

Figure 2-2: Work Flow for SWAT model setup and SWAT-CUP

2.5.2. Runoff-Volume Models

ArcSWAT computes runoff volume in (mm) by computing the volume of water that percolated to deep aquifer, return flow, evaporated from shallow aquifer, evapo-transpiration and subtracting it from the precipitation. Infiltration represents the movement of water to areas beneath the land surface.

2.5.3. Rainfall–runoff relationships

Rainfall–runoff relationships are used primarily for design, forecasting and evaluation. If stream flow data are unavailable or are too limited for reliable interpretation, rainfall–runoff relationships can be very helpful because of their ability to extract stream flow information from the precipitation records. Because of the relative simplicity and inexpensive nature of the collection of rainfall data, they are generally more abundant than are stream flow data. If a strong relationship can be established between the rainfall and runoff for a catchment of interest, the combination of the rainfall–runoff relationship and the rainfall data may, for example, give more reliable estimates of the frequency of high stream flows than either a regional flood relationship or an extrapolation of meager stream flow data from the catchment.

In general, rainfall–runoff relationships are developed in two distinct steps: the determination of the volume of runoff that results from a given volume of rainfall during a given time period and the distribution of the volume of runoff in time. The first step is necessary because of the partitioning of rainfall among evapotranspiration, infiltration and runoff. The second step is required to account for the travel time and the attenuation of the wave of runoff that is generated by the rainfall (WMO, 2004).

2.5.4. Supplementary software for this study

XLSTAT-2014: In my case XLSTAT software is used for filling of missing temperature and rainfall data, checking of trend and homogeneity. XLSTAT started in 1995 in order to make accessible to anyone a powerful, complete and user-friendly data analysis and statistical solution. This software can execute preparing, describing, visualizing, analyzing, and modeling data and correlation tests, parametric and non parametric tests, testing for outliers, homogeneity, trends and etc. The accessibility comes from the compatibility of XLSTAT with all the Microsoft Excel versions that are used nowadays (starting from Excel 97 up to Excel 2013), from the interface that is available in several languages and downloaded from the XLSTAT website www.xlstat.com. Last, the usability comes from the user-friendly interface, which after a few minutes of trying it out, facilitates the use of some statistical methods that might require hours

of training with other software. This tool allows you to complete or clean your dataset using advanced missing value treatment methods.

Easy Fit 5.6: Easy Fit is a data analysis and simulation application allowing to fit probability distributions to sample data, select the best model, and apply the analysis results to make better decisions. EasyFit can be used as a stand-alone Windows application or with Microsoft Excel and other third party Excel-based simulation tools, leaving the complex technical details behind the scenes and enabling you to focus on your business goals. The latest version of EasyFit can be downloaded from http://www.mathwave.com/downloads.html.

The goodness of fit (GOF) tests measures the compatibility of a random sample with a theoretical probability distribution function. In other words, these tests show how well the distribution you selected fits to your data. The results are presented in the form of interactive tables that help you decide which model describes your data in the best way.

2.5.5. Homogeneity Tests for rainfall Time series in XLSTAT

Use this tool to determine using one of four proposed tests (Pettitt, Buishand, SNHT, or von Neumann), if we may consider a series is homogeneous over time, or if there is a time at which a change occurs. Homogeneity tests involve a large number of tests for which the null hypothesis is that a time series is homogenous between two given times. The variety of the tests comes from the fact that there are many possible alternative hypotheses: change in distribution, changes in average (one or more times) or presence of trend.

The tests presented in this tool correspond to the alternative hypothesis of a single shift. For all tests, XLSTAT provides p-values using Monte Carlo resamplings. Exact calculations are either impossible or too costly in computing time.

i. Pettitt's test

The Pettitt's test is a nonparametric test that requires no assumption about the distribution of data. The Pettitt's test is an adaptation of the tank-based Mann-Whitney test that allows identifying the time at which the shift occurs.

ii. Alexanderson's SNHT test

The SNHT test (Standard Normal Homogeneity Test) was developed by Alexanderson (1986) to detect a change in a series of rainfall data. The test is applied to a series of ratios that compare the observations of a measuring station with the average of several stations. The ratios are then standardized. The series of Xi corresponds here to the standardized ratios. The null and alternative hypotheses are determined whether they follow the distribution

iii. Buishand's test

The Buishand's test (1982) can be used on variables following any type of distribution. But its properties have been particularly studied for the normal case. In his article, Buishand focuses on the case of the two-tailed test, but for the *Q* statistic presented the one-sided cases are also possible. Buishand has developed a second statistic *R*, for which only a bilateral hypothesis is possible.

iv. von Neumann's ratio test

XLSTAT evaluates the p-value and an interval around the p-value by using a Monte Carlo method. This test does not allow detecting the time at which the change.

2.6. Frequency Analysis

Frequency analysis done based on statistical analysis to relate flood magnitude with their frequency occurrence. High flow exceeding risk levels and entering in flood plains is the result of heavy or continuous rainfall exceeding the absorptive capacity of soil, and the flow capacity of the streams (Nibedita Guru[a], Ramakar Jha[b], 2015). It causes widespread damage to property and life in different parts of the catchment. Despite the fascinating achievements of science and technology in the 21st century, floods and droughts continue to hit every generation of human beings, bringing suffering, death, and material losses. The knowledge of magnitude-frequency relationships can be used in the design of dams, spillway of dams, highway, bridges, culverts, water supply systems and flood control structures. In the past, flood frequency analysis techniques were developed to relate the magnitude of floods with their frequency of occurrences (Hosking and Wallis, 1997). Such studies have also been done to estimate flood based on catchment characteristics and statistical analysis. It is understood that a minimum of 30-40 years of records are needed for flood frequency analysis (Nibedita Guru[a], Ramakar Jha[b], 2015). If the length of records is too short, specifically on inadequate data situation, then regional flood frequency curves together with at-site mean provides consistent estimates of floods.

Hazen (1921) revised his own work and found some data sets plotted are as curved lines in log normal distribution. He suggested using a three parameter distribution including skewness and plotting it on logarithmic probability paper. Foster (1924) introduced the Pearson type III (P3) frequency distribution for describing the flood data. Gumbel (1941) brought the basis of analysis to a new level by applying extreme value theory. Using the findings of Fisher and Tippett (1928), Gumbel (1941) introduced the Extreme Value Type I distribution (EV1) to flood frequency analysis. Chow et.al (1988), related the magnitude of such extreme events with their frequency of occurrence through the use of probability distributions. By fitting the past observations to selected probability distributions, the probability of future high flow events can be predicted.

In the case of the officially mandated models, their original selection was based almost exclusively on the basis of empirical goodness-of-fit to the events of record: it is implicitly assumed that the best fit will provide the most reliable extrapolation. Classically, the appropriateness of a given model is assessed via a goodness-of-fit test (e.g., Chowdhury et al., 1991).

The purpose of frequency analysis is to analyze past records of hydrologic variables so as to estimate future occurrence probabilities. The data used in the analysis must be evaluated in terms of the objectives, length of records available and completeness of records. It must also satisfy certain statistical criteria such as randomness, independence, homogeneity and stationary. A frequency analysis can be performed using single-site data, regional data or both. It can also include historical information and reflect physical constraints.

3. MATERIALS AND METHODS

3.1. Description of the Study Area

Didesa sub-basin is mainly located in East and West Welega zone, Illubabor zone, Jimma (special zone of Oromiya region) and some part in Kamashi zone of Benishangul-Gumuz. Geographically the sub-basin is located between $07^0$40'- $10^0$0'N and $35^0$32'-$37^0$15'E latitude and longitude respectively in western part of Ethiopia. The general elevation in the basin ranges between 653 meter a.m.s.l. and 3144 meter a.m.s.l. Physically, Didessa basin drains four zones (Jima, Illubabor, East Wollega, and West Wollega) of the National Regional State of Oromia as well as Benishangul Regional State.

Didessa River, which is the largest tributary of the Blue Nile (Abay) contributes roughly a quarter of the total flow of Blue Nile. The total catchment area drained by the river is estimated to be 28,229 km^2 originating from the mountain ranges of Gomma in South Western Ethiopia. The main upper streams namely; Dembi river in the South flow eastwards for about 75kms until they are joined by the Eastern tributaries such as Wama, Indris and so on, then after, turning rather sharply to the north until it reaches the Blue Nile (Abay) River. In the North East direction, the main tributary of Didessa River with the largest catchment area is Anger River (Tena, 2015). The mean annual rainfall in the study area is about 1745mm. The majority of the area is characterized by a humid tropical climate with heavy rainfall and most of the total annual rainfall is received during one rainy season called kiremt. The maximum and minimum temperature varies between 21.3 – 30.9^{0}C and 10.9 - 15.1^{0}C, respectively.

Physiographically, Didesa sub basin can be categorized in to two broad units which are the high land plateau and the associated low lands. The high land plateaus mainly embrace the Jimma- Ilu Abba Bora high lands, the Guduru highlands of Horo Guduru Wellega while the associated low lands include the Didesa low lands. The study area under Didesa Sub basins Integrated Land Use Planning Project include Jimma, Ilu Abba Bora highlands, Horo Guduru Wollega highlands, and associated low lands of Didesa valleys.

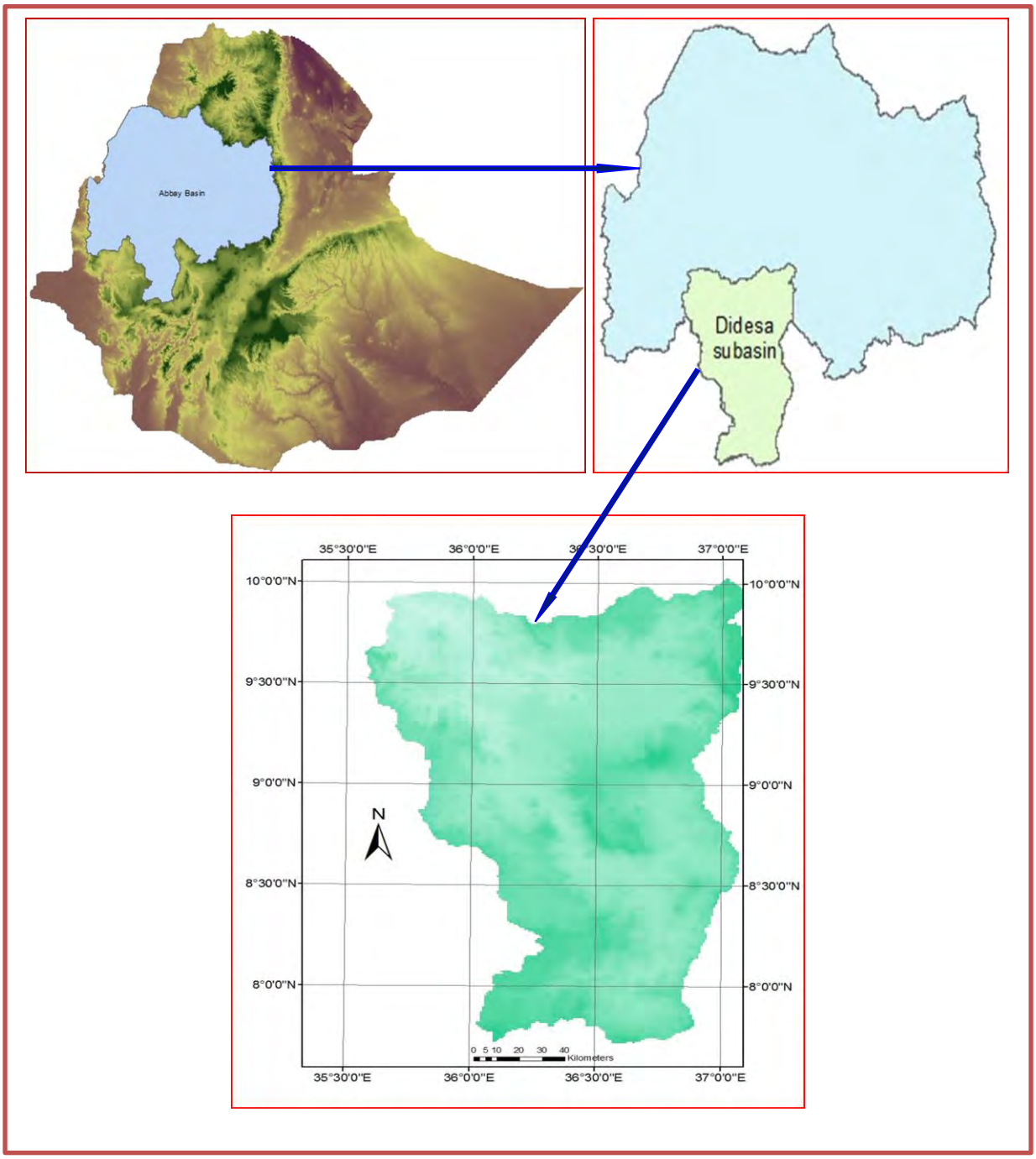

Figure 3-1:Didesa Sub-basin Locations

From the assessment of land use/land cover, major land cover types identified include moderately cultivated, dense woodland, intensively cultivated land, wooded grassland, open woodland, natural forest cover, natural forest with coffee, coffee farm with shade trees, riverine forest, bamboo forest, plantation forest, settlement, shrub land and open grassland. Different land use types in different land cover have been identified in the sub basin (OWWDSE, 2014). These include mixed cultivation, coffee production, livestock production, subsistence and commercial forest products utilization, non-timber products utilization, beekeeping, Wildlife management and utilization, infrastructure development, mining and investment activities on different activities.

Identification of these land use/ land cover types is important to indicate the conditions of the land potentials and constraints that could help integrated land use planning for the sustainable development of the communities living in and around the studied sub basins.

3.1.1. Climate

According to Hurni (1986) classification, the sub basin has five agro climatic zones. These are wet Dega, moist Dega, wet Weyna Dega, moist Weyna Dega and moist Kolla. It has got uni-modal rain fall distribution.

3.1.2. Major land forms

The project area is made up of three main broad soil and landscape units based on the general physiographic character of the landforms. These are: Low land plains and plateau with some undulating to steep land forms including depressions and valley floors, Moderate to high relief hills, severely dissected side slopes and plateaux and high to mountainous relief hills and plains of seasonally wetland and waterlogged. The slope or gradient of the project area varies from 0 to >36%.

3.1.3. Geology

The upper part of Didesa sub basin is dominated by Jimma Volcanic and the central part with Wellega Basalt and the lower parts are dominated by undifferentiated lower complex, Wellega Basalt and Adigrat Sand Stone.

3.2. Dataset and Data Sources for SWAT Model

The major data types that were used in this study include climate, hydrology, soils, land use/land cover data and Digital Elevation Model. The climate variables required are daily precipitation, maximum and minimum air temperature. Table 2.1 summarizes the dataset used in SWAT modeling of the study area, and their corresponding sources.

Table 3-1: Sources of available input data and its period

Data Type	Source	Scale/Period	Description	Remark
Weather	National Meteorological Agency of Ethiopia	1980-2015	Daily precipitation, Maximum and minimum temperature	Many of thestation have long period missing
Hydrology	Ministry of Water, Irrigation and Energy of Ethiopia	1980-2014	Daily and monthly flow data	Many of the station have long period missing
Land use/cover	(MERIS land use land cover,2009)	2009	Land use classification map	
Soils	Soil geo-database of Ethiopia' prepared by (Belete B.,et al,2013).	2013	Soil classification map	Single layer
Digital Elevation Model	NASA	30x30m	ASTER DEM	

3.2.1. Weather data

SWAT requires daily weather data including maximum and minimum air temperature, precipitation, wind Speed, Relative humidity and solar radiation. In case of lack of data, the weather generator in SWAT can provide alternative climate input, but it is not recommended for applications outside the USA. This data was acquired at the National Meteorological Agency of Ethiopia for stations within the Blue Nile Basin for the years of 1980 to 2015. The stations' locations are shown in figure 2.5. The meteorological stations are scatterly populated and and some stations are base period are recent with high missing record. In the case of unavailability of relative humidity, wind speed, and sun shine hour's data SWAT model was run with daily rainfall and maximum and minimum temperature. Below Table 3-2 shows listed weather monitoring Stations and available data and the time period used for the Didesa sub-basin.

Table 3-2: List of Selected weather monitoring Stations and Available data sets for rainfall and climatic variables

StationName	Zone	Station Elevation	Latitude	Longitude	Data coverage	% of missing Rainfall	% of missing Temp.(°C)
			Decimal Deg.	Decimal Deg.			
Bedele	Illubabor	2011	8.5	36.3	1980-2015	17	24.9
Arjo	Misrak Wellega	2565	8.8	36.5	1989-2015	27	33.1
Shambu	Misrak Wellega	2460	9.6	37.1	1980-2015	14	41.0
Nekemte	Misrak Wellega	2080	9.1	36.5	1980-2014	7	11.5
Gimbi	Mirab Wellega	1970	9.2	35.8	1980-2015	18	41.4
Nedjo	Mirab Wellega	1800	9.5	35.5	1980-2015	20	21.8
Jimma	Jimma	1718	7.7	36.8	1980-2015	5	4.6
Agaro	Jimma	1666	7.9	36.6	1995-2014	55	20
Dedessa	Misrak Wellega	1310	9.4	36.1	1980-2015	18	38.1

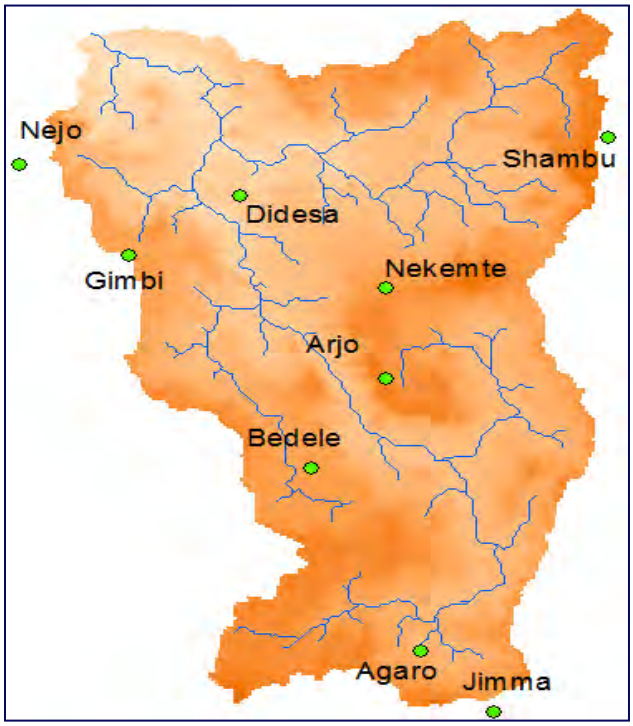

Figure 3-2: map of weather gauging location

3.2.2. Flow Data

Flow measurements were obtained from the Ministry of Water and Energy in Ethiopia. The relevant gauging station of Didesa river basin is located near Dembi (Toba),Arjo Didesa near Arjo,Dabana near Abasina,Wama near Nekemte and Angar near Nekemte which are employed for calibration and validation to find sensitive parameters and its approximate value. Similar to rainfall data Average monthly flow data also checked for absence of trend, consistency and homogeneity. And monthly data of hydrometric monitoring stations are free of trend, consistent and homogeneous.

Table 3-3: Basic Hydrometric monitoring description for Didesa sub-basin River Basin

Code	River	Station	Latitude		Longitude		Catchment area (km^2)	Data coverage	% Missing
			Deg.	Min	deg.	min			
114001	Didessa	Arjo	8	41	36	25	9,981	1980-2014	6
114002	Anger	Nekemte	9	26	36	31	4,674	1995-2004	7
114005	Dabana	Abasina	9	02	36	03	2,881	1980-1985	12
114014	Didesa	Nr. Dembi	9	30	36	35	1806	1985-2014	7
114004	Wama	Nr. Nekemte	8	47	36	47	844	1980-1985	39%(1981&1983 missing)

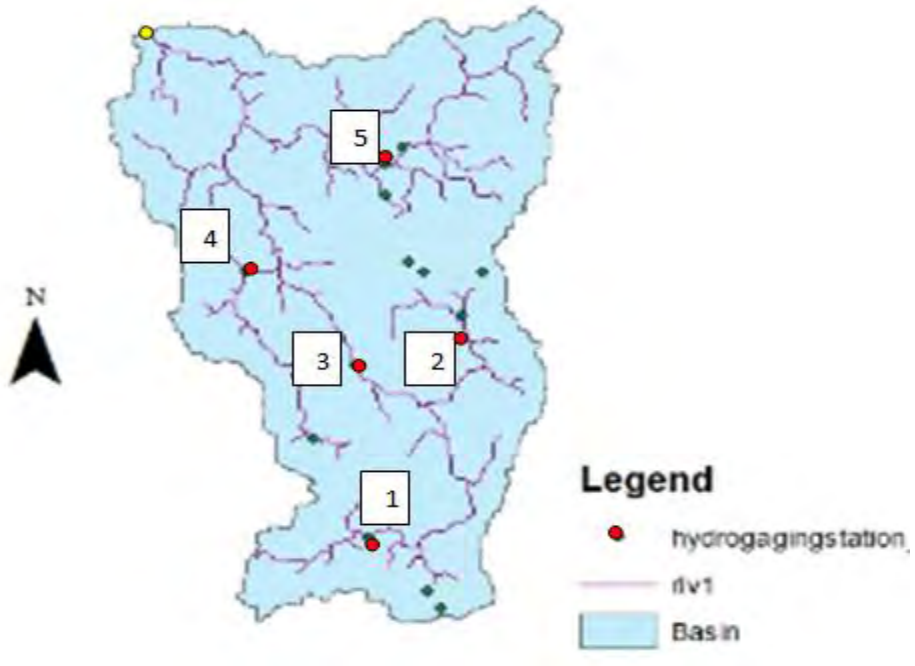

Figure 3-3: location of hydro gauging stations (1,2,3,4,5) for Dembi(Toba),Wama, Arjo, Dabana, Angar) respectively

3.2.3. Land-use data

Land use is one of the main factors affecting surface erosion, and Evapotranspiration in a watershed. The source of land use map of the study is the MERIS (Medium Resolution Imaging Spectrometer) based Glob-Cover 2009 land cover map is used after clipping it for my study area and modified to correspond with the SWAT predefined land uses classification. It contains a raster version of the Glob-Cover land cover map produced for the year 2009. The map is in geographic coordinates in a Plate-Carrée projection (WGS84 ellipsoid). You will find the following files within the zip file (Globcover_2009_V1.0.zip).

3.2.4. Soil Data

Different types of soil texture and physical-chemical properties are required for SWAT simulations. These data were obtained from various sources. The soil map obtained from Ministry of Water Resources of Ethiopian at Water Resources Information and Metadata Base Centre department. However, several properties like moisture bulk density, saturated hydraulic conductivity, percent clay content, percent silt content and percentage sand content of the soil which are required by SWAT model were not incorporated. Due to these deficient information additional data were substantiated from another source like 'soil geo-database of Ethiopia' prepared by (Belete B.,et al,2013). As it is shown in (Fig. 3-4), the major soil types Humic Nitosols. Comparison of this generated soil database of the country with the previously available FAO soil database (FAO, 1998) shows that the soil database from the former has more detail classification than the FAO soil data base.

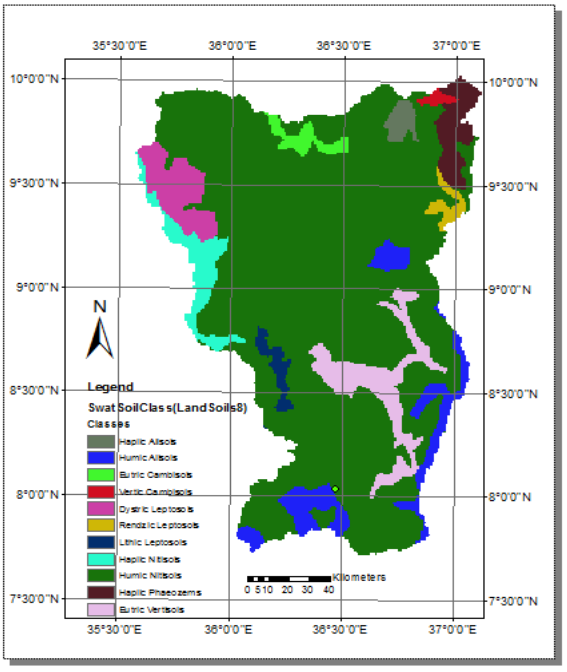

A)

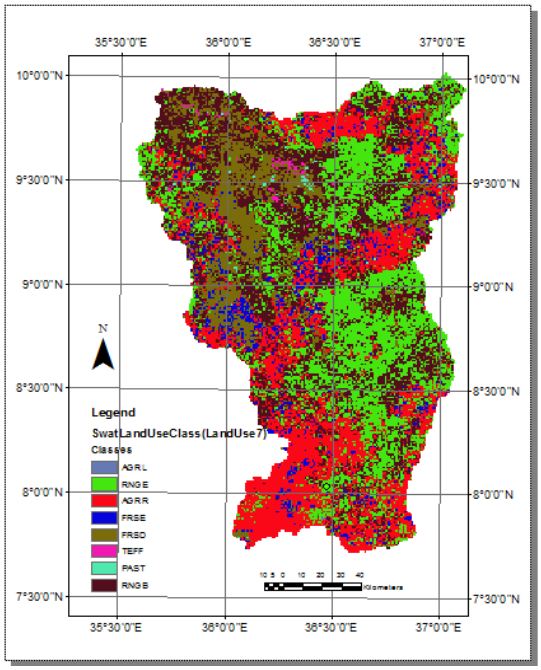

B

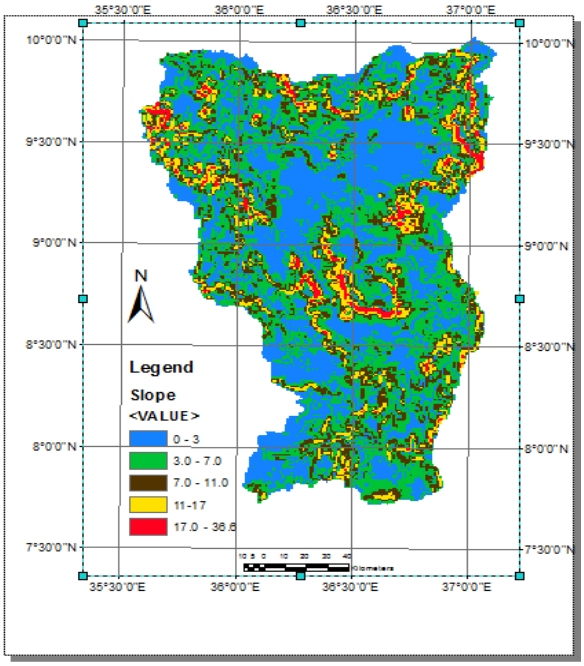

C)

Figure 3-4: Soil map, B) Land use map C) Slope class map

Source :((A) Soil geo-database of Ethiopia prepared by (Belete B.,et al,2013,(B)MERIS based Globe cover,2009. (C) ASTER DEM)

3.2.5. Digital elevation model

The digital elevation model ASTER GDEM was obtained from NASA (National Aeronautics and Space Administration) (2015). It is a product of the Ministry of Economy, Trade and Industry of Japan and the NASA. The DEM (see Fig. 3-5) was used to delineate the watershed and the drainage patterns of the surface area analysis. Sub basin parameters such as slope gradient, slope length of the terrain, and the stream network characteristics such as channel slope, length, and width were derived from DEM. The grid resolution lies at 30 m (see figure 3.4). It is necessary for the stream network processing in SWAT. The calculations establishing the river system are included in the ArcSWAT procedure facilitating the application. They are based on the functions Fill, Flow Direction and Flow Accumulation included in ArcMap Hydrology toolbox from ArcGIS program. Further the sub basins are generated. In total there were 116 sub basins established for Didesa River catchment area. The basin has Minimum Elevation and maximum elevation of 653m and 3144m respectively. Additionally, the average slopes were derived. The slope conditions are depicted in figure 3.5. Slope was classified into four groups: 0-5 %, 5-10 %, 10-20 % and >20 %. Slope classes were necessary for the HRU generation later on. The lowest slopes (0-5%) cover about 58% of watershed area.

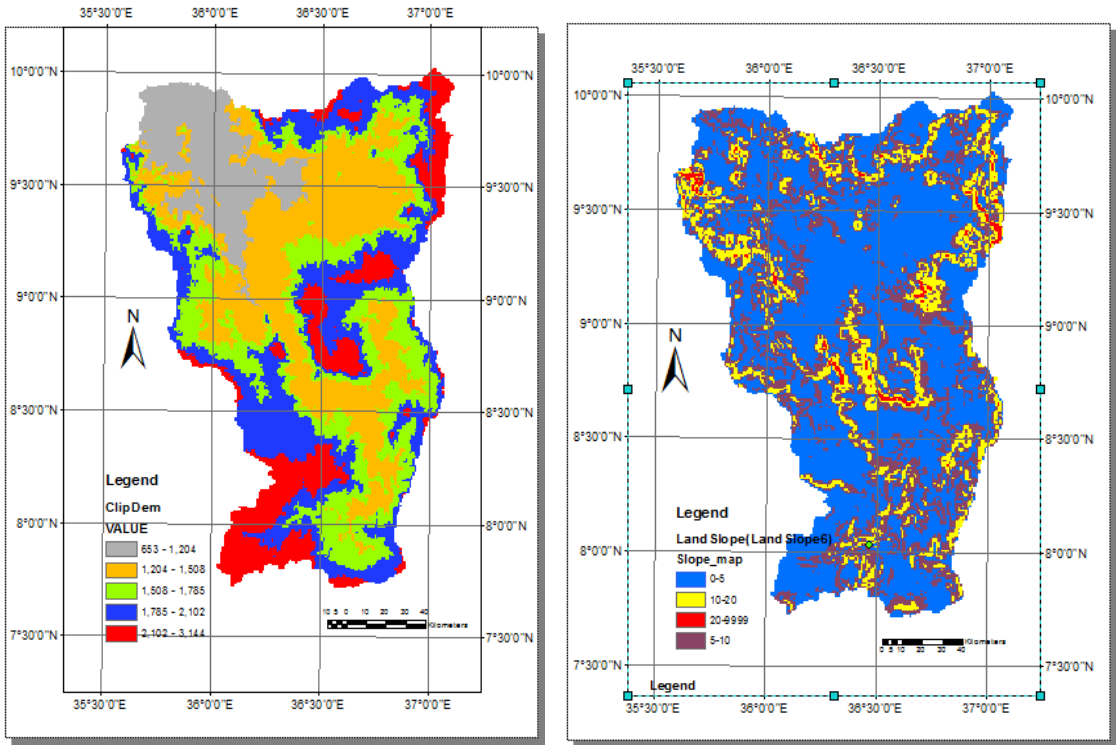

A) B)

Figure 3-5: (A). DEM map and (B) Slope map

After including DEM, soil and land use map, the HRUs are defined. Following the evaluations of Setegn (2008) for Blue Nile Basin area, the threshold percentages were defined at 20 % land use, 20 % soil and 15 % slope. The thresholds determine beyond which percentage of land use within a sub basin, the land use is accounted for in the HRU generation. Likewise this holds for soil within land use class and slope within soil class.

3.3. Method of filling Missing Rainfall and temperature Data

XLSTAT software is used as filling of missing temperature and rainfall data. XLSTAT started in 1995 in order to make accessible to anyone a powerful, complete and user-friendly data analysis and statistical solution. The accessibility comes from the compatibility of XLSTAT with all the Microsoft Excel versions that are used nowadays (starting from Excel 97 up to Excel 2013), from the interface that is available in several languages and downloaded from the XLSTAT website www.xlstat.com.

The power of XLSTAT comes from both the C++ programming language, and from the algorithms that are used. The algorithms are the result of many years of research of thousands of statisticians, mathematicians, computer scientists throughout the world. Each development of a new functionality in XLSTAT is preceded by an in-depth research phase that sometimes includes exchanges with the leading specialists of the methods of interest. Last, the usability comes from the user-friendly interface, which after a few minutes of trying it out, facilitates the use of some statistical methods that might require hours of training with other software. Most XLSTAT functions include options to handle missing data. However, only few approaches are available. This tool allows you to complete or clean your dataset using advanced missing value treatment methods.

Different methods are available depending on your needs and data:

- For quantitative data, XLSTAT allows you to:
    - Remove observations with missing value.
    - Use a mean imputation method.
    - Use a nearest neighbor approach.
    - Use the NIPALS algorithm.
    - Use an MCMC multiple imputation algorithm.
- For qualitative data, XLSTAT allows you to:
    - Remove the observations with missing value.
    - Use a mode imputation method.

- Use a nearest neighbor approach.

The NIPALS method is a method presented by H. Wold (1973) to allow principal component analysis with missing values. The NIPALS algorithm is applied on the dataset and the obtained PCA model is used to predict the missing values. XLSTAT proposes a multiple imputation algorithm based on the Markov Chain Monte Carlo (MCMC) approach also called fully conditional specification (Van Buulen, 2007).Hence missing data of rainfall, maximum and minimum temperature are filled by Using a nearest neighbor approach.

3.4. Checking the Consistency of data at rain gauge stations

Sometimes a significant change may occur in and around a particular rain gauge stations. Such change occurring in a particular year will start affecting the rain gauge data, being reported from a particular station. In order to detect such inconsistency and to correct and adjust the reported rainfall values, a technique called double mass curve method is generally adopted. In this method a group of 5 to 10 neighboring stations are chosen in the vicinity of doubtful station. The mean daily rainfall values are serially arranged in reverse chronological order to determine relative consistency; one compares the observations from a certain station with the mean of observations from several nearby stations. This mean is called the 'base' or 'pattern'. It is difficult to say how many stations the pattern should comprise. The more the stations, the smaller the chance that inconsistent data from a particular one will influence the validity of the average of the pattern. In conventional double-mass analysis, this checking requires removing from the pattern the data from a certain station and comparing them with the remaining data. If these data are consistent with the general totals in the area, they are re-incorporated into the pattern. Data of each station are arranged in descending order. The cumulative sums, station to be tasted and base station; are plotted against each other and a line (or lines) of best fit are drawn in excel work sheet.

The cumulative precipitation values of doubtful station, X say ΣPx, and cumulative values of group average say ΣPav are then plotted on a graph paper. Px' (corrected precipitation) and given by the following formula.

$$Px' = Px\frac{M'}{M}$$

Where, Px'= corrected precipitation at station x

Px= original recorded precipitation at station x

M'= corrected slope of double mass curve

M= original slope of double mass curve

Fig.2.2 Corrected Rainfal of Bedele station by double mass

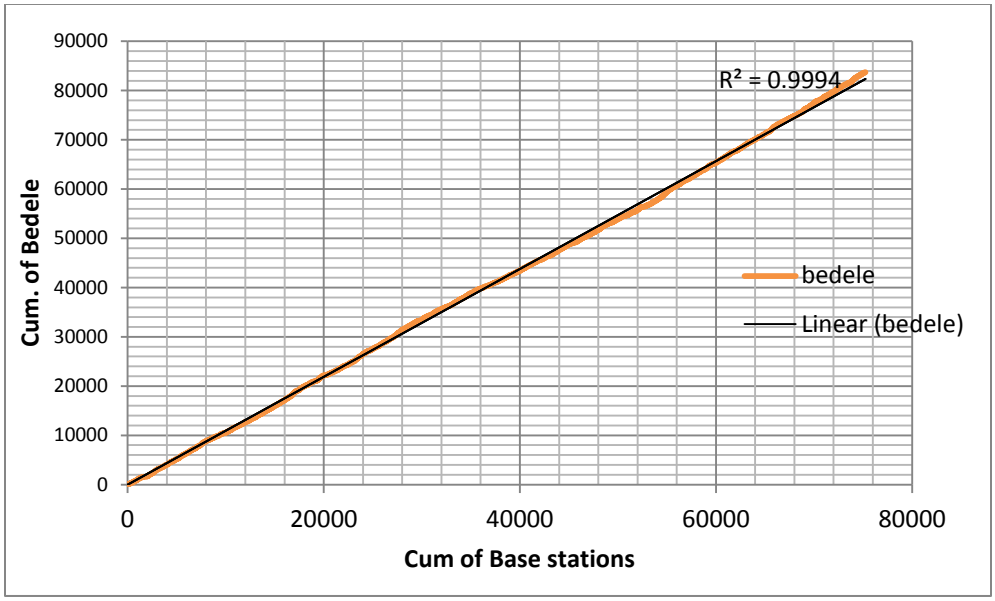

Figure 3-6: linear consistency for Bedele stations

3.5. Test for Absence of Trend

Mann-Kendall Trend Tests: Use this tool to determine with a nonparametric test if a trend can be identified in a series, even if there is a seasonal component in the series. A nonparametric trend test has first been proposed by Mann (1945) then further studied by Kendall (1975) and improved by Hirsch *et al* (1982, 1984) who allowed taking into account seasonality. The null hypothesis H0 for these tests is that there is no trend in the series. The three alternative hypotheses that there is a negative, non-null, or positive trend can be chosen. The Mann-Kendall tests are based on the calculation of Kendall's tau measure of association between two samples, which is itself based on the ranks with the samples. To calculate the p-value of this test, XLSTAT can calculate, as in the case of the Kendall tau test, an exact p-value if there are no ties in the series and if the sample size is less than 50. If an exact calculation is not possible, a normal approximation is used, for which a correction for continuity is optional but recommended. If the time series does have a trend, the data cannot be used for frequency analyses or modelling.

3.6. The Mean Rainfall of gauging stations

Average precipitation over the sub basin is calculated with Thiessen's polygon method. The area coverage of each weather gauging station is calculated in ArcGIS software.

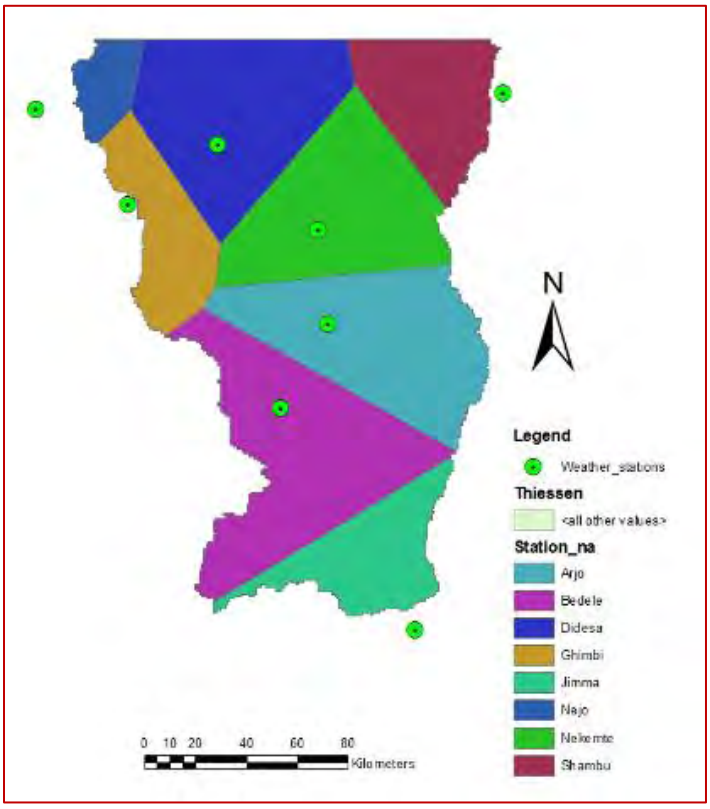

Figure 3-7:Thiessen's polygon for Didesa sub basin

The mean annual rainfall of 1980 to 2015 used to calculate average precipitation on the sub basin for Thiessen's polygons method. The annual precipitation and station coverage is given in table 3-4.

Table 3-4:stations coverage and annual precipitation

Station name	Area(km2)	Annual Precipitation (mm)
Bedele	5102.8	1913.88
Jimma	2238.2	1503.1
Shambu	2453.0	1539.4
Didesa	4395.9	1547.1
Arjo	4454.3	2120.7
Nekemte	4130.6	2073.4
Nejo	768.3	1581.3
Ghimbi	2014.4	1919.4

3.7. Model calibration and Validation

Calibration describes the effort to support the model with fitted parameters for a given set of local conditions in order to reduce the prediction uncertainty (Arnold et al. 2012a). The Didesa sub-basin model's calibration includes water balance on monthly and daily time step. Calibration was carried out with the SWAT Calibration and Uncertainty Program (SWAT-CUP) 2012, Version 2.7.1.2, which facilitates the calibration process (Abbaspour, 2014).

3.7.1. Automatic calibration procedure using SUFI2 algorithm

SWAT-CUP provides algorithms for auto-calibration, from which Sequential Uncertainty Fitting, Version 2 (SUFI2) was chosen. SUFI2 accounts for several sources of uncertainties such as uncertainty in driving variables (e.g. rainfall), conceptual model, parameters and measured data (K. C. Abbaspour and Genuchten 2004). It is not a fully automated calibration tool, since it still requires interaction of the modeller and knowledge about the parameters and their effects on the output (Yang et al. 2008).

The algorithm has been applied successfully in former applications to the Blue Nile Basin (e.g. in Setegn (2008). The SUFI2 algorithm does not use sole parameters, but parameter ranges. Consequently calibrated parameters are given as ranges as well. Before the model is executed, Latin Hypercube sampling assigns as many parameter combinations as model runs are to be carried out. For each combination every single parameter is given a value within a suggested range. Then the iteration with SUFI2 is executed. As a result the algorithm proposes optimum parameter ranges and the so called "best" estimation. Furthermore SUFI2 orients on a given objective function (NSE, R2,...) resulting from the parameter sets besides other quality criteria, in particular the p-factor and the r-factor (Abbaspour, 2014). Those provide information about the model's strength and certainty of the calibration result.

3.7.2. Selection of parameters for Sensitivity Analysis

Before calibration to start parameters those were sensitive for Abbay basin were arranged from articles published, since Didesa sub basin is found in Abbay basin. Parameters required for calibration are described in (table 3.4) below**.** Table 1 provides a description of the 19 parameters included in the manual calibration and sensitivity analysis: CN2, ESCO, SOL_AWC, GW_DELAY, GW_REVAP, REVAPMN, GWQMN, ALPHA_BF, RCHRG_DP, CH_K2, SURLAG, CH_N2, and SOL_K, CH_K2, ALPHA_BNK, SLSUBBSN, OV_N, LAT_TIME, ESCO, EPCO, and HRU_SLP. The smaller the p-value indicates the more sensitive parameter whereas the larger the p-value point toward the less sensitive

for the given watershed. The values close to zero has more significance. Sensitivity checking of parameters is done at five major hydro gauging stations (Dembi,Wama,Dabana,Arjo and Angar near Nekemte) found in Didesa sub basin. Hence, to check this, sensitivity analysis is one of SWAT model tool to show the rank and the mean relative sensitivity of parameters identification and this step was ordered to analysis. This appreciably eases the overall calibration and validation process as well as reduces the time required for it. Besides, as Lenhart et al. (2002) indicated, it increases the accuracy of calibration by reducing uncertainty.

Table 3-5: Parameter definitions and initial ranges used in SUFI-2.

Stream flow parameters selected for calibration	Description of parameters	Ranges
GW_DELAY	Groundwater delay (days).	0-500
ALPHA_BF	Base flow alpha factor (days).	0-1
GWQMN	Threshold depth of water in the shallow aquifer required for return flow to occur (mm).	0-5000
GW_REVAP	Groundwater "revap" coefficient.	0-0.2
REVAPMN	Threshold depth of water in the shallow aquifer for "revap" to occur (mm).	0-500
RCHRG_DP	Deep aquifer percolation fraction.	0-1
CN2	SCS runoff curve number	(-0.25) - 0.25
SOL_AWC	Available water capacity of the soil layer.	(-0.25) - 0.25
SOL_K	Saturated hydraulic conductivity.	(-0.25) - 0.25
CH_N_2	Manning's "n" value for the main channel.	0 – 0.3
CH_K_2	Effective hydraulic conductivity in main channel alluvium.	0 – 500
ALPHA_BNK	Base flow alpha factor for bank storage.	0 – 1
SLSUBBSN	Average slope length.	10 - 150
OV_N	Manning's "n" value for overland flow.	0.01 - 30
LAT_TTIME	Lateral flow travel time.	0 - 180
ESCO	Soil evaporation compensation factor.	0 - 1
EPCO	Plant uptake compensation factor.	0 - 1
SURLAG	Surface runoff lag time	0.05 - 24
HRU_SLP	Average slope steepness	0 - 1

3.7.3. Model performance evaluation

In order to decide whether the model is capable to reproduce predictions close enough to observed data, some quality criteria are used. Apart from simple graphical and visual interpretation of model results, statistical values were used to quantify the model's performance. The following objective functions to measure the model's goodness of fit for discharge was taken into consideration:

1. **NSE**

The Nash-Sutcliffe Efficiency (Nash and Sutcliffe 1970) is a dimensionless, normalized statistical value and expresses the noise to information ratio (equation 1). It shows how well the plot of observed versus simulated data fits the 1:1 line. Its usage is recommended from ASCE (1993).

$$\mathrm{NSE} = 1 - \frac{\sum_{i=1}^{n}(\mathrm{Qi}^{m} - \mathrm{Qi}^{s})^2}{\sum_{i=1}^{n}(\mathrm{Qi}^{m} - \overline{\mathrm{Q}^{m}})^2} \quad ----------(3a)$$

Where,

Qi^m= observed discharge at time step i

Qi^s = Simulated discharge at time step i

$\overline{Q^m}$= mean of observed discharge

The range of NSE goes from -1 to 1. NSE < 1 indicates that the model's prediction is worse than the mean observed discharge and NSE = 1 signifies an optimal t of observed and simulated values. For values between 0 and 1 the performance is generally seen as acceptable (Moriasi et al.2007).

2. **R^2**

The coefficient of determination describes the proportion of variance of the measured data. It has to be treated carefully due to its over sensitivity to outliers. Further it is insensitive to proportional differences (Legates and McCabe Jr, 2010). For the calculation, the following equation is used.

$$R^2 = \frac{\left[\sum_{i=1}^{n}(\boldsymbol{Q_{m.i}} - \overline{\boldsymbol{Q_m}})(\boldsymbol{Q_{s,i}} - \overline{\boldsymbol{Q_s}})\right]^2}{\sum_{i=1}^{n}(\boldsymbol{Q_{m,i}} - \overline{\boldsymbol{Q_m}})^2 (\boldsymbol{Q_{s,i}} - \overline{\boldsymbol{Q_s}})^2} \quad ---------(\boldsymbol{3b})$$

Coefficient of determination *R*2 where *Q* is a variable (e.g., discharge), and *m* and *s* stand for measured and simulated, *i* is the *i* th measured or simulated data.

R^2 lies within the bounds of 0 and 1. A value of 0 indicates that there is no relationship between observed and measured data, 1 signifies a perfect linear relation. Hence, the closer R^2 is to 1, the less is the error variance (Moriasi et al. 2007).

3. PBIAS

The Percent Bias is an error index, which measures the average tendency of the simulated data to be larger or smaller than the observations (Gupta, Sorooshian, and Yapo 1999). It is taken as a clear quantifier for water balance errors (Moriasi et al. 2007). ASCE (1993) recommends its usage for watershed models. Calculation of PBIAS follows equation 3

$$PBIAS = 100 * \frac{\sum_{i=1}^{n}(Q_m - Q_s)i}{\sum_{i=1}^{n} Q_{m,i}} - - - - - - - - - - - - - - - (3c)$$

where Q is a variable (e.g., discharge), and m and s stand for measured and simulated, respectively.

Percent bias measures the average tendency of the simulated data to be larger or smaller than the observations. The optimum value is zero, where low magnitude values indicate better simulations. Positive values indicate model underestimation and negative values indicate model over estimation (Gupta et al., 1999).

4. RSR

The RMSE-observations standard deviation ratio error index is the standardized form of the Root Mean Square Error (RMSE). Moriasi et al. (2007) recommends using this standardized version of error index, because it combines error index and a normalization factor, the standard deviation (STDEV). The normalization on the standard deviation of observed data provides the opportunity to compare RSR to other models. For computation of RSR equation 6 is used.

$$RSR = \frac{\sqrt{\sum_{i=1}^{n}(Q_m - Q_s)_i{}^2}}{\sqrt{\sum_{i=1}^{n}(Q_{i,m} - \overline{Q_m})^2}} - - - - - - - - - - - - (3d)$$

Where, Q is a variable (e.g., discharge), and m and s stand for measured and simulated, respectively.

3.8. Hydrological characterization

3.8.1.Defining watersheds

Once the model region is defined, calibrated and validated for Didesa sub basin, optimum parameters found in calibration at gauging stations was used for flow estimation at junctions or river confluence. it is also necessary to define sub basins within this region. Sub basin delineation in this study is based on possible river junction locations. Because runoff volume is calculated on a sub basin scale, a hydrograph can only be produced at the outlet of each sub basin and at river junctions. A hydrograph is needed at each potential location to determine the optimum river gauge location. These locations are used to redefine watershed outlet points. SWAT was rerun to estimate flow hydrograph at outlet, water balance, and to determine physical parameters in order to derive Snyder synthetic unit hydrograph for the resulting 5watersheds (Wama, Dembi, Dabana, Didesa near Arjo, Angar at confluence with Didesa, and Arjo Didesa at confluence of Angar)

3.8.2.Deriving Physical Watershed Parameters

After defining the watershed sub basins, Arc Hydro tool is used to calculate the physical parameters associated with each watershed and river reach used in the Snyder synthetic unit hydrograph preparation. These parameters are:

- Sub basin Area
- Longest flow path
- Length from sub basin outlet to a point nearest the sub basin centroid
- differentiate the most sensitive hydrological parameters

3.8.3. Defining Overland Flow in each sub basin

The overland flow process describes how the volume of excess precipitation is transformed to runoff at a specific point. In this study, the Snyder Unit Hydrograph method is chosen. This well-established empirical method is based on the analysis of many studies conducted in agricultural watersheds in the United States (Bedient, et al., 2008). From these studies, a relationship was derived relating the magnitude and time of the peak hydrograph to the lag time and area of each sub basin.

The lag time is defined as the time between the centroid of excess precipitation and the peak of the resultant hydrograph (Bedient, et al., 2008). Lag time can be calculated through a variety of methods; two common methods are the SCS Unit Hydrograph Method and the Snyder Method.

3.9. Frequency Analysis

Hydrologic systems are sometimes impacted by extreme events, such as severe storms, floods, and droughts. The magnitude of an extreme event is inversely related to its frequency of occurrence, very severe events occurring less frequently than more moderate events. The objective of frequency analysis of hydrologic data is to relate the magnitude of extreme events to their frequency of occurrence through the use of probability distributions. The results of flood flow frequency analysis can be used for many engineering purposes: for the design of dams, bridges, culverts, and flood control structures; to determine the economic value of flood control projects; and to delineate flood plains and determine the effect of encroachments on the flood plain.

Flood frequency analysis is done at each junction using: Different methods are employed to determine frequency analysis. The Extreme Value Type I (EVI) distribution, log normal distribution, Log-Pearson type-III distribution. Storm rainfalls are most commonly modeled by the Extreme Value Type I distribution (Chow, 1953; Tomlinson, 1980), and drought flows by the Weibull distribution, that is, the EV III distribution applied to -x(Gumbel,1954,1963). Frequency analysis was performed with all the above mentioned three methods and type I (Chow, 1953) is compared with parameters found during calibrations (lag time) compared during unit hydrograph preparation and give good results. Flood with its frequency of occurrence is done at junction 1, 2 and 3. The modest timescales such as 100 years, which offer the best promise for testing alternative models of extreme flood behaviour across a wider range of basins (R. Kidson1,* and K.S. Richards[2],2005). At stake is the accurate estimation of flood magnitude, used widely for design purposes.

Furthermore, the best distribution is selected by using Easy Fit soft ware. Kolmogorov Smirnov rank of goodness of fit is used to determine the best method to analyze my distribution is lognormal (3P) which is almost similar to extreme value type-I in which KT is determined by chow (1953). However, for peak over threshold flood data series Log Normal (3P) distribution showed best results with all goodness of fit test.

i. **EV-Type I Distribution**: For the Extreme Value Type I distribution, Chow (1953) derived the expression

$$K_T = \frac{\sqrt{6}}{\pi}\left\{0.5772 + ln\left[ln\left(\frac{T}{T-1}\right)\right]\right\} \text{ ---------- (3-1)}$$

Where, K_T, frequency factor, T= return period

$x_T = \bar{x} + K_T * s$ ---------- (3-2)

Where,$\bar{x}$ peak flow mean, s=standard deviation of peak flow and, x_T, magnitude of extreme event at time at return period T.

ii. **For lognormal distribution**

The value of z corresponding to an exceedence probability of p (p=1/T) can be calculated by finding the value of an intermediate variable w:

$$w = \left[ln\left(\frac{1}{p^2}\right)\right]^{1/2} \qquad (0 < p \leq 0.5) - - - - - - - - - - -(3-3)$$

Then calculating z using the approximation

$$z = K_T = w - \frac{2.515517 + 0.802853w + 0.010328w^2}{1 + 1.432788w + 0.189269w^2 + 0.001308w^3} - - - - - - - - - - - - - -(3-4)$$

When p>0.5, 1—p is substituted for p in (3) and the value of z computed by (4) is given a negative sign. The error in this formula is less than 0.00045in z (Abramowitz and Stegun, 1965).The frequency factor K_T for the normal distribution is equal to z, as mentioned above.

For the lognormal distribution, applied to the logarithms of the variables, and their mean and standard deviation are used in Eq. (2). And then antilog of data is taken to get extreme value.

iii. **Log-Pearson type-3 distribution**. For this distribution, the first step is to take the logarithms of the hydrologic data, y=logx. Usually logarithms to base10 are used. The mean y, standard deviation s_y, and coefficient of skewness C_s are calculated for the logarithms of the data. The frequency factor depends on the return period T and the coefficient of skewness C_s.When Cs=0, the frequency factor is equal to the standard normal variable z.When Cs≠ 0,K_T is approximated by Kite(1977) as

$$K_T = z + (z^2 - 1)k + \frac{1}{3}(z^3 - 6z)k^2 - (z^2 - 1)k^3 + zk^4 + \frac{1}{3}k^5, where, k = \frac{C_s}{6} \text{------- (3-5)}$$

3.10. Time of Concentration

The channel flow time of concentration, can be computed using the equation:

$$t_c = \frac{L_c}{3.6 * V_c} - - - - - - - - - - - - - - - - - - (3-14)$$

Where L_c is the average flow channel length for the sub basin (km), *vc* is the average channel velocity (m s-1), and 3.6 is a unit conversion factor.

The average channel flow length can be estimated using the equation

$$L_c = \sqrt{L * L_{cen}} - (3-15)$$

Where *L* is the channel length from the most distant point to the sub basin outlet (km), and *Lcen* is the distance along the channel to the sub basin centroid (km).

The average velocity can be estimated from Manning's equation assuming a trapezoidal channel with 2:1 side slopes and a 10:1 bottom width-depth ratio.

$$v_c = \frac{0.489 * Q^{0.25} * S^{0.375}}{n^{0.75}} - - - - - - - - - - - - - - - - - - (3-16)$$

Where v_c is the average channel velocity (m s^{-1}), Q is the average channel flow rate (m^3 s^{-1}), S is the channel slope (m m-1), and n is Manning's roughness coefficient for the channel. To express the average channel flow rate in units of mm/hr, the following expression is used (Source: SWAT 2005 Theoretical Documentation)

4. RESULTS AND DISCUSSIONS

4.1. Data Processing and Model Set Up

Data processing in this case includes trend test and homogeneity tests for monthly precipitation data of 8 stations in Didesa sub basin from 1980 to 2014. Moreover, monthly flow data of the sub basin is also tested for Arjo gauging station from year 1980 to 2014, Dembi station from 1985 to 2014, Angar stations from 1995 to 2004, for Dabana stations from 1982 to 1985 depending availability of flow data.

4.2. Trend and Homogeneity Test

4.2.1. Trend test for observed Rainfall

Monthly data of rainfall from 1980 to 2014 is employed for trend analysis. In this test, seasonal Mann-Kendall test is applied, and we take into account the seasonality of the series. This means that for monthly data with seasonality of 12 months, one will not try to find out if there is a trend in the overall series, but if from one month of January to another, and from one month February and another, and so on, there is a trend. In order to use this test my daily data are converted to monthly data and the calculation of parameters is executed with XLSTAT whether we accept or reject the null hypothesis i.e data has no trend. As it can be seen from the following XLSTAT output summery table in all stations p-value is greater than Alpha (5%), means there is no seasonal trend in gauging stations.

As the computed p-value is greater than the significance level alpha=0.05, one cannot reject the null hypothesis H0.

Table 4-1: seasonal trend test for monthly rainfall of Weather gauging stations

Summary statistics:

Station	Observations	Obs. with missing data	Obs. without missing data	Minimum	Maximum	Mean	Std. deviation
JIMMA	420	0	420	0.3	572.1	126.9	102.0
BEDELE	420	0	420	0.0	500.1	156.8	128.2
NEKEMTE	420	0	420	0.0	593.8	174.5	149.3
DIDESA	420	0	420	0.0	514.9	126.4	118.4
GIMBI	420	0	420	0.0	1007.3	152.9	139.6
NEJO	420	0	420	0.0	390.0	128.4	104.1
ARJO	420	0	420	0.3	720.5	161.9	125.8
SHAMBU	420	0	420	0.6	566.2	128.5	98.4

Station	Kendall's tau	p-value (Two-tailed)	alpha
JIMMA	0.041	0.281	0.05
BEDELE	-0.02	0.93	0.05
NEKEMTE	-0.00138	0.986	0.05
DIDESA	-0.0470	0.228	0.05
GIMBI	0.0451	0.216	0.05
NEJO	0.038	0.268	0.05
ARJO	0.0143	0.694	0.05
SHAMBU	0.057	0.126	0.05

Note: p-values are greater than alpha (0.05), hence data of all stations are consistent

4.2.2. Homogeneity test of observed Rainfall

Alexanderson's SNHT test for Homogeneity is applied for testing of monthly rainfall. The SNHT test (Standard Normal Homogeneity Test) was developed by Alexanderson (1986) to detect a change in a series of rainfall data. The test is applied to a series of ratios that compare the observations of a measuring station with the average of several stations. The ratios are then standardized. Monthly Sum of rainfall is used to analyses presence homogeneity and the results are evaluated in XLSTAT software. We followed the same procedure as trend test and found that data are homogeneous (see table below).

Table 4-2: Alexanderson's SNHT test for Homogeneity of monthly rainfall data

Station	Kendall's tau(τ_o)	p-value (Two-tailed)	alpha
JIMMA	7.7	0.146	0.05
BEDELE	2.5	0.93	0.05
NEKEMTE	4.8	0.5	0.05
DIDESA	3.6	0.72	0.05
GIMBI	3.3	0.8	0.05
NEJO	2.81	0.89	0.05
ARJO	2.2	0.96	0.05
SHAMBU	4.1	0.63	0.05

As shown in table all p-values are greater than alpha (0.05), hence data are homogenous.

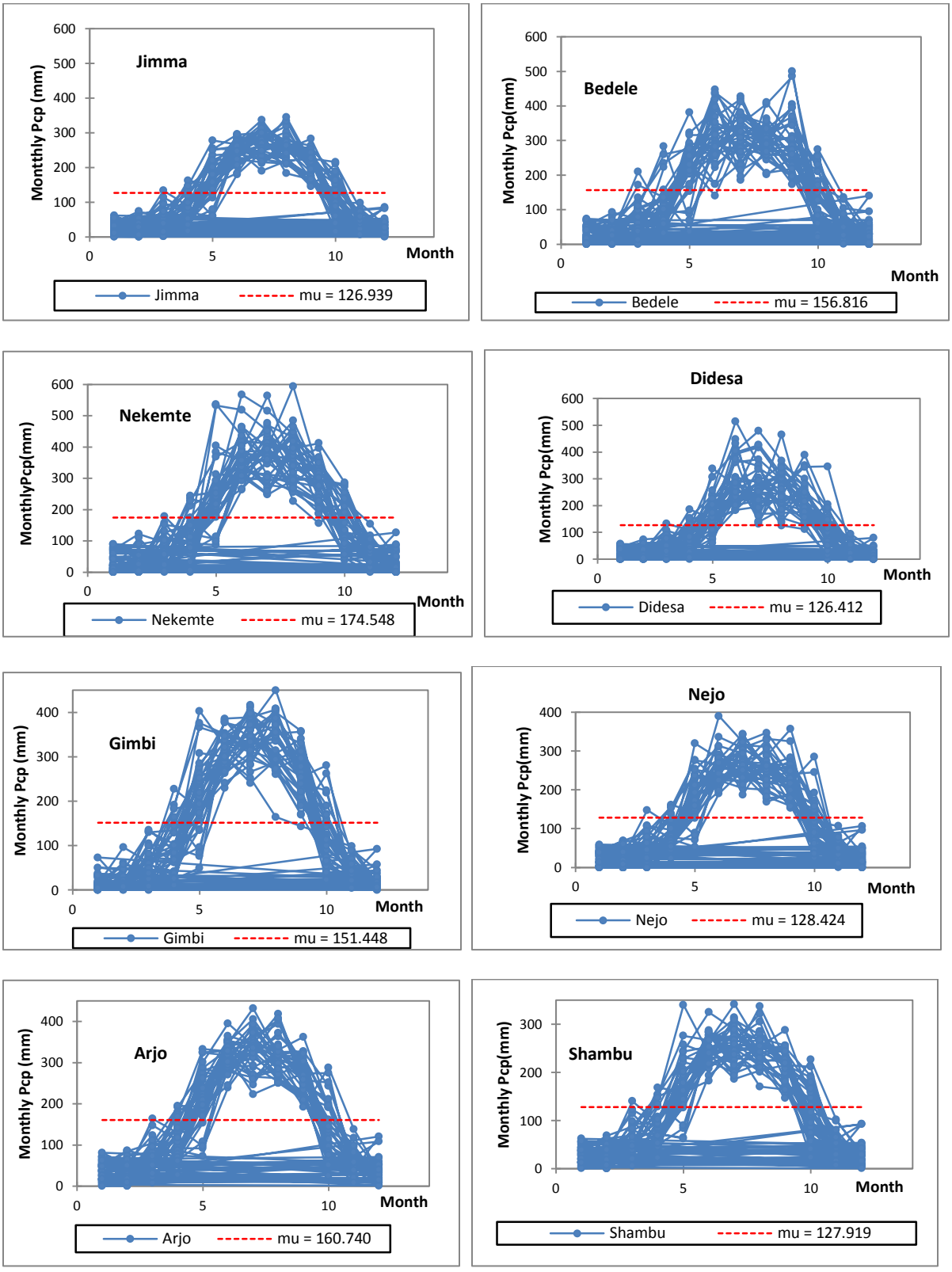

Figure 4-1: Graphical representation of homogeneity test of monthly flow data

4.2.3. Trend test and homogeneity test for monthly flow data

Similarly discharge homogeneity and trend test is done at discharge gauging stations of Didesa near Arjo (from 1980-2014), Dabana Near Abasina (1980-1984), Didesa Near Dembi (1985-2014) and Angar Near Nekemte (1995-2004). And from trend and homogeneity test it is found that the flow data used for calibration and validation are homogeneous and no significant trend is found at all discharge gauging stations. Alexanderson's SNHT test for Homogeneity is applied for testing of monthly flow and found flow data are inconsistent.

Table 4-3: Alexanderson's SNHT test for Homogeneity of monthly Discharge

Station	Observations	Obs. with missing data	Obs. without missing data	Minimum	Maximum	Mean	Std. deviation
Angar	108	0	108	0.000	295.2	60.0591	71.9
Nr. Arjo	420	12	408	0.000	540.9	107.6	125.7
Nr. Dembi	360	16	344	0.542	238.4	40.7	48.6
Nr. Abasina	60	3	57	2.7	196.5	52.2	58.9

Station	Kendall's tau(τ_o)	p-value (Two-tailed)	alpha
Angar	10.75	0.059	0.05
Nr. Arjo	10.8	0.06	0.05
Nr. Dembi	4.8	0.47	0.05
Nr. Abasina	4.0	0.47	0.05

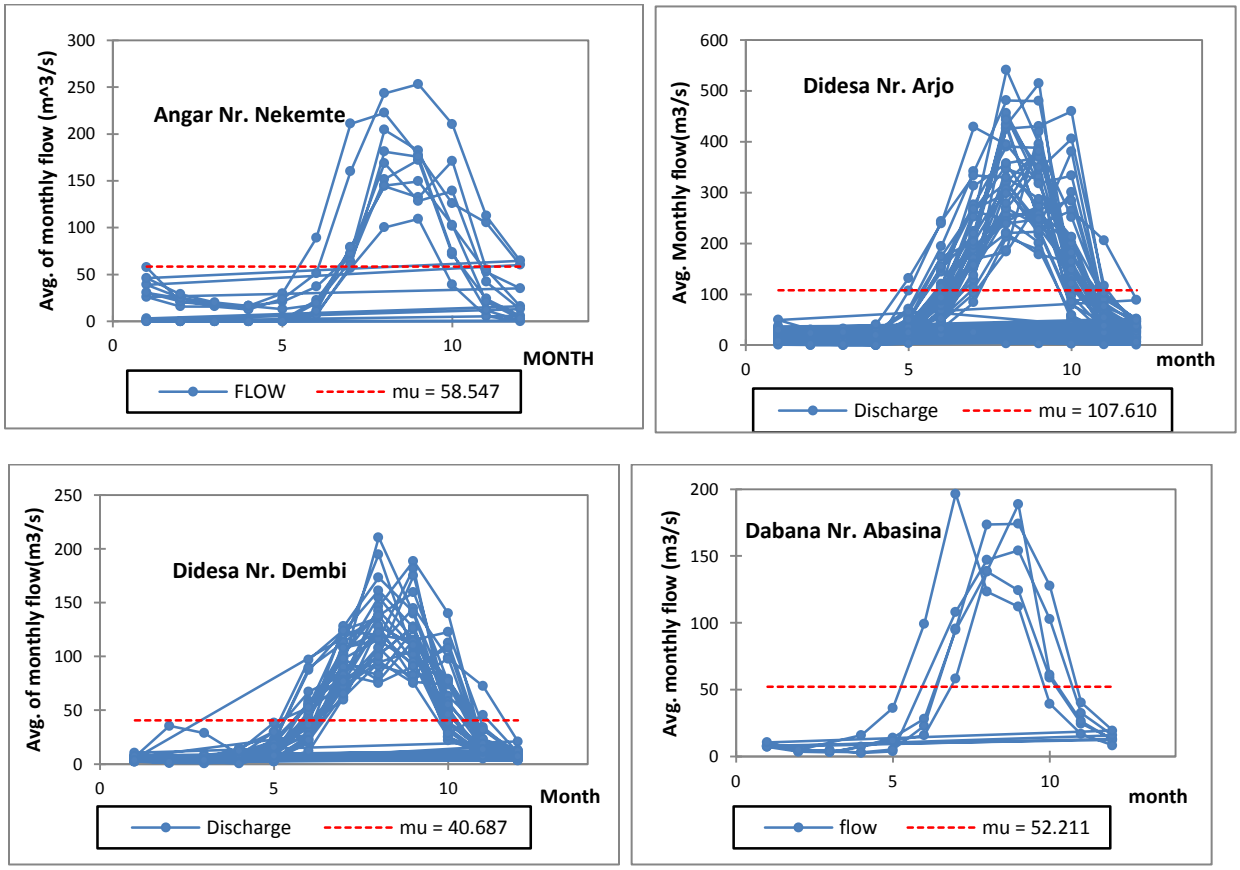

Figure 4-2: Graphical representation of homogeneity test of monthly observed flow data

4.3. Model Calibration and Validation

The first step in the calibration and validation process in SWAT is the determination of the most sensitive parameters for a given watershed or sub watershed. It shows to determine which variables to adjust based on expert judgment or on sensitivity analysis. It is necessary to identify key parameters and the parameter precision required for calibration (Jeffrey G. Arnold et al., 2012). Most reported SWAT studies contain both calibration and validation, while others performed only calibration due to a lack of observed data (Jeffrey G. Arnold, 2012). For gauging stations Dabana near Abasina and Wama near Nekemte left only with calibration as limited data of less than 5 years are available after 1980.

After running of SWAT hydrological water balance is observed and base flow is overestimated. For Angar and Dabana calibration and validation was done with semi automated sufi-2 in SWAT-CUP without manual adjustment of biased base flow. Manual calibration attempted to minimize total flow (minimized average annual percent bias), accompanied by visual inspection of daily hydrographs and duration of daily flow curves. The sum of squares of residuals objective function could have been used in the manual calibration, but preliminary testing showed that the total mass balance method in combination with the inspection of duration of daily flow curves gave a better representation of the range of simulated flows (Van Liew et al., 2005). A preliminary calibration was conducted on a monthly basis to identify the order of magnitude of all parameters to reproduce proper runoff volumes and seasonal characteristics. Then daily calibration is succeeded to get more perfect parameter about watershed as well as to properly estimate flow volumes at necessary point or junction (figure.4-3).

Figure 4-3: location of flow-gauging stations (1= Dembi (Toba),2= Wama, 3= Arjo, 4= Dabana, 5= Angar)) respectively

Parameter values are adjusted to fit observed and simulated hydrograph. To decrease Base flow, increase deep percolation (GW_DEEP), (GWQMN), increase the groundwater revap-coefficient (GW_REVAP), and increase the threshold depth of water in shallow aquifer (REVAPMN) was done. To correct the late shift, the slope (HRU_SLP) increased, and Manning's roughness coefficient (OV_N) as well as the value of overland flow rate (SLSUBBSN) decreased.

Model calibration and validation is done depending on location of gauging stations as well as presence of available gauged discharge data. For Dembi and Arjo daily flow data of 18 consecutive years with negligible missing is used for calibration and validation. Angar near Nekemte has 10 years available data within the range of SWAT run period where as Lower Dabana and Wama have 5 years and 4 years data within the range respectively. Hence due to absence sufficient data calibration is done without validation at Dabana and Wama discharge gauging stations. Even though model performance values are not shown in table 4-4 for these two gauging stations observed flow is calibrated. The calibration statistical value is found in (table.4-4). Didesa near Arjo gauging station data are classified in to two depending on hydrological change during 2005in Didesa sub basin. This change was due to settlers Hararghe population, land clearing for sugar cane production and etc. Flow data from 1997 to 2004 and from 2007 to 2014 are used for this watershed to understand the basin characteristics within the two ranges.

Table 4-4: Model performance statistics for the Didesa Sub basin at 5 discharge gauging stations.

Time Step	Calibration	(1997-2008)	(1997-2001)	(2006-2011)	(1997-2001)
	Criterion	**Dembi**	**Arjo**	**Arjo**	**Angar**
Daily	R^2	0.66	0.74	74	0.8
	NSE	0.6	0.74	0.65	0.8
	PBIAS	-10.5	-6.1	-19.4	0.5
	RSR	0.64	0.56	0.6	0.45
	Validation	**(2009-2014)**	**(2002-2004)**	**(2012-2014)**	**(2002-2004)**
	R^2	0.70	0.70	0.64	0.62
	NSE	0.66	0.62	0.6	0.61
	PBIAS	-6	0.0	-4	-16.3
	RSR	0.59	0.61	0.66	0.68
Monthly	**Calibration**	**(1997-2008)**	**(1997-2001)**	**(2006-2011)**	**(1997-2001)**
	Criterion	**Dembi**	**Arjo**	**Arjo**	**Angar**
	R^2	0.80	0.87	0.75	0.82
	NSE	0.72	0.82	0.71	0.79
	PBIAS	-16.4	-10.5	2.5	-3.5
	RSR	0.53	0.42	0.54	0.45
	Validation	**(2009-2014)**	**(2002-2004)**	**(2012-2014)**	**(2002-2004)**
	R^2	0.86	0.89	0.82	0.92
	NSE	0.83	0.84	0.81	0.91
	PBIAS	-13.3	-20	7.7	-13.4
	RSR	0.42	0.47	0.44	0.4

Overall, calibration and validation of the hydrological model SWAT on the Didesa sub basin at all the gauging stations yielded good results in terms of NSE, PBIAS, RSR and R^2 for both daily and monthly time steps. In both daily calibration and monthly calibration returned a NSE $\geq$ 0.5 and were thus considered as behavioral. In most stations dramatically daily performance are greater than that of monthly in terms of PBIAS. Specifically, very good NSE and R^2 values were obtained and were greater than 0.75 for the best simulations of monthly basis. Moreover, it can be noticed that the performance is slightly lower for daily calibration compared to monthly calibration. Only one station i.e. Arjo showed low performance with a PBIAS of -20 even though NS and R^2 are very good on monthly basis. The water balance prediction can be considered as accurate at a daily time-step but becomes hardly satisfactory for monthly calibration, which is characterized by higher PBIAIS values showing increasing errors in the prediction. For example, the PBIAIS values increased from daily to monthly time intervals for both calibration validations, for all stations: Furthermore, since average of data is simulated on monthly time step, it is not good as daily time step in water balance prediction at necessary junction to estimate flow for

design purpose. With regard to high flow events, visual analysis of simulated and observed hydrographs represented in figure came out with the following results: timing of peak is well reproduced although the simulation tends to overestimate peak flows especially during wet season of the years for Arjo. For the left watersheds flow is well reproduced for both wet and dry season.

a)

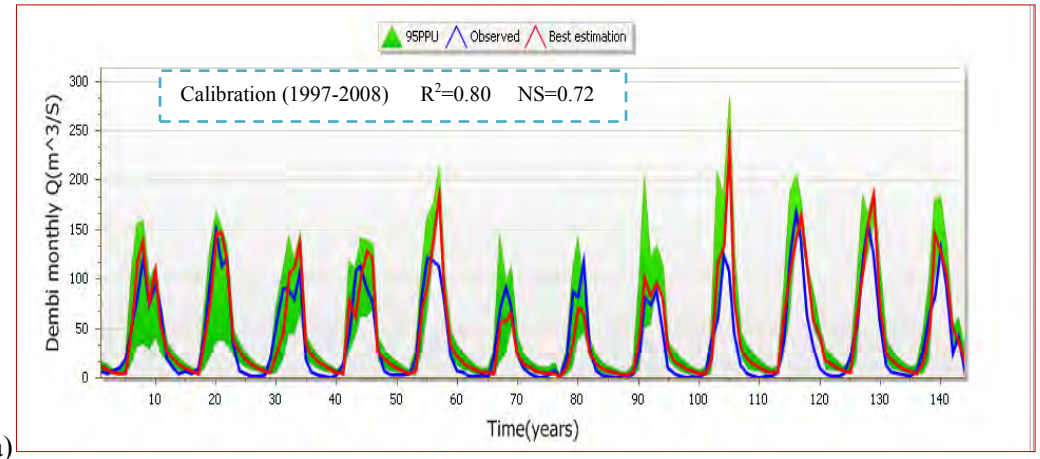
95PPU
Observed
Best estimation
Calibration (1997-2008) R²=0.80 NS=0.72
Dembi monthly Q(m^3/S)
Time(years)

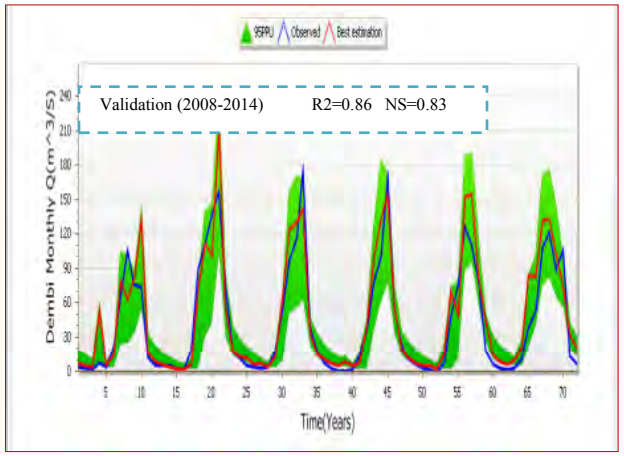
95PPU
Observed
Best estimation
Validation (2008-2014) R2=0.86 NS=0.83
Dembi Monthly Q(m^3/S)
Time(Years)

b)

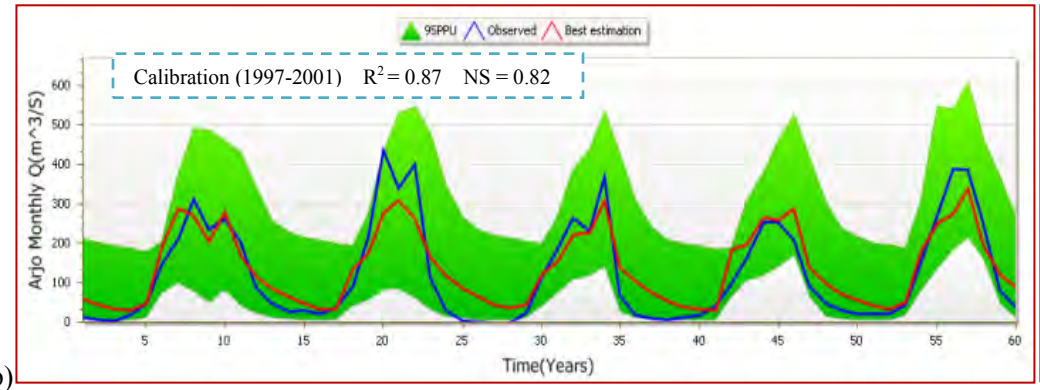
95PPU
Observed
Best estimation
Calibration (1997-2001) R² = 0.87 NS = 0.82
Arjo Monthly Q(m^3/S)
Time(Years)

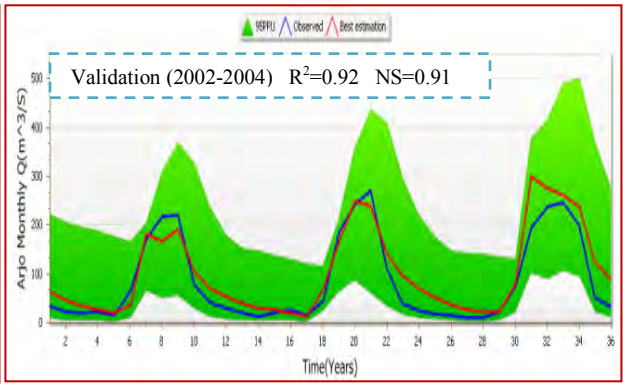
95PPU
Observed
Best estimation
Validation (2002-2004) R²=0.92 NS=0.91
Arjo Monthly Q(m^3/S)
Time(Years)

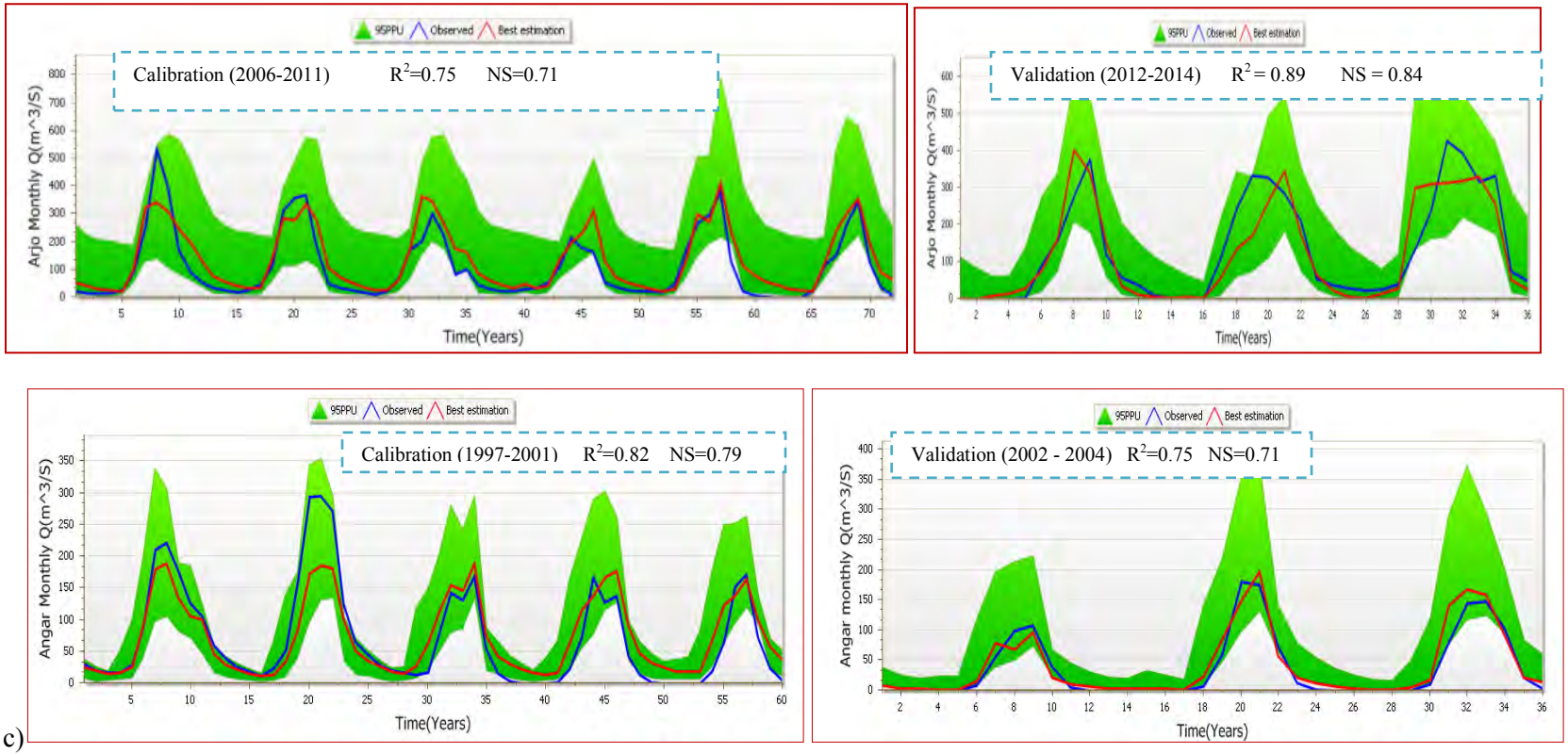

Figure 4-4:Monthly Simulated and observed hydrographs at the 5 gauging station (a) Dembi calibration and validation,(b) Arjo calibration and validation and,(c) Angar calibration and validation at monthly time steps.

a)

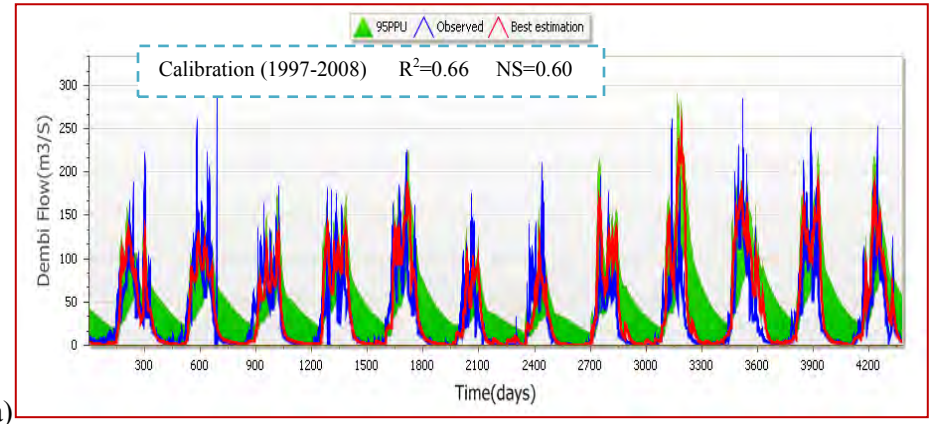
95PPU
Observed
Best estimation
Calibration (1997-2008) R^2=0.66 NS=0.60
Dembi Flow(m3/S)
Time(days)

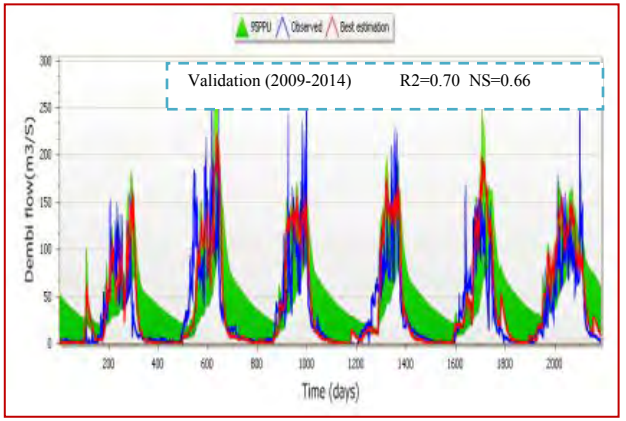
95PPU
Observed
Best estimation
Validation (2009-2014) R2=0.70 NS=0.66
Dembi flow(m3/S)
Time (days)

b)

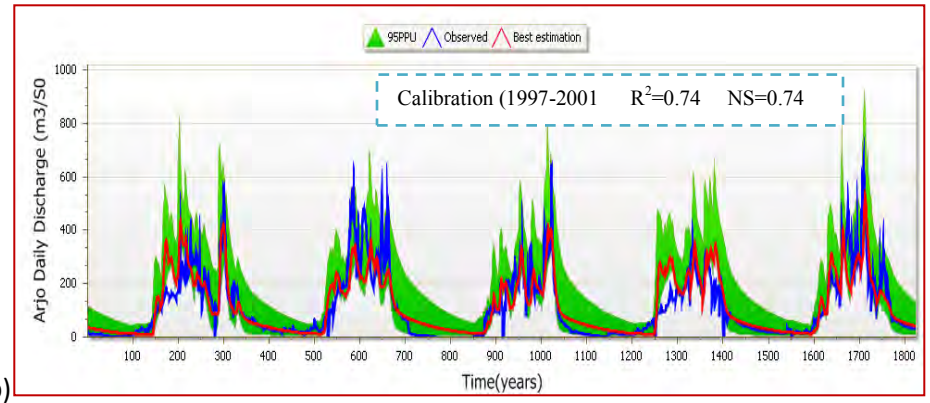
95PPU
Observed
Best estimation
Calibration (1997-2001 R^2=0.74 NS=0.74
Arjo Daily Discharge (m3/S0
Time(years)

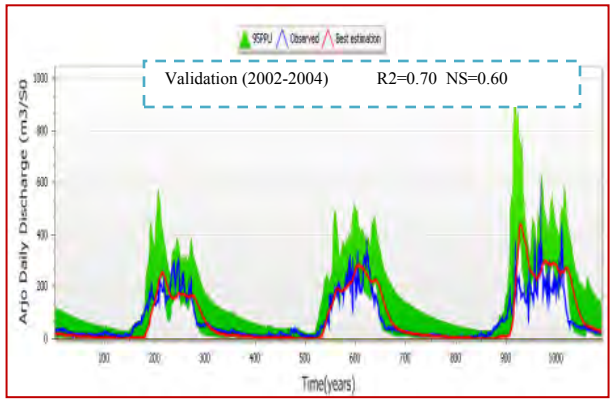
95PPU
Observed
Best estimation
Validation (2002-2004) R2=0.70 NS=0.60
Arjo Daily Discharge (m3/S0
Time(years)

b)

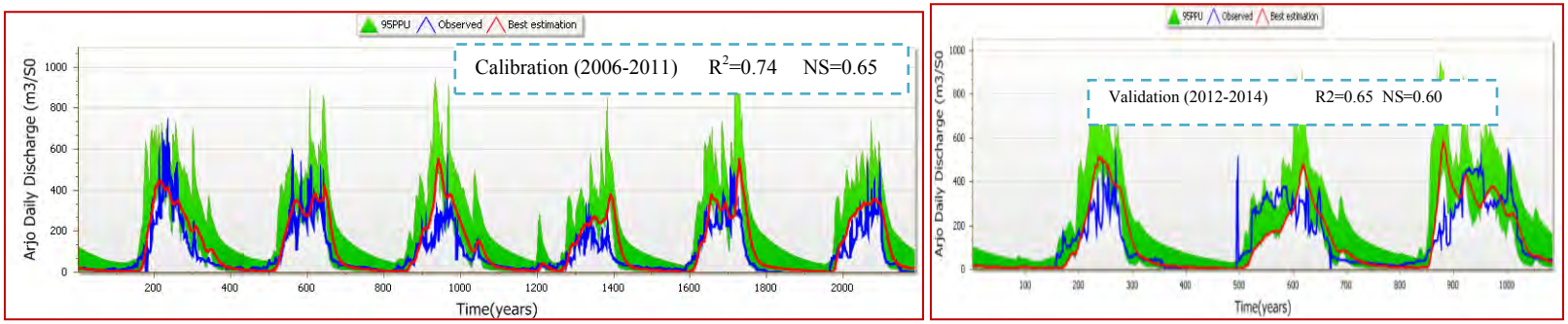

c)

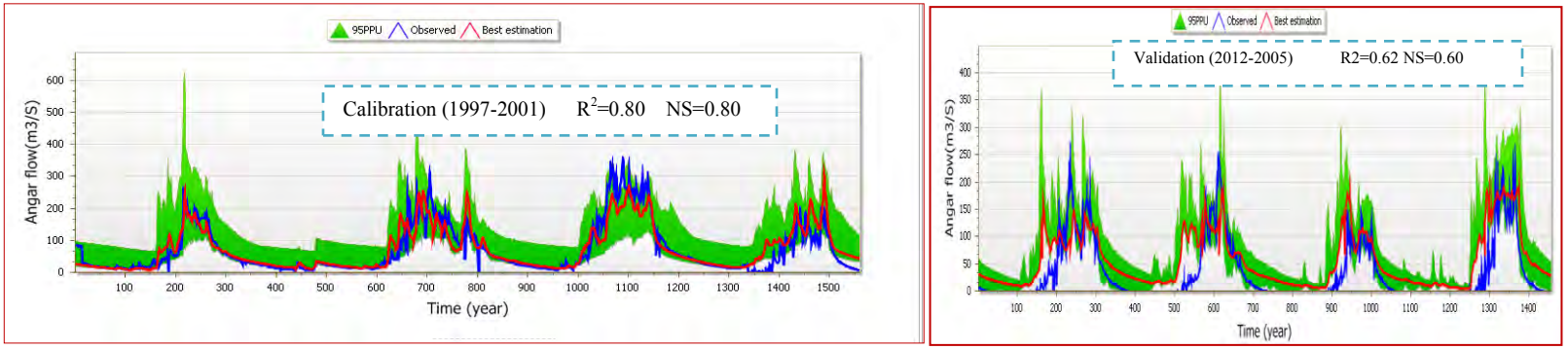

Figure 4-5:Daily Simulated and observed hydrographs at the 5 gauging station (a) Dembi calibration and validation,(b) Arjo calibration and validation ,and (c) Angar calibration and validation at daily time steps

4.4. Sensitivity Analysis

4.4.1. Purpose of sensitivity Analysis

The purpose of sensitivity analysis is to identify the parameters that have the greatest influence on model results (Feyereisen, G. et al, 2007). The division of parameters into various degrees of sensitivity is subjective. There are a few methods available in assessing a sensitivity of input parameters in hydrological models. In SWAT model, input parameters can be either manually adjusted in the SWAT model or can be accessed in the SWAT-CUP. SWAT-CUP is a computer program for calibration of SWAT models and the programs link SUFI-2 algorithms to SWAT. It enables sensitivity analysis, calibration, validation, and uncertainty analysis of SWAT models. In manual sensitive parameter identification for balancing biased base flow adjustment: RCHRG_DP,GW_REVAP,SOL_AWC, SOL_K and ESCO were found to be the most important parameters those play crucial role to estimate water balance ratio.

4.4.2. Dotty plots

Dotty plots command show the dotty plots of all parameters. These are plots of parameter values vs objective function. The main purpose of these graphs is to show the distribution of the sampling points as well as to give an idea of parameter sensitivity. Dotty plots for Dembi watershed is shown as an example in Figure 4-6. The X-axis ranges of calibration parameters where, the Y-axis is objective function (Nash-Sutcliffe Efficiency).

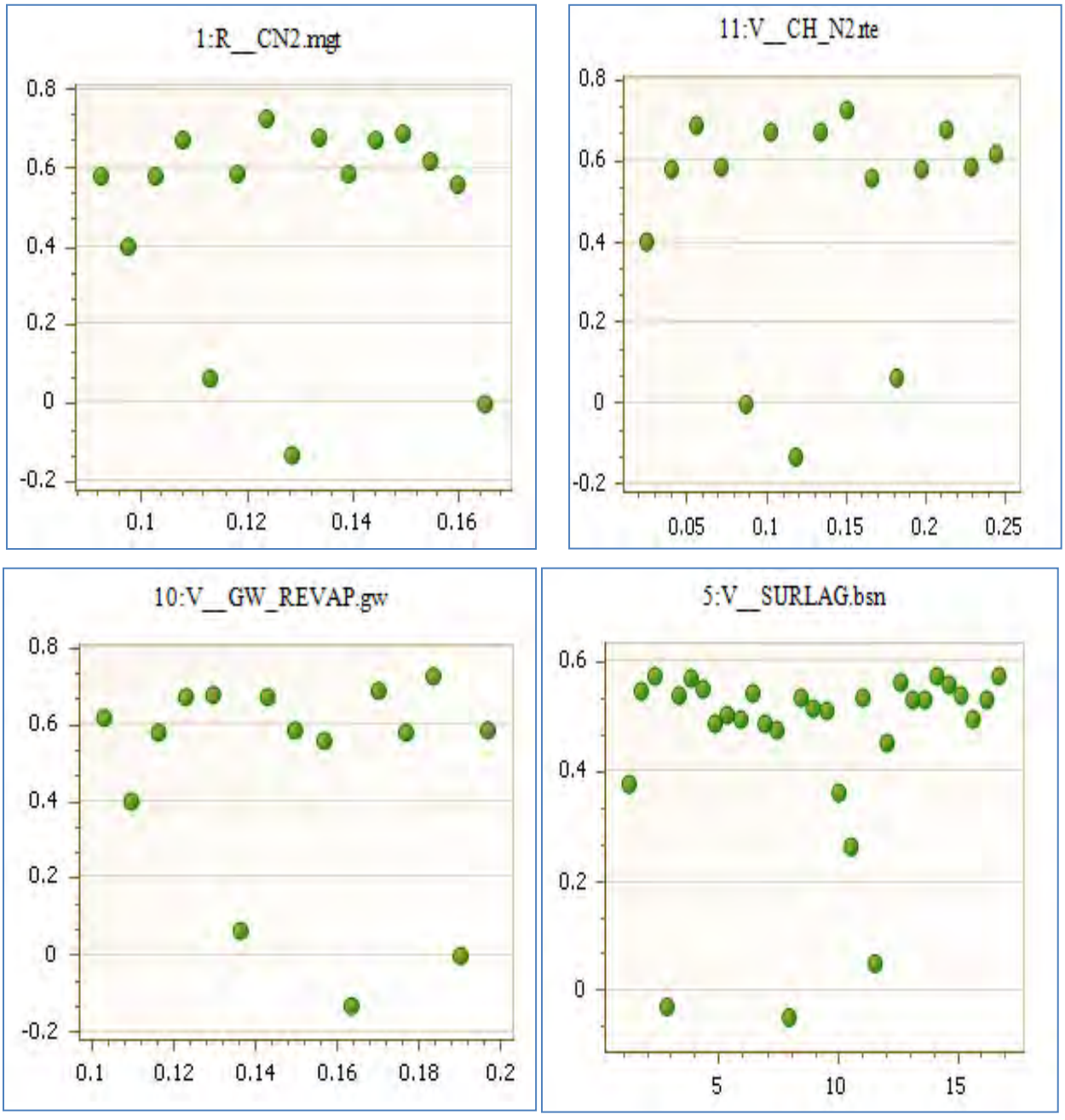

Figure 4-7: Plots showing most identified sensitive parameters during monthly calibration in Sufi-2 in SWAT-CUP

4.4.3. Global sensitivity Analysis

The global sensitivity of stream-flow parameters has been calculated using Latin hypercube regression systems. The parameters have given ranks for their sensitivity to the model calibration for both procedures (Table 4-5). The most sensitive parameters recorded after sensitivity analysis for daily calibration in SUFI-2 procedures are shown in table 4-5. The sensitive parameters are similar to those found by (D. T. Mengistu[1,2] and A. Sorteberg[2,3],2012) sensitive parameters for Abbay basin. Out of 19 selected parameters the curve number, available water capacity, average slope steepness, saturated hydraulic conductivity, ground water revaporation coefficient, threshold water depth in the shallow aquifer for flow, and base flow alpha factor were identified as being parameters to which the flow has medium to high sensitivity. New sensitive parameters those can affect flow are Manning's "n" value for the main channel (CH_N2), Lateral flow travel time (LAT_TIME), and Manning's "n" value for overland flow (OV_N) were gotten. The ranking of the parameters were different at various outlets where sensitivity test was carried out. However the curve number (CN2) was the main sensitivity parameter for all outlets.

Table 4-5:Parameters' sensitivity level

PARAMETER	Sensitivity Rank									
	DEMBI		ARJO		ANGAR		DABANA		WAMA	
	P-value	Rank	P-value	Rank	P-value	Rank	P-value	Rank	P-value	Rank
ALPHA_BF	0.51	8	0.27	4	0.42	6	0.73	14	0.56	10
ALPHA_BNK.	0.03	1	0.47	9	0.84	16	0.89	15	0.28	6
CH_K2	0.53	11	0.15	3	0.35	4	0.27	2	0.33	7
CH_N2	0.13	2	0.88	18	0.35	5	0.58	12	0.51	9
CN2.mgt	0.571	13	0	1	0.32	3	0.51	8	0.09	1
EPCO	0.4	6	0.82	14	0.61	10	0.96	17	0.72	13
ESCO	1	19	0.53	10	1	19	1	19	0.94	17
GW_DELAY	0.82	16	0.87	17	0.55	9	0.5	7	0.79	14
GW_REVAP	0.131	3	0.78	13	0.71	12	0.4	5	0.6	11
GWQMN	0.63	15	0.82	15	0.19	1	0.54	9	0.6	12
HRU_SLP	0.511	9	0.57	11	0.86	18	0.04	1	0.11	2
LAT_TTIME	0.57	12	0.13	2	0.54	8	0.57	11	0.18	3
OV_N	0.52	10	0.95	19	0.3	2	0.56	10	0.21	4
RCHRG_DP	0.61	14	0.41	8	0.72	13	0.92	16	0.61	18
REVAPMN	0.94	17	0.27	5	0.81	14	0.34	3	0.86	15
SLSUBBSN	0.45	7	0.57	12	0.81	15	0.5	6	0.96	19
SOL_AWC	0.96	18	0.33	7	0.84	17	0.6	13	0.24	5
SOL_K	0.38	5	0.85	16	0.51	7	0.37	4	0.91	16
SURLAG	0.3	4	0.28	6	0.69	11	0.99	18	0.34	8

- SCS runoff curve number (CN2) was found to be the most sensitive parameters for a Arjo watershed. The finding was observed agreed to a first input parameter need to be adjusted using SWAT manual calibration flowchart as conducted by previous researchers. Other two most sensitive input parameters were a Lateral flow travel time (LAT-TIME) and Effective hydraulic conductivity in main channel alluvium (CH_K2).
- Base flow alpha factor for bank storage (ALPHA_BNK) was found to be the most sensitive parameter for Dembi watershed. While both (Manning's "n" value for the main channel) CH_N2 and Groundwater re-evaporation coefficient (GW_REVAP) found to take second and third rank for this watershed respectively.
- Next Average slope steepness (HRU_SLP), Effective hydraulic conductivity in main channel alluvium (CH_K2), and Threshold depth of water in the shallow aquifer for revaporation to occur (REVAPMN) were found to the most sensitive parameters for Dabana watershed.
- Furthermore, SCS runoff curve number (CN2) found to be the most sensitive parameters for Wama watershed like Arjo watershed. Average slope steepness (HRU_SLP), and Lateral flow travel time (LAT_TIME) are the second and the third sensitive parameters those are found through sensitive analysis.
- Lastly, Threshold depth of water in the shallow aquifer required for return flow to occur (GWQMN), Manning's "n" value for overland flow (OV_N), SCS runoff curve number (CN2) were found the most sensitive parameters for Angar watershed.

4.4.4. Optimum Parameter estimate

After calibration best parameters are found Best_par.txt in Sufi-2. These file shows the" best parameter" values as well as their ranges. These are the parameters, which gave the best objective function values in the current iteration. The fitted value of these best parameters can really explain the mineral characteristics of the sub basin. For Arjo, Wama, and Dembi since base flow is over estimated manual calibration is needed increase, Sol-AWC close 0.4m/m, decrease ESCO close 0.002 to increase soil Evapo-transpiration which shows properties of vegetation land before calibration was done in SWAT CUP. Soil saturated hydraulic conductivity (mm/hr) is all kept 5 for reach along Didesa main line. And all 19 parameters are estimated for the six watersheds in Didesa sub basin both on daily basis in semi automated Sufi-2 and the best value is given in table 5-3. Ground water flow into main channel increases

when ALPHA_BF increases. It was highest for Dabana and Angar watershed when compared to other watersheds.

Effective hydraulic conductivity in main channel alluvium (CH_K2) (mm/hr) is highest for Arjo, Wama, and Dabana watersheds in consecutive order. High effective hydraulic conductivity in main channel alluvium (CH_K2) (mm/hr) means during periods when a stream receives no groundwater contributions, high water to be lost from the channel via transmission through the side and bottom of the channel.

The smaller ALPHA_BNK Coefficient is the small the water released from bank storage, means the quick the water is released from channel bank. This characteristic is seen in Dembi watershed where Water released from bank storage is very small.

The manning coefficient of the main channel (CH_N2) rules the velocity of the flow in the reaches. If the CH_N2 value gets higher, the velocity is reduced and the simulated flow will become lagged compared to the measured flow. This can be attributed to the decreasing channel velocity with higher values of CH_N2, introducing a lag in the daily model output.

Soil saturated conductivity (SOL_K) of the sub basin is found to be in the range of 4 to 6 mm/h. To account for different soils' ability to infiltrate, NRCS has divided soils into four hydrologic soil groups (HSGs). So HSG Group B fits the sub basin soil group because these soils have a moderate rate of water transmission (final infiltration rate of 3.81 to 7.62mm./h). Soils with moderate infiltration rates when thoroughly wetted. These consist chiefly of soils that are moderately deep to deep, moderately well drained to well drained with moderately fine to moderately coarse textures.

As we can see from hydrological water balance, flow is surface flow dominated. Hence, It is best idea to find what are the dominant parameter those affects surface flow to be highest? The average value of CN_2 of the sub basin lies between 75 and 82. The value of saturated soil conductivity can also affect ground water flow. Consequently this maximum value of CN2 and moderate conductivity SOL_K indicates flow to be surface flow dominated.

As value of ESCO is very small means evaporative demand for soil layer is very high for each watershed.

PARAMETER	Optimum Value of Parameters and Their Sensitivity Rank											
	DEMBI		ARJO(1997-2004)		ARJO(2006-2014)		ANGAR		DABANA		WAMA	
	BEST VALUE	Rank	BEST VALUE	Rank	BEST VALUE	Rank	BEST VALUE	Rank	BEST VALUE	Rank	BEST VALUE	Rank
V_ALPHA_BF	0.45	8	0.357	4	0.511	4	0.721	6	0.741	14	0.545	10
V_ALPHA_BNK	-0.01	1	0.745	9	0.327	9	0.457	16	0.175	15	0.755	6
V_CH_K2	125.68	11	488.78	3	309.204	3	285.0	4	451.31	2	486.2	7
V_CH_N2	0.273	2	0.191	18	0.056	18	0.389	5	0.276	12	0.213	9
R_CN2	0.11	13	0.124	1	0.15	1	0.107	3	0.153	8	0.1	1
V_EPCO	0.062	6	0.529	14	0.213	14	0.042	10	0.11	17	0.103	13
V_ESCO	0.002	19	0.001	10	0.003	10	0.0022	19	0.0023	19	0.0021	17
V_GW_DELAY	0.01	16	0.604	17	0.234	17	-0.001	9	0.01	7	0.005	14
V_GW_REVAP	0.199	3	0.183	13	0.17	13	0.181	12	0.177	5	0.179	11
V_GWQMN	3044.64	15	4850	15	4616.7	15	1683.72	1	3705.5	9	4596.8	12
R_HRU_SLP	-0.871	9	0.784	11	-0.112	11	0.287	18	0.196	1	-0.665	2
V_LAT_TTIME	5.934	12	12.643	2	28.4	2	4.957	8	5.217	11	1.141	3
V_OV_N	6.237	10	7.426	19	5.776	19	1.502	2	1.577	10	6.718	4
V_RCHRG_DP	0.258	14	0.222	8	0.124	8	0.422	13	0.265	16	0.832	18
V_REVAPMN	147.78	17	299.45	5	125.7	5	149.06	14	303.0	3	485.9	15
V_SLSUBBSN	123.12	7	87.891	12	169.2	12	57.057	15	123.0	6	91.9	19
R_SOL_AWC	-0.049	18	-0.101	7	0.025	7	0.356	17	0.052	13	0.077	5
R_SOL_K	-0.136	5	0.009	16	0.121	16	0.166	7	0.038	4	-0.02	16
V_SURLAG	16.74	4	20	6	10.4	6	4.711	11	6.258	18	12.5	8

Table 4-6: Optimum SWAT model parameters for 5 catchments

4.5. Flow Hydrograph

Flow Hydrograph at Junctions as shown (fig. 5-7) was prepared based on parameters found in calibration and validation at each hydro gauging station. SWAT is rerun to find flow from each watershed at three junctions or confluence. Discharge (m^3/s) is filtered at each junction from SWAT output of reach data base: Junction 1(Dembi watershed and Wama watershed confluence), junction 2(Arjo watershed and Dabana watershed confluence), junction 3(Angar watershed and Arjo Didesa watershed confluence). (And out flow hydrograph (m^3/s) from 1982 to2014 on daily basis for Dembi, Wama, Dabana, Arjo Didesa and Angar sub basin are estimated are shown in figure 4-8.

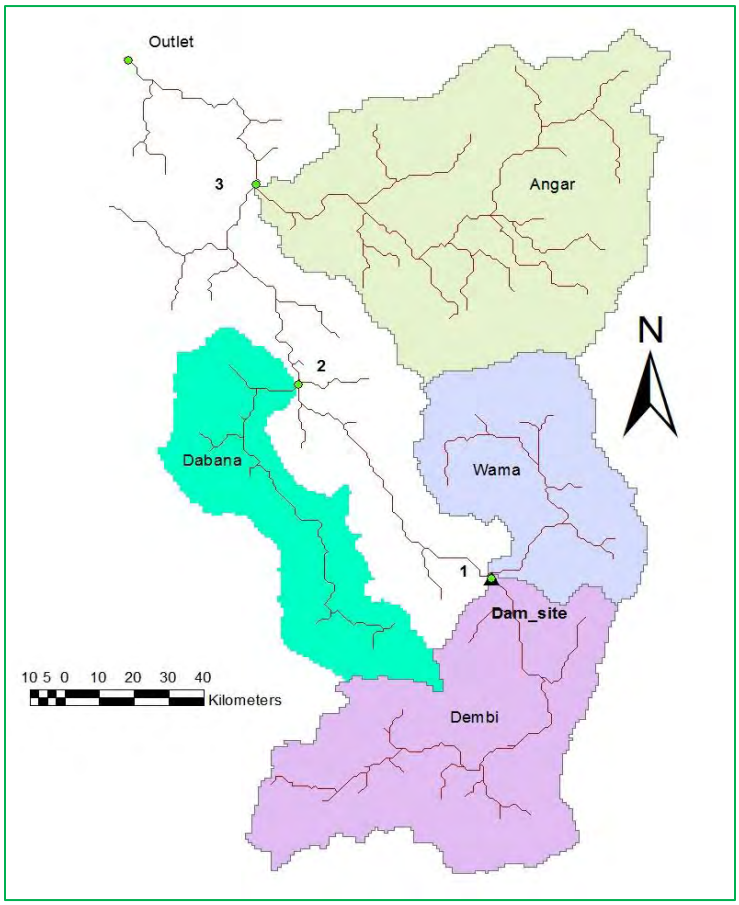

Figure 4-8: Map to show points or junction at which flow is estimated (Junction 1=Dembi and Wama confluence, 2=Dabana and Didesa confluence, 3=Arjo Didesa and Angar confluence)

The dam for Arjo-Didessa Irrigation Development Project is being constructed at about 1.5 km upstream of the confluence of Wama and Upper Didessa rivers. The dam site drains a catchment area of about 5,536.0 km^2. The mean annual flow at the dam site is about 84.6 m3/s (total of 3.03 BCM), a sub - watershed average of about 482.55 mm. It can be observed that there is variability in water yield between the tributary watersheds and the basin average. This may be due to the differences in catchment behavior (land use/land cover, soil types and relief).

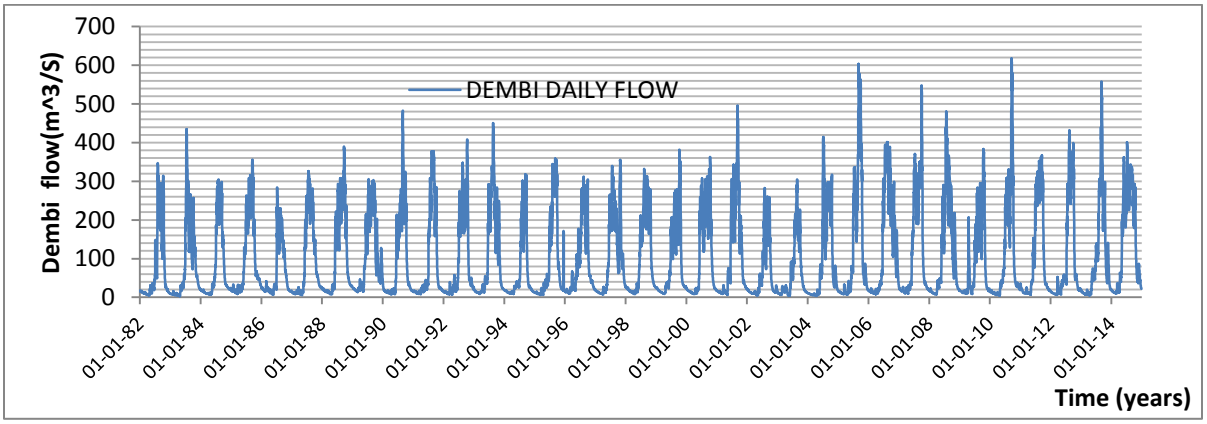

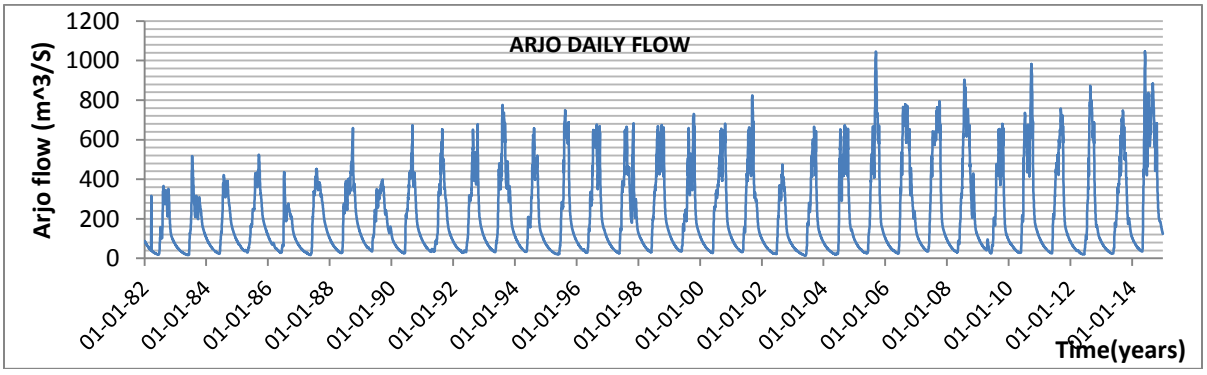

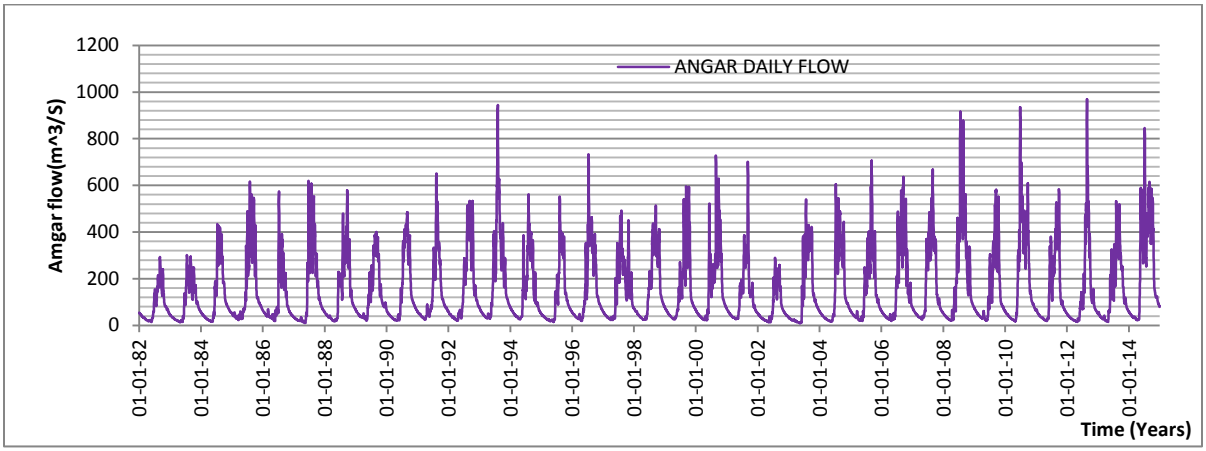

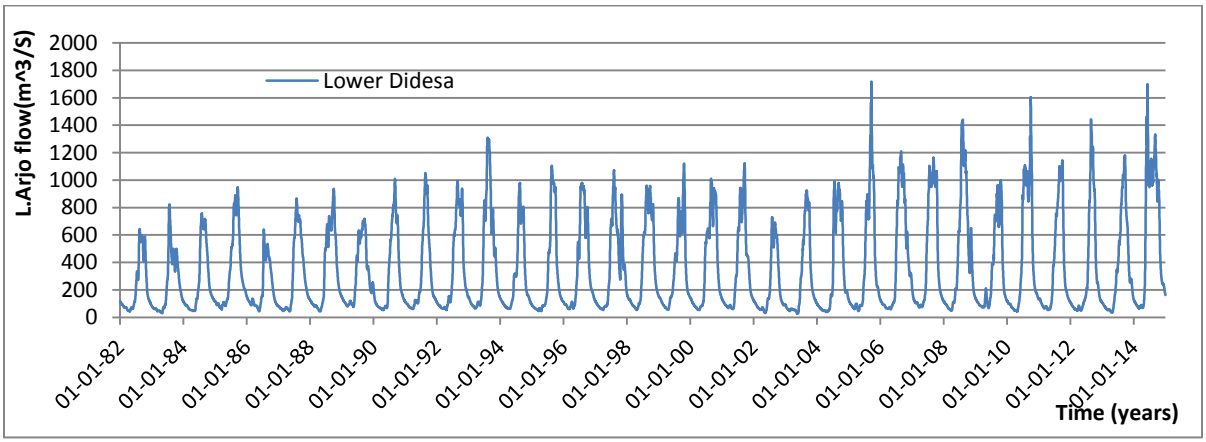

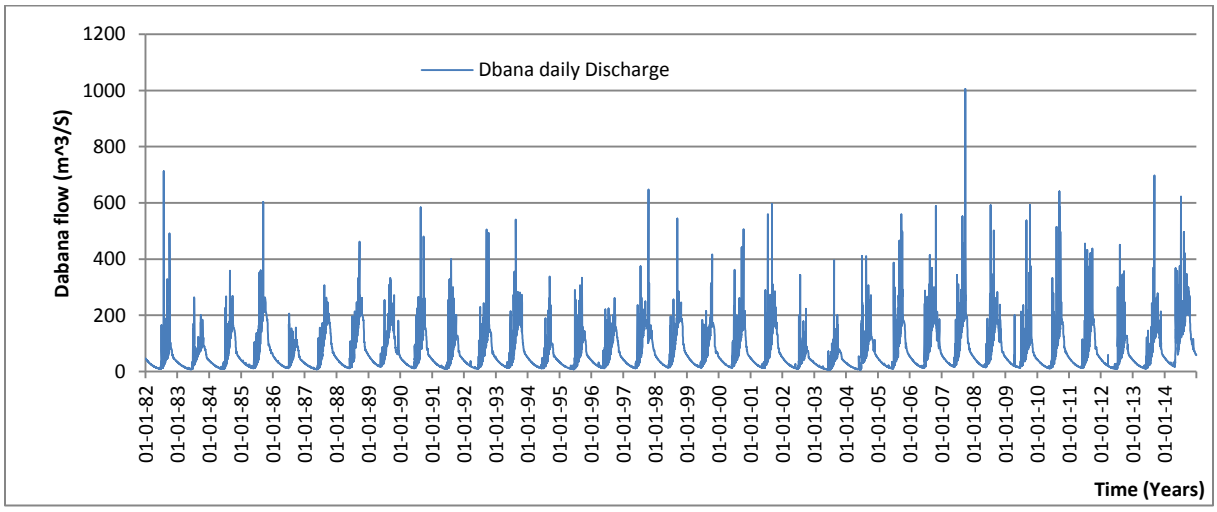

Figure 4-9: Daily flow Hydrograph

4.6. Hydrological Characteristics of Didesa Sub basin

After including DEM, soil and land use map, the HRUs are defined for each watershed. Following the evaluations of Setegn (2008) threshold is defined for HRU definition. The thresholds determine beyond which percentage of land use within a sub basin, the land use is accounted for in the HRU generation. Likewise this holds for soil within land use class and slope within soil class. Area of watershed, for each watershed: Threshold, number of HRUs and number of sub basin generated by ArcSWAT are shown in table 4-7.

Table 4-7: Simulation details of SWAT model set-up for Arjo Didesa Sub basin

WATERSHED	AREA	NO. OF SUBASIN	THRESHOLD	NO. OF HRUs	Simulation length (years)	Warm up (years)
Dembi	5532.1	27	15/15/10	191	35	2
Arjo	11358.1	47	15/15/10	348	35	2
Dabana	3246.4	13	15/15/10	98	35	2
Wama	3336.8	13	15/15/10	94	35	2
Angar	7988.2	28	10/10/5	284	35	2
Lower Didesa	17791.8	78	10/10/10	760	35	2

4.6.1. Land use Characteristics

According to MERIS, 2009 land use map, most of Didesa sub basin is entirely covered with vegetation. More than 60 % of Dembi watershed is covered with mixed crop land and the left is enclosed with shrub or bush and mosaic range land. About 70% of Arjo watershed is shaded with agricultural land and mostly grasslands, whose plants can provide food (i.e., forage) for grazing or browsing animals. In addition, about 60% of Dabana watershed is covered with crop land and shrub land. This watershed has high percentage of deciduous forest comparing to other watersheds. Furthermore, about 60% of Wama watershed is covered with mixed vegetation. Angar and Lower Arjo Didesa are related in land use; both have almost similar vegetation, crop land and shrub land. These land use categories are substituted with equivalent land use those are found in SWAT database as given in table 4-8 below.

Table 4-8: characteristics of land use

Land-use category	LU-Swat	Watershed area (%) Covered					
		Dembi	Arjo	Dabana	Wama	Angar	L/Didesa
Mosaic Croplands/Vegetation	RNGE	24.91	38.96	8.48	61.63	29.07	29.76
Mosaic Vegetation/Croplands	AGRR	61.14	35.36	38.37	4.95	24.55	29.52
Closed to open broadleaved evergreen or semi-deciduous forest	FRSE	0.60	0.94	4.00	0	1.61	3.17
Open broadleaved deciduous forest	FRSD	0	0.52	21.77	0	13.03	11.68
Closed to open Shrub land	RNGB	13.35	24.23	27.38	33.42	31.73	25.86

4.6.2. Soil Characteristics

Using Soil geo-database of Ethiopia' prepared by (Belete B.,et al,2013), more than 75% of the sub basin is enclosed with Humic Nitosols which is loam in textural class of soil. Loam is soil that is good for growing crops and plants in because it contains a lot of decayed vegetable matter and does not contain too much sand or clay. For this reason, each watershed in this sub basin has soil with good infiltration rate which is preferred for agriculture with comparing to other soil type.

Table 4-9: characteristics of soil in Didesa sub basin

Soil category	Watershed area (%) Covered					
	Dembi	Arjo	Dabana	Wama	Angar	L/Didesa
Humic Nitisols	76.18	78.2	79.34	81.85	80.8	75.25
Dystric Leptosols	0	0	0	0	0	4.08
Haplic Nitisols	0	0	13.75	0	0	4.42
Humic Alisols	15.87	9.62	0	6.64	1.86	6.95
Eutric Vertisols	7.95	12.18	0	11.51	0	7.98
Lithic Leptosols	0	0	6.91	0	0	1.32
Haplic Phaeozems	0	0	0	0	8.65	0
Vertic Cambisols	0	0	0	0	0.97	0
Haplic Alisols	0	0	0	0	3.15	0
Eutric Cambisols	0	0	0	0	20.3	0
Rendzic Leptosols	0	0	0	0	2.53	0
TOTAL	100	100	100	100	100	100

4.6.3. Slope Characteristics

This watershed is known with gentle slope. More than 55% of each watershed of Didesa sub basin is spatially distributed with slope of 0% up to 5%. The upper limit of gradient in this sub basin is 36.6% (figure 3-4). Hence, most area of this sub basin is suitable for surface irrigation.

Table 4-10: characteristics of Slope

	Watershed area (%) Covered					
slope class(deg.)	Dembi	Arjo	Dabana	Wama	Angar	L/Didesa
0-5	57.35	56.8	68.15	59.76	56.8	59.56
5 to 10	34.60	32.16	28.33	32.06	32.16	31.32
10 to 20	8.05	10.49	3.52	8.17	10.49	7.09
>20	0.0	0.54	0.0	0.0	0.54	2.03

4.6.4. Water Balance of Didesa Sub Basin

Water balance analysis of the sub basin is done with a given land use. In addition the calibrated parameters are reinserted during ArcSWAT run for each watershed to get appropriate balance. This type of analysis has historically been used to obtain an understanding of the overall hydrologic response of an area or watershed. While not generally being overly detailed, the analysis gives a basic understanding of the rainfall-runoff relationship over a long term planning period (e.g., seasonal or yearly). The outcome of such an analysis allows for the general breakdown of the components and their percentages which go into defining runoff from a site, surface and subsurface. A typical water balance analysis will compare meteorological input data to a measured (or transferred) set of flow data within the receiving stream. The flow data along with typical estimates of Evapotranspiration losses and the input meteorological information allows for breakdown of each component and a determination of infiltration, base flow and the surface flow components of individual site water balance. This information can assist in determining the potential sensitivities of the watershed to alteration features which may affect these functions (e.g., land use change, climate change). The general hydrological water balance and hydrological parameters estimated and tabulated in table 4-11.

Table 4-11: Hydrological water balance ratio and hydrological parameters

Hydrology (water balance ratio)	Dembi	Arjo	Dabana	Wama	Angar	L/Didesa
Stream flow/precipitation	0.21	0.2	0.28	0.15	0.20	0.22
Base flow/total flow	0.21	0.28	0.27	0.32	0.39	0.4
Surface run-off/total flow	0.79	0.72	0.73	0.68	0.61	0.60
Percolation/precipitation	0.28	0.34	0.29	0.36	0.35	0.30
Deep recharge/precipitation	0.07	0.13	0.08	0.3	0.15	0.11
ET/precipitation	0.55	0.51	0.50	0.48	0.52	0.52

Hydrological parameters (all units in mm)	Dembi	Arjo	Dabana	Wama	Angar	L/Didesa
Average curve number	82.11	79.06	80.41	75.65	75.46	76.8
ET and transpiration	964.5	951.7	932.8	961.5	860.3	960.0
Precipitation	1740	1862.9	1861.7	1990.2	1669.9	1850.6
Surface run-off	287.4	264.71	376.41	209.1	204.5	245.8
Lateral flow	3.37	5.2	13.42	98.92	17.66	91.1
Return flow	74.9	95.24	124.6	0.0	115.14	71.9
Percolation to shallow aquifer	482.36	638.18	537.97	716.7	586.03	551.6
Recharge to deep aquifer	117.21	247.04	142.29	596.3	75.46	196.6
Revaporation from shallow aquifer	238.19	224.78	230.9	128.3	247.07	227.3

4.6.4.1. Stream flow at the Dry and wet Season

Average monthly basin rainfall, Evapo-transpiration, surface flow, Potential Evapo-transpiration and average basin yield is obtained From ArcSWAT output. From this out put one can understand hydrological characteristics of the basin in terms of months with high and minimum surface and base flow. To easily understand the output hydrological property, it is better to divide output results into two seasons which are wet and dry has been used in this study. Hence according to the total amount of rainfall, dry season stands for all months between November and April and the Wet season refers to May to October. In addition the long term average monthly stream flow is lowest in April and highest in August. See figure 4-10. And highest rainfall is simulated from June to September. Season of heavy rainfall is known by high surface runoff and high water yield. Average monthly rainfall (mm), Surface flow (mm), and average monthly water yield (mm) are shown on Primary X-axis and y-axis whereas average monthly Potential Evapotranspiration (mm) and actual Evapotranspiration (mm) are shown on secondary x-axis and y-axis.

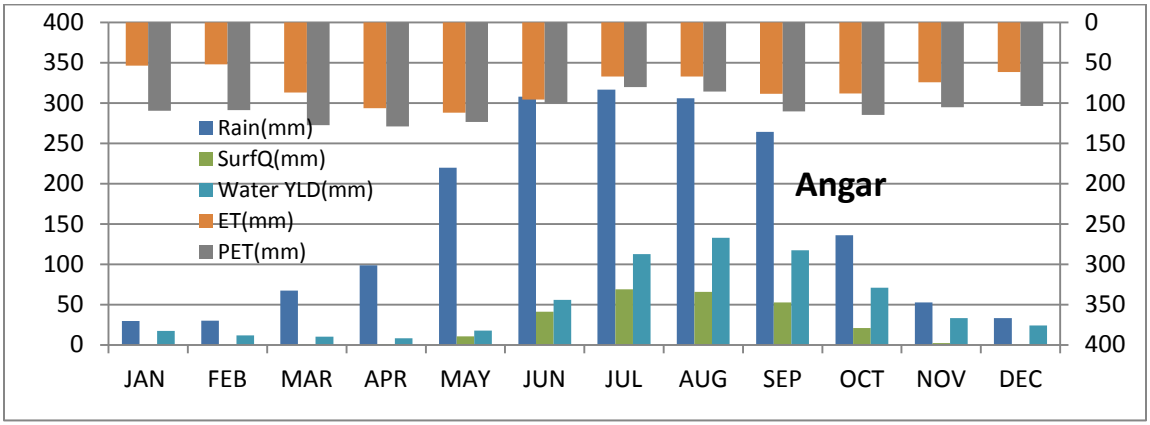
Rain(mm)
SurfQ(mm)
Water YLD(mm)
ET(mm)
PET(mm)
Angar
400
350
300
250
200
150
100
50
0
0
50
100
150
200
250
300
350
400
JAN FEB MAR APR MAY JUN JUL AUG SEP OCT NOV DEC

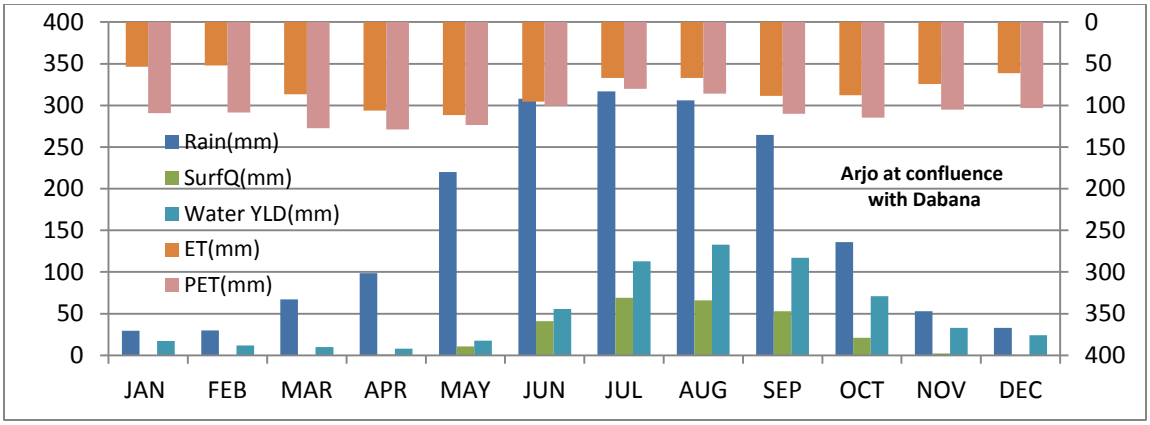
Rain(mm)
SurfQ(mm)
Water YLD(mm)
ET(mm)
PET(mm)
Arjo at confluence with Dabana
400
350
300
250
200
150
100
50
0
0
50
100
150
200
250
300
350
400
JAN FEB MAR APR MAY JUN JUL AUG SEP OCT NOV DEC

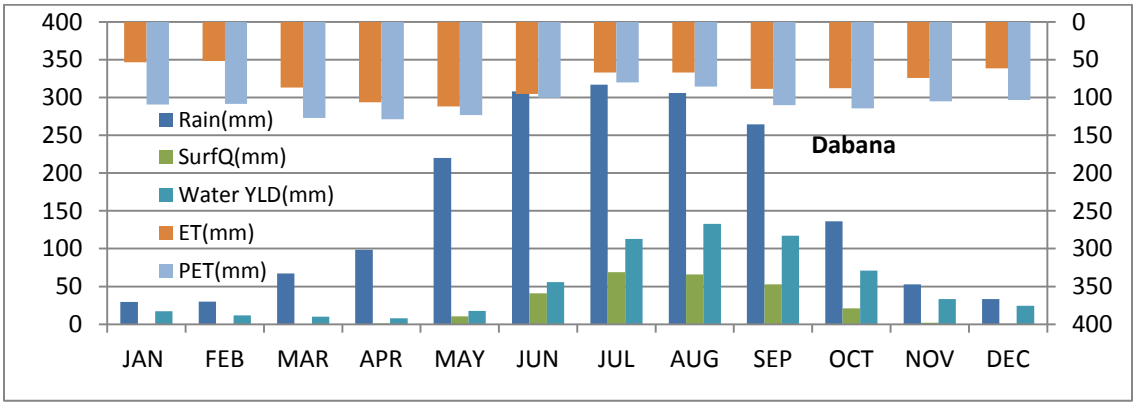
Rain(mm)
SurfQ(mm)
Water YLD(mm)
ET(mm)
PET(mm)
Dabana
400
350
300
250
200
150
100
50
0
0
50
100
150
200
250
300
350
400
JAN FEB MAR APR MAY JUN JUL AUG SEP OCT NOV DEC

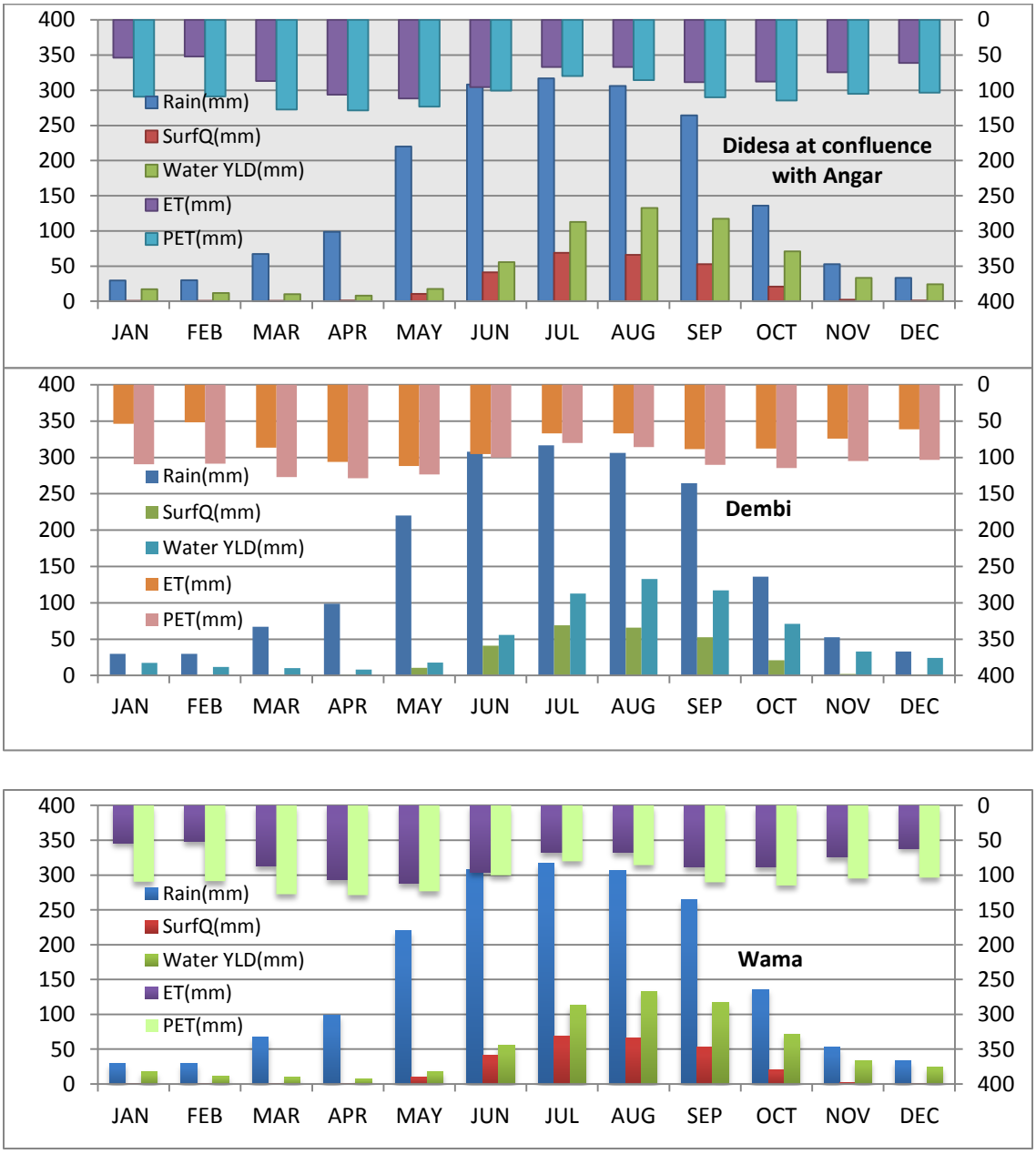

Figure 4-10: Average monthly Rainfall, Evapotranspiration, Surface runoff, Potential Evapotranspiration and Water yield

Outputs of the SWAT hydrological model for Didessa Sub-basin on the water yield of the major tributaries have also been evaluated. The four major tributaries of Didessa River are Anger, Dabena, Wama and Dembi.

In terms of size of the catchment area and contribution to the total runoff of Didessa River, Anger Sub – watershed stands first among the tributary watersheds of the sub-basin. The mean annual rainfall in Anger Sub-watershed is about 1670 mm, and the mean annual runoff is about 265 mm (lower than the figure reported by Awulachew, et al. (2008). Hence, the runoff coefficient is 0.12. Anger Sub-watershed contributes an annual total water yield of 4.46 BCM (i.e, about 8% of the total flow of Abbay River as measured at the Sudan boarder) to Didessa and thereby, Abbay.

The other important sub-watershed in Didessa Sub-basin is Dabena Sub-watershed, with a catchment area of 3246.4 km2. This watershed receives a mean annual precipitation of 1861.7 mm, with the highest Evapotranspiration rate of 932.4 mm per year. The mean annual runoff from the watershed is 376.41mm, resulting in a runoff coefficient of 0.20.

Wama is among the top important sub-watersheds in terms of share in Didessa Sub-basin's annual runoff volume. It drains a catchment area of about 3336.8km2. It receives a mean annual rainfall of 1990.2 mm (the highest among Didessa Sub-watersheds) and the mean annual runoff is about 209.11 mm. Hence, the average runoff coefficient in the watershed is 0.11.

The mean annual rainfall in Dembi Sub-watershed, the reach of Didessa River upstream of its confluence with Wama River, is about 1740 mm, and the mean annual runoff is about 287.4 mm, resulting in a coefficient of runoff of 0.17. It drains an area of 5532.1 km2. It is an important sub -watershed where the dam and reservoir for Arjo-Didessa Irrigation Development Project, a project which is intended to develop about 80,000 ha of land through irrigation, is being constructed. The results are summarized on table 4-12.

The total flow from the sub-basin amounts to about 10.71 BCM per year accounts for about 26 % of the total estimated mean annual flow from the Abbay Basin (54.8 BMC) as measured at the Sudan boarder (Awulachew, et al, 2007).

Table 4-12: Mean Annual Water Budget of the Major Tributaries

S.No	Name. of Tributary/ Reach	Precipitation (mm)	Mean annaul Flow (m3/s)	SURQ (mm)	PET (mm)	ET (mm)	Total Annual Water Yield	
							Depth (mm)	Volume ($10^9 m^3$)
1	Dembi	1740	84.5	287.4	1404.1	964.1	482.6	3.1
2	Dabana	1861.7	67.6	376.4	1456.7	932.4	656.4	2.15
3	Wama	1990.2	86.1	209.1	1195.5	961.0	902.3	2.71
4	Angar	1669.9	147.2	204.4	1359.6	860.2	583	4.6
5	Lower Didesa	1850.6	341.2	245.8	1374.5	959.6	604.83	10.7

Comparing simulated monthly flow with Abbay master plan study of 1999, the SWAT model underestimates the monthly flow during peak for Arjo Didesa and Angar gauging station. The small difference may be the model used in estimation of flow and the data range used in Master plan study (1962 to 1992 for Didesa at Arjo, and 1960 to 1992 for Angar at Nekemte) in monthly estimation.

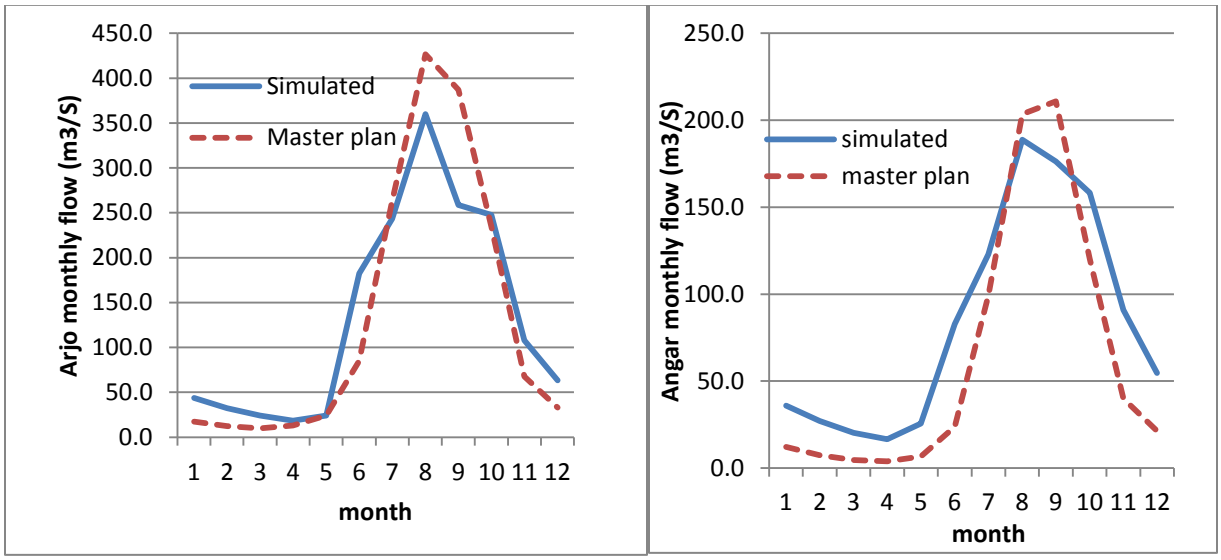

Figure 4-11:Comparision of simulated monthly flow with Abay basin master plan

4.6.4.2. Groundwater

The occurrence of subsurface water can vary according to soil type, the nature of the underlying parent material and the depth of weathering. Water may also move from the shallow aquifer up again towards the vadose zone. The amount is regulated by the groundwater revap coefficient (GW REVAP). It was found to be a large value of between 0.15 and 0.199 in order to ensure high movement from the shallow aquifer to the root zone. Deep aquifer recharge directly from the root zone can be managed by the RCHRG DP parameter. It is third component in which water is lost from the sub basin except Wama sub watershed. Namely the groundwater delay time GW_ DELAY was lowered to achieve a quick percolation of water through the soil layer reaching the shallow aquifer. There is insignificant Groundwater delay (GW_ELAY) near zero value means recession time for hydrograph is so small. Deep aquifer percolation fraction (RCHRG_DP) accounts the fourth component in which water is lost to deep aquifer except Wama watershed. The soil affecting parameters of available water content SOL_ AWC had to be risen to allow more water to be stored by the soil.

4.6.5. Frequency Analysis

4.6.5.1. Frequency rank

The frequency distribution results executed in Easy Fit analysis shows that all the watershed fit Lognormal model except Wama which is found to give good fit with Logpearson-3.Values of parameters μ, σ and γ are calculated for each watershed and the result is found in Easy fit test is tabulated in (table 4-13).

Table 4-13: Goodness of fit rank (a=Ajo at confluence with with Dabana, b=Dembi at confluence with Wama=Dabana at confluence with Didesa, d=Angar at confluence with Didesa, e=Wama at confluence with Dembi, f=Didesa at confluence with Angar)

a)

Goodness of Fit - Summary

#	Distribution	Kolmogorov Smirnov		Anderson Darling		Chi-Squared	
		Statistic	Rank	Statistic	Rank	Statistic	Rank
10	Lognormal (3P)	0.10006	1	72.757	1	672.65	4
14	Pearson 5 (3P)	0.10722	7	77.015	2	434.45	1
15	Pearson 6	0.10899	9	79.793	3	497.43	3
13	Pearson 5	0.10894	8	79.991	4	493.94	2
7	Log-Gamma	0.11111	10	91.517	5	688.7	5
16	Pearson 6 (4P)	0.1012	2	94.13	6	987.56	7
8	Log-Pearson 3	0.10472	5	99.83	7	924.27	6

b)

Goodness of Fit - Summary

#	Distribution	Kolmogorov Smirnov		Anderson Darling		Chi-Squared	
		Statistic	Rank	Statistic	Rank	Statistic	Rank
10	Lognormal (3P)	0.05486	1	26.276	1	234.49	1
8	Log-Pearson 3	0.05977	2	42.776	7	356.99	7
16	Pearson 6 (4P)	0.06066	3	32.244	2	270.12	5
7	Log-Gamma	0.0621	4	37.905	6	299.61	6
14	Pearson 5 (3P)	0.06807	5	35.192	4	267.58	3
13	Pearson 5	0.06809	6	35.027	3	266.23	2
15	Pearson 6	0.06809	7	35.382	5	269.32	4

c)

Goodness of Fit - Summary

#	Distribution	Kolmogorov Smirnov		Anderson Darling		Chi-Squared	
		Statistic	Rank	Statistic	Rank	Statistic	Rank
10	Lognormal (3P)	0.08933	2	54.165	1	371.7	1
14	Pearson 5 (3P)	0.0944	3	70.626	2	373.46	2
15	Pearson 6	0.09443	4	70.637	3	381.91	4
13	Pearson 5	0.09449	5	70.675	4	375.19	3
7	Log-Gamma	0.09789	8	74.799	5	495.22	6
16	Pearson 6 (4P)	0.10035	9	75.46	6	398.2	5
19	Weibull (3P)	0.08084	1	76.96	7	885.17	9

d)

Goodness of Fit - Summary

#	Distribution	Kolmogorov Smirnov		Anderson Darling		Chi-Squared	
		Statistic	Rank	Statistic	Rank	Statistic	Rank
10	Lognormal (3P)	0.03665	2	9.4205	1	128.93	2
16	Pearson 6 (4P)	0.04826	10	13.862	2	126.99	1
8	Log-Pearson 3	0.04199	4	16.852	3	161.59	3
6	Gen. Pareto	0.03583	1	17.153	4	N/A	
7	Log-Gamma	0.04544	5	18.072	5	183.03	5
9	Lognormal	0.04054	3	20.421	6	176.29	4
15	Pearson 6	0.04704	9	20.454	7	216.74	6

e)

Goodness of Fit - Summary

#	Distribution	Kolmogorov Smirnov		Anderson Darling		Chi-Squared	
		Statistic	Rank	Statistic	Rank	Statistic	Rank
10	Log-Pearson 3	0.05236	2	27.135	1	273.07	1
18	Pearson 6	0.061	6	28.351	2	276.25	2
11	Lognormal	0.05486	3	29.437	3	284.99	3
12	Lognormal (3P)	0.06002	5	30.125	4	305.06	4
19	Pearson 6 (4P)	0.0628	7	35.371	5	331.98	5
7	Gen. Extreme Value	0.06649	8	36.61	6	341.43	6
17	Pearson 5 (3P)	0.05999	4	36.676	7	344.78	7

f)

Goodness of Fit - Summary

#	Distribution	Kolmogorov Smirnov		Anderson Darling		Chi-Squared	
		Statistic	Rank	Statistic	Rank	Statistic	Rank
10	Lognormal (3P)	0.10712	1	84.388	3	732.79	5
16	Pearson 6 (4P)	0.11108	2	82.241	1	501.74	1
14	Pearson 5 (3P)	0.11179	3	82.894	2	507.23	2
8	Log-Pearson 3	0.11228	4	117.31	7	1062.7	7
9	Lognormal	0.11228	5	127.77	9	1182.4	8
7	Log-Gamma	0.113	6	110.02	6	932.83	6
19	Weibull (3P)	0.1131	7	120.79	8	N/A	

The goodness of fit tests, including Kolmogorov- Smirnov (KS), Anderson-Darling (AD), and Chi-square for all the data sets were done for all the watershed at outlet point with 12 years daily data and parameters distribution parameters are found in table 4-14. Anderson-Darling test is much more sensitive to the tails of distribution, whereas Kolmogorov-Smirnov test is more aware of the center of distribution. To sum up, Anderson-Darling would recommend you to use, to get much more powerful test. The Kolmogorov-Smirnov and Anderson-Darling tests are restricted to continuous distributions.

Table 4-14: Distribution parameters value for each watershed

Watershed	Distribution type	parameters	Parameters value
ARJO	Lognormal(3P)	μ, σ and γ	4.6736,1.3499 and 12.894
DEMBI	Lognormal(3P)	μ, σ and γ	3.6748,1.5244 and 3.5162
DABANA	Lognormal(3P)	μ, σ and γ	3.6494,1.1052 and 5.2552
ANGAR	Lognormal(3P)	μ, σ and γ	4.23871.1563 and 9.46.17
LOWER DIDESA	Lognormal(3P)	μ, σ and γ	5.1171,1.3257 and 26.414
WAMA	Logpearson(3P)	α ,β and γ	284.76,-0.04162 and 16.096

Note: these parameters are calculated with 12 year data since EasyFit used cannot handle (>5000) data for trial version.

Similarly, using easy fit best distribution is selected as rank of goodness of fit is simulated. The basins annual peak flows were extracted from daily flow hydrograph estimated with ArcSWAT model for each watershed. Logarithm of annual peak flow from each watershed at out let was calculated. The value of

average of peak discharge, $\bar{x}$ and standard deviation, σ are calculated from estimated flow hydrograph at each outlet of watershed found in table A6 of appendix table. And the value of K_T can be calculated for any required return period from equation (3-4) for lognormal and (3-5) for logpearson distribution.

Table 4-15: Expected probable flood with its frequency of occurrence from model determined annual peak at confluence of watersheds (1=Angar at confluence with Didesa, 2=Arjo at confluence with Dabana, 3=Dembi at confluence with Wama, 4=Dabana at confluence with Arjo, 5= Wama at confluence with Dembi, 6=Didesa at confluence with Angar)

Return Period	Threshold Values of (X_T)					
	1	2	3	4	5	6
2	583.7	657.9	458.0	316.8	237.8	1037.2
5	755.5	811.6	539.8	396.9	285.7	1279.6
10	864.6	913.4	594.0	446.6	317.2	1428.2
20	966.5	1011.0	646.0	492.2	347.5	1563.9
25	998.4	1042.0	662.4	506.4	357.2	1605.7
50	1095.7	1137.4	713.2	549.3	387.1	1731.9
100	1191.1	1232.1	763.6	590.9	417.3	1853.9
200	1285.8	1326.5	813.9	631.7	448.0	1973.0
1000	1505.4	1545.0	930.2	725.1	522.3	2243.3
10000	1825.3	1857.4	1096.5	858.1	638.4	2624.4

According to Arjo Irrigation feasibility of 2007 and 2009 frequency analysis is done for Upper Arjo Didesa at dam site which is approximately same with Dembi watershed. Outlet of Dembi watershed and Dam site is nearer to each other. Hence, Frequency Analysis from simulated flow are compared and found to be similar to that of feasibility study with negligible difference. For example, the estimated 100 years flood was 763.6m^3/s and feasibility study estimates as 787 m^3/s. The difference of the value may be the distribution we use may be different.

4.6.6. Time of concentration

Q is the average channel flow rate (m3 s^{-1}) and taken from SWAT reach out put which is calibrated and validated, *S* is the channel slope (m m-1) and , and *n* is Manning's roughness coefficient for the channel which is called CH_N2, best value taken from calibration parameter. *L* is the channel length from the most distant point to the sub basin outlet (km), and *Lcen* is the distance along the channel to the sub basin centroid (km) and their values are got from basin map. The average channel velocity in m s^{-1} (v_c), average channel flow length (Lc) and time of concentration (t_c) are calculated from equation 3-16, 3-15, and 3-14 respectively.

Table 4-16: Values of time of concentration for the tributaries (1= Dabana at confluence with Arjo Didesa,2= Angar at confluence with Didesa,3= Dembi at confluence with Wama,4= Arjo Didesa at confluence with Dabana,5= Wama at confluence with Arjo Didesa,6=Didesa at confluence with Angar)

tributary

PARAMETERS	1	2	3	4	5	6
Q(m^3/s)	68.1	147.2	97.7	209.3	86.0	339.6
n (unitless)	0.2760	0.0875	0.2730	0.1910	0.1790	0.1910
L(Km)	150.3	198.2	191	279.9	126	357.9
L_{cen} (Km)	37.5	66	51.2	82	32.9	112.7
S (m/m)	0.0165	0.0199	0.0164	0.0127	0.0273	0.0110
V_c (m/s)	0.8	2.4	0.9	1.3	1.4	1.3
L_c (Km)	75.1	114.4	98.1	151.5	64.4	200.8
t_c (hour)	29.2	13.23	27.2	36.1	24.3	43.5
t_L (hour)	17.5	7.94	16.32	21.65	14.6	26.1

A correct estimate of time of concentration and lag time were calculated and these parameters will insure the effectiveness of flood warning systems as a major component of an overall watershed management system.

4.6.7. Comparison of Peak flow rate with the flow 2015

4.6.7.1. Estimation of Peak Flow Rate for year 2015

Hence SWAT is rerun to estimate discharge of year 2015 by using the parameters found during calibration and validation for each sub basin. Filled data of 2012 up to 2014 is used as warm up period. The monthly peak flow and average monthly rainfall hydrograph for each watershed during 2015 estimated as given in (figure 4-12). The annual peak discharges of the six watersheds are extracted from output reach data base and briefly clarified in (table 4-12). Primary x-axis and y-axis is simulated monthly peak discharge, while secondary x-axis and y-axis is simulated average monthly rainfall.

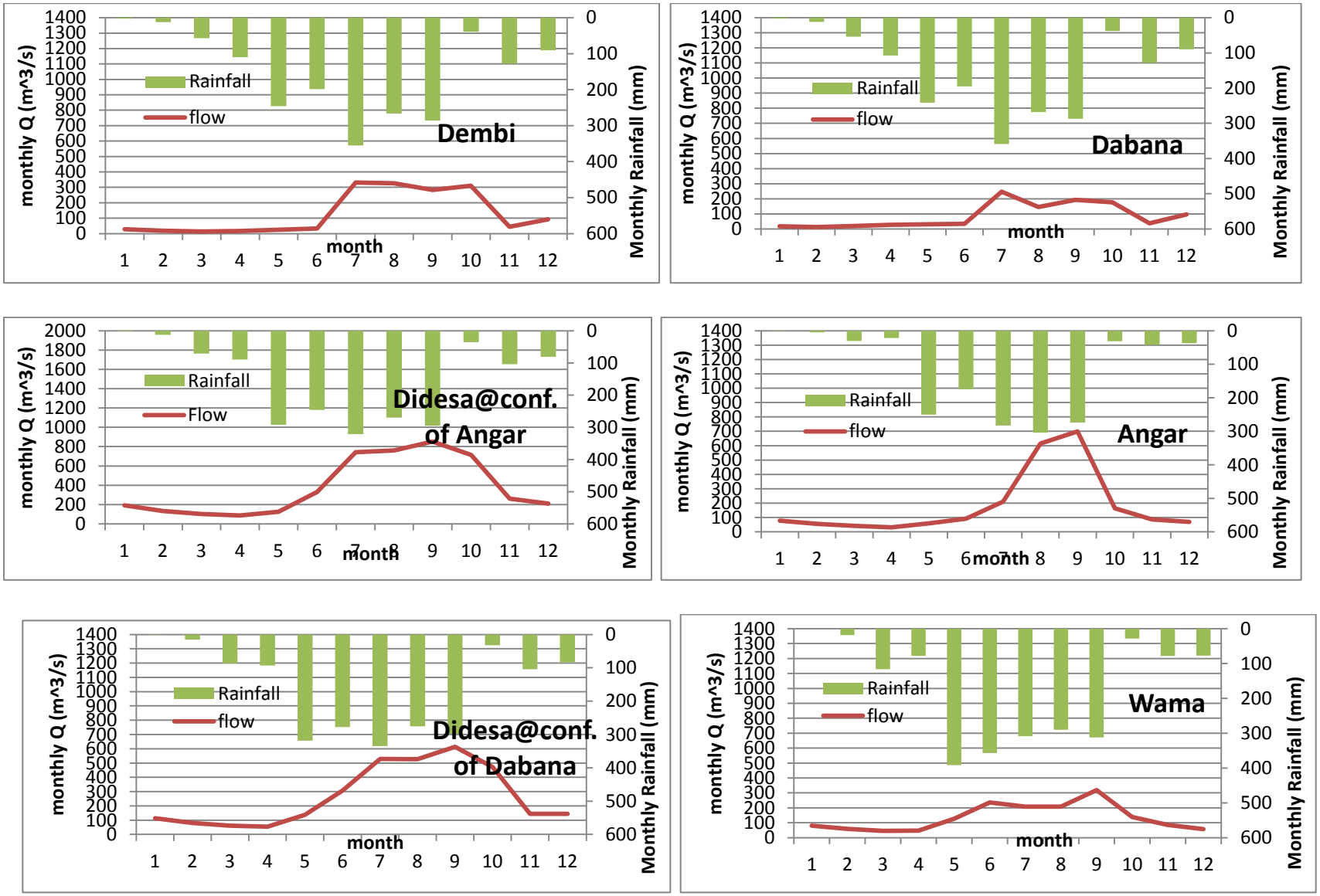

Figure 4-12: Monthly Peak flow hydrograph for each watershed in 2015

Table 4-17: Annual peak flow of Didesa sub basin during 2015

Criterion	Dembi	Arjo	Angar	Dabana	Wama	Lower Didesa
Annual peak flow(m3/S)	390.5	691.9	698.4	246.4	319.7	853.5

Comparing Annual Peak Discharge of 2015 with previously Determined Threshold value

If the peak flow of the year 2015 compare with the peak flow frequency analysis results of the sub basins, it fall in the range of 2-5 year return period for Arjo at confluence with Dabana, Dembi at convergence with Wama, Dabana at confluence with Ajo and Arjo Didesa at convergence with Angar; and 10 -20 years return period for Wama at confluence with Dembi. It indicates that the flood at the year 2015 was smaller than any of the design flood expected on the relief culvert and coffer dam since they were designed with 100 year return period flood.

5. CONCLUSION AND RECOMMENDATIONS

5.1. Conclusion

Understanding of the hydrological characteristics of different watersheds as sources of stream flow is of considerable importance in the effective utilization of water resources. Didesa sub basin has not well studied and understood as compare with the northern sub basins of Blue Nile such as (Tana sub basin).The hydrological characterization of Didesa sub basin was handled with different hydrological procedures and methods in this study. First the observed metrological and hydrological data were statistically tested and found to be consistent and free of trend. A SWAT Hydrological model for the sub basin was established, calibrated and validated using the observed stream flow data at five gauged stations in the sub basin. The calibration and validation of the model were measured by the coefficient of determination R^2 and the Nash-Sutcliffe model efficiency (NS) parameter of at daily and monthly time scale. The values of R^2 and NS range 0.66 to 0.70 and 0.60 to 0.66, 0.66 to 0.70 and 0.64 to 0.74, 0.62 to 0.80 and 0.61 to 0.8 for Dembi, Arjo Didesa, and Angar tributary watershed respectively, at daily time scale. The values of R^2 and NS increases at monthly time scale and range 0.80 to 0.86 and 0.72 to 0.83, 0.87 to 0.89 and 0.82 to 0.84, 0.82 to 0.92 and 0.79 to 0.91 for Dembi, Arjo Didesa, and Angar tributary watershed respectively.

Sensitivity analysis realizes parameters those were the most sensitive for the sub basin. And each parameter is arranged based on their sensitivity rank for each watershed as CN2, GWQMN, CH_K, ALPHA_BNK and LAT_TIME are the most sensitive parameters in Didesa sub basin.

Therefore, the hydrological process in Didesa sub basin is characterized using the simulated stream flow at five major tributaries watersheds. This characterization include stream flow hydrograph, watershed attributes including land use, slope and soil characteristics, peak flow analysis using fitted probabilistic distribution and unit.

Land use land cover shows that the sub basin is entirely covered with vegetation. The dominate land use of the sub basin is mixed vegetation/crop lands followed by closed to open shrub land. Soil of the sub basin is spatially distributed. More than 79% of the sub basin is enclosed with Humic Nitosols which is loam in textural class of soil. The sub basin has gentle slope. Slope of 0% up to 5% covers nearly 63% of Didesa sub basin.

Frequency analysis was performed using the simulated Annual peak flood series data sets watersheds of Didesa sub basin. Lognormal (3P) distribution gives the best fitted probabilistic distribution for all watersheds except Wama watershed which fitted with Logpearson (3P) distribution. Using these fitted probabilistic distribution the peak flow of the watersheds computed for 2- 10000 years return period.

The Snyder synthetic unit hydrograph parameters are developed to characterize the watersheds in the sub basins. The determined Values of lag time (t_P) were 17.5, 7.94, 16.32, 21.65, 14.6, 26.1 respectively, for Dabana at confluence with Arjo Didesa, Angar at confluence with Didesa, Dembi at confluence with Wama, Arjo Didesa at confluence with Dabana, Wama at confluence with Arjo Didesa, Didesa at confluence with Angar. Similarly, the evaluated values of time of concentration (t_c) were 29.2, 13.23, 27.2, 36.1, 24.3, 43.5 respectively, for Dabana at confluence with Arjo Didesa, Angar at confluence with Didesa, Dembi at confluence with Wama, Arjo Didesa at confluence with Dabana, Wama at confluence with Arjo Didesa, Didesa at confluence with Angar.

5.2. Recommendations

- ✓ There is always possibility of differ hydrological characteristics for sub basins in a large basin, therefore researchers, designers, and practitioners hast to check the characteristics of the basin before taking parameter values.

Reference

Abbay River Basin Integrated Development Master Plan Project. (April,1999). Addis Ababa,Ethiopia

Adane, A. a. (2006). Catchment characterization as predictors of baseflow index (BFI) in Wabi Shebele river Basin, East Africa,Conference on International Agricultural Research for Development. University of Bonn, Germany.

Arnold, J, Kiniry, J, Srinivasan, R, Williams, J, Haney, E, & Neitsch, S. (Version2009). Soil and Water Assessment Tool Input/Output File Documentation. Texas A&M University System, 2011.

Arnold, J. G, Moriasi, D. N, Gassman, P. W, Abbaspour, K. C, White, M. J, Srinivasan, R, et al. (2012). Swat: Model Use, Calibration and Validation , . American Society of Agricultural and Biological Engineers, Vol. 55(4): 1491-1508.

Arnold, J.G., R. Srinivasan, R.S. Muttiah, and J.R. Williams. (1998). Large-area hydrologic modeling and assessment. Part I. Model development.J. American Water Res. Asso, 34(1): 73-89.

Awulachew, S. B, McCartney, M, Steenhuis, T. S, & Ahmed, A. A. (n.d.). (2008). A Review of Hydrology, Sediment and Water Resource Use in the Blue Nile Basin. IWMI Working Paper 131 . Colombo, Sri Lanka: International Water Management Institute.

Belete Berhanu, Y. S. (2015). Flow Regime Classification and Hydrological Characterization: A Case Study of Ethiopian Rivers. Water , 3149-3165.

Black, P. (1996). Watershed Hydrology . CRC Press, Boca Raton, Fla. , 450 pp.

Burn, D. H. (1992). Catchment classification applied to the estimation of hydrological parameters at ungauged catchments. Institute of Hydrology Report No. 118, Wallingford, UK .

Conway, D. (1997). A water balance model of the upper Blue Nile in Ethiopia. Hydrological Sciences, 42 , 265-282.

Conway, D. (2000). Conway, D. The climate and hydrology of the Upper Blue Nile River. The Geographical Journal, 166 , 49-62.

Cornelissen, T., Diekkrüger, B., & Giertz, S. (2013). A comparison of hydrological models for assessing the impact of land use and climate change on discharge in a tropical catchment. *Journal of Hydrology*, 498, 221–236.

Costa, M. H., Botta, A., & Cardille, J. A. (2003). Effects of large-scale changes in land cover on the discharge of the Tocantins River, Southeastern Amazonia . *Journal of Hydrology* , 283, 206–217.

Curtis, B. P. (1994). WATER BALANCE OF BLUE NILE RIVER BASIN IN ETHIOPIA. J. Irrig. Drain Eng , 573-590.

Elfert, S., & Bormann, H. (2010). Simulated impact of past and possible future land use changes on the hydrological response of the Northern German lowland "Hunte"catchment. *Journal of Hydrology*, 383, 245–255.http://dx.doi.org/10.1016/j.jhydrol.2009.12.040.

Francisco Olivera, David R. Maidment and Randall J. Charbeneau. (1996). Spatially Distributed Modeling of Storm Runoff and Non-Point Source Pollution Using Geographic Information Systems (GIS). The University of Texas at Austin.

Fu G, C. S. (2007). A two-parameter climate elasticity of streamflow index to assess climate change effects on annual streamflow -. Water Resources Research.

G.S. Dwarakish and B.P. Ganasri. (2015). Impact of land use change on hydrological systems: A review of current modeling approaches. *Cogent Geoscience*, http://dx.doi.org/10.1080/23312041.2015.1115691.

Gupta, H. V., S. Sorooshian and P. O. Yapo. (1998). Toward Improved Calibration of Hydrologic Models: Multiple and Noncommensurable Measures of Information. In Water Resources research (pp. 34(4): 751-763).

Gupta, H. V., S. Sorooshian and P. O. Yapo. (1998). Toward Improved Calibration of Hydrologic Models: Multiple and Noncommensurable Measures of Information . Water Resources Research, 34(4): 751-763.

Hamed, K. H. (2008). Trend detection in hydrologic data: The Mann–Kendall trend test under the scaling hypothesis. Journal of Hydrology Volume 349, Issues 3–4, 1 February 2008 , 350–363.

Johnson, P. A. (1994). Water balance of Blue Nile River Basin in Ethiopia. Journal of Irrigation and Drainage Engineering – ASCE 120 , 573-590.

Laouacheria, F., & Mansouri, R. (2015). Comparison of WBNM and HEC-HMS for runoff hydrograph prediction in a small urban catchment. *Water Resources Management*, 29,2485–2501.

Lin, Y. P., Verburg, H. P., Chang, C. R., Chen, H. Y., & Chen, M. H. (2009). Developing and comparing optimal and empirical land-use models for the development of an urbanized watershed forest in Taiwan. *Landscape and Urban Planning*, 92, 242–254.

Linsley, R. K., M. A. Kohler and J. L. H. Paulhus. (1982). Hydrology for Engineers, 3rd Edition . McGraw-Hill, New York, 508 p.

Liu, B. Y. (2008). Overcoming limited information through participatory watershed management: Case study in Amhara, Ethiopia. Physics and Chemistry of the Earth 33 , 13–21.

Lørup, J. K., Refsgaard, J. C., & Mazvimavi, D. (1998). Assessing the effect of land use change on catchment runoff by combined use of statistical tests and hydrological modelling: Case studies from Zimbabwe. *Journal of Hydrology*, 205,147-163.

Mamo, T. M. (2014). Morphometric Analysis of Didessa River Catchment in Blue Nile Basin, Western Ethiopia. Science, Technology and Arts Research Journal , 3(3): 191-197.

Mao, D., & Cherkauer, K. A. (2009). Impacts of land-use change on hydrologic responses in the Great Lakes region. *Journal of Hydrology*, 374, 71–82.

Martinez-Mena, M. J. (1998). Factors influencing surface runoff generation in a Mediterranean semi-arid environment: Chicamo watershed . SE Spain, Hydrological Processes , 12 , 741-754.

McCartney, M. P, Alemayehu, T, Easton, Z. M, & Awulachew, S. B. (2012). The Nile River Basin: Water, Agriculture, Governance and Livelihood. sAbingdon, UK: International Water Management Institute.

McColl, C., & Aggett, G. (2007). Land-use forecasting and hydrologic model integration for improved land-use decision support. *Journal of Environmental Management*, 84, 494–512.

McDonnell, J. J. (2007). Moving beyond heterogeneity and process complexity: A new vision for watershed hydrology, WaterResour. Res., 43, W07301, doi:10.1029/2006WR005467.

Mishra, A. a. (2006). A grid-based runoff generation and flow routing model for the upper Blue Nile Basin. Hydrological Sciences Journal, 51 , 191-206.

Mishra, A. T. (2004). Models for recession flows in the upper Blue Nile River. Hydrological Processes, 18 , 2773-2786.

Mohammad Karamouz, Ferenc Szidarovszky,Banafsheh Zahraie. (2003). Water resources systems analysis. LEWIS PUBLISHERS.

Nash, J. E. (1970). River flow forecasting through conceptual models part I: A discussion of principles. Journal of Hydrology, 10 , 282-290.

Niehoff, D., Fritsch, U., & Bronstert, A. (2002). Land-use impacts on storm-runoff generation: scenarios of land-use change and simulation of hydrological response in a meso-scale catchment in SW-Germany. *Journal of Hydrology* , 267, 80–93.

P. A. Troch, G. C. (2013). Climate-vegetation-soil interactions and long-term hydrologic partitioning: signatures of catchment co-evolution. Hydrology and Earth System Sciences , 2209–2217.

Sarkar, A., & Kumar, R . (2012). Artificial neural networks for event based rainfall–runoff modeling . *Journal of Water Resource and Protection*, 04, 891–897.

Saxena, R. K., Verma, K. S., Chary, G. R., Srivastava, R., and Barthwal, A. K. (2000). IRS-1C data application in watershed characterization and management, Int. J. Remote Sens. 21, 17, 3197–3208.

S. G. Gebrehiwot, U. I. (2011). Hydrological characterization of watersheds in the Blue Nile Basin,Ethiopia. Hydrology and Earth System Sciences , 11–20.

Shirke, Y., Kawitkar, R., & Balan, S. (2012). Artificial neural network based runoff prediction model for a reservoir. *International Journal of Engineering Research and Technology*, 1(3), 1–4.

Sima, B. A. (2011). Flow Regime and Land Cover Changes in the Didessa Sub-Basin of the Blue Nile River, South-Western Ethiopia: Combining Empirical Analysis and Community Perception. Master Thesis in Integrated Water Resource Management presented at Swedish University of Agricultural Sciences .

Sivapalan.M..G. Bloschl. R. Merz and D. Gutknecht. (2005). Linking flood frequency to long term water balance: incorporating effects of seasonality. Water resource research. 41(6). 1-17.

Singh, V. P. (2002). Mathematical Models of Large Watershed Hydrology. Water Resour. Publ., 891 pp., Highlands Ranch,Colo.

Snyder. (1938). Synthetic unit graphs. Trans Americans Geophysics, Un. 19.

Spittlehouse, D.L. and R. D. Winkler. (2002). Modelling snowmelt in a forest and clearcut. Proceedings 25th Conference on Agricultural and Forest Meteorology., Norfolk Virginia, American Meteorological Society, Boston, MA. pp. 121-122.

Suliman, A. A., Jajarmizadeh, M., Harun, S., & Mat Darus, I.Z . (2015). Comparison of semi-distributed, GIS-based hydrological models for the prediction of streamflow in a large catchment. *Water Resources Management*, 29,3095–3110

Tamrat, Y. A. (2005). Ethiopia and the Eastern Nile Basin. Aquatic Sciences, 16 , 15- 27.

Tang, L., Yang, D., Hu, H., & Gao, B. (2011). Detecting the effect of land-use change on streamflow, sediment and nutrient losses by distributed hydrological simulation . *Journal of Hydrology*, 409, 172–182.

Tariku, M. (2007). Surface Irrigation Suitability Analysis Of Southern Abbay Basin By Implementing Gis Techniques . Unpublished Masters Thesis Presented To Graduate School Of Addis Ababa University Technology Faculty .

Tena Bekele Adgolign, G. V. (2015). Assessment Of Spatio-Temporal Occurrence of Water Resources in Didessa Sub-Basin, West Ethiopia. IJCSEIERD , 105-120.

Thanapakpawin, P., Richey, J., Thomas, D., Rodda, S.,Campbell, B., & Logsdon, M. (2006). Effects of landuse change on the hydrologic regime of the Mae Chaem river basin, NW Thailand . *Journal of Hydrology*, 334, 215–230.

ThorstenWagener, M. R. (2007). Catchment Classification and Hydrologic Similarity. Blackwell Publishing Ltd , 1749-8198.

Uhlenbrook, S. (2003). An empirical approach for delineating spatial units with the same dominating runoff generation processes. Phys.Chem. Earth, 28, 297–303.

Verburg, P. H., Schot, P. P., Dijst, M.J., & Veldkamp, A. (2004). Land use change modelling: current practice and research priorities. *GeoJournal*, 61, 309–324.

Wagener, T. a. (2006). Parameter estimation and regionalization for continuous rainfall-runoff models including uncertainty. . Journal of Hydrology 320, , pp. 132–154.

Wagener, T. M. (2007). Catchment classification and hydrologic similarity. Geogr. Compass, 1,doi:10.1111/j.1749-8198.2007.00039.x.

Wagener, T. W. (2004). Rainfall-runoff modelling in gauged and ungauged catchments. .London, UK: Imperial College Press.

Xu, C. Y., & Singh, V. P. (1998). A review on monthly water balance models for water resources investigations. *Water Resources Management*, 12, 31–50.

Yadav, M., Wagener, T., and Gupta, H. (2007). Regionalization of constraints on expected watershed response behavior for improved predictions in ungauged basins. Adv. Water Resour, 30, 1756–1774.

Ye, X., Zhang, Q., Liu, J., Li, X., & Xu, C. Y. (2013). Distinguishing the relative impacts of climate change and human activities on variation of streamflow in the Poyang Lake catchment, China . *Journal of Hydrology*, 494, 83–95.

A. APPENDIX

Table A-1: Annual Rainfall Data

YEAR	JIMMA	BEDELE	NEKEMTE	DIDESA	GIMBI	NEJO	ARJO	SHAMBU
1980	1522.2	1975.7	1808.7	1531.8	1801.5	1519.0	1922.0	1554.0
1981	1416.3	1880.9	1899.5	1396.7	1778.1	1392.6	1791.6	1433.4
1982	1307.7	1663.2	1863.4	1290.2	1628.4	1371.4	1686.3	1353.0
1983	1411.0	1898.7	1870.7	1154.9	1321.8	1587.4	1886.9	1463.3
1984	1350.4	1704.7	1927.6	1309.7	1657.6	1426.6	1738.2	1341.7
1985	1676.6	2062.5	2338.1	1750.3	2187.3	1534.3	2099.0	1649.0
1986	1225.0	1555.9	1769.2	1310.3	1404.2	1265.7	1601.7	1230.1
1987	1595.4	1952.7	2083.5	1737.6	1829.7	1617.0	2019.1	1604.6
1988	1651.4	2039.9	2080.7	1559.6	1912.9	1652.1	2131.0	1654.1
1989	1595.2	2045.5	2130.0	1549.8	1875.3	1626.2	2062.2	1607.0
1990	1402.4	1711.5	2013.2	1402.2	1739.1	1458.6	1866.4	1412.9
1991	1538.1	1723.5	2144.4	1586.4	1730.8	1535.1	1997.3	1552.5
1992	1622.2	1909.2	2286.5	1686.6	2019.0	1594.4	2097.2	1634.0
1993	1680.3	1775.8	2514.9	1759.9	2101.1	1746.0	2160.1	1690.5
1994	1346.1	1410.1	2090.0	1395.5	1620.9	1436.1	1747.9	1378.4
1995	1433.4	1838.8	2058.9	1465.6	1640.2	1675.2	1886.9	1444.1
1996	1604.7	1921.3	2320.9	1571.4	1818.5	1284.7	2050.3	1609.6
1997	1606.8	2048.1	2247.4	1595.0	1925.1	1614.8	2121.7	1646.9
1998	1551.9	1945.9	2080.5	1489.0	1875.7	1578.6	2037.4	1604.7
1999	1530.8	1772.2	1977.3	1484.7	1808.1	1750.2	1899.6	1501.5
2000	1489.5	1859.9	2066.0	1836.6	1768.4	1393.8	1911.5	1520.6
2001	1399.0	2165.0	1913.5	1270.8	1608.3	1516.6	1825.5	1469.1
2002	1172.0	1449.5	1647.3	905.2	1577.4	1200.5	1552.0	1152.8
2003	1501.9	1445.5	2161.4	1571.9	1657.9	1511.8	1897.6	1513.3
2004	1484.3	1937.3	1899.9	1472.2	1848.3	1507.7	1810.5	1500.7
2005	1516.3	2233.9	2248.7	1534.6	1849.2	1573.1	1902.4	1552.9
2006	1679.5	2358.3	2139.4	1812.2	1853.9	1768.6	2189.5	1730.8
2007	1597.7	1982.4	2173.0	1319.5	2077.2	1622.6	1883.2	1586.2
2008	1809.3	2030.5	2441.3	2098.1	2175.3	1823.5	2222.1	1812.8
2009	1538.2	1776.8	2022.8	1447.0	1909.9	1601.4	1862.0	1570.8
2010	1654.0	1949.3	2482.1	1641.7	2016.9	1659.0	2105.3	1697.6
2011	1454.9	1918.2	2010.4	1304.7	1896.1	1492.0	1763.8	1485.6
2012	1404.5	1887.4	2109.3	1402.2	1697.1	1453.0	1790.5	1430.8
2013	1499.0	1943.1	1965.3	1639.3	1826.3	1511.1	1908.2	1513.8
2014	2046.6	2089.4	2524.3	1809.7	2775.0	1637.0	2566.1	2049.1

Table A-2: summary of pearson correlation test result of daily rainfall (1980-2014) gauging stations

Summary statistics:

Variable	Observations	Obs. with missing data	Obs. without missing data	Minimum	Maximum	Mean	Std. deviation
JIMMA	12784	0	12784	0.000	38.165	4.170	5.074
BEDELE	12784	0	12784	0.000	83.500	5.152	8.689
NEKEMTE	12784	0	12784	0.000	137.500	5.735	9.310
DIDESA	12784	0	12784	0.000	116.600	4.153	8.074
GIMBI	12784	0	12784	0.000	55.568	5.023	7.046
NEJO	12784	0	12784	0.000	92.000	4.219	6.149
ARJO	12784	0	12784	0.000	48.493	5.319	6.285
SHAMBU	12784	0	12784	0.000	41.046	4.220	4.973

Correlation matrix (Pearson):

Variables	JIMMA	BEDELE	NEKEMTE	DIDESA	GIMBI	NEJO	ARJO	SHAMBU
JIMMA	**1**	**0.711**	**0.764**	**0.655**	**0.917**	**0.795**	**0.966**	**0.971**
BEDELE	**0.711**	**1**	**0.485**	**0.380**	**0.575**	**0.564**	**0.705**	**0.714**
NEKEMTE	**0.764**	**0.485**	**1**	**0.462**	**0.775**	**0.610**	**0.763**	**0.760**
DIDESA	**0.655**	**0.380**	**0.462**	**1**	**0.514**	**0.529**	**0.650**	**0.648**
GIMBI	**0.917**	**0.575**	**0.775**	**0.514**	**1**	**0.748**	**0.864**	**0.869**
NEJO	**0.795**	**0.564**	**0.610**	**0.529**	**0.748**	**1**	**0.794**	**0.794**
ARJO	**0.966**	**0.705**	**0.763**	**0.650**	**0.864**	**0.794**	**1**	**0.968**
SHAMBU	**0.971**	**0.714**	**0.760**	**0.648**	**0.869**	**0.794**	**0.968**	**1**

Table A-3:Maximum of 24 Hr Rainfall (mm) from 1980-2015

Year	Max of JIMMA	Max of BEDELE	Max of NEKEMTE	Max of DIDESA	Max of GIMBI	Max of NEJO	Max of ARJO	Max of SHAMBU
1980	24.7	47.8	27.4	22.8	31.9	24.2	28.3	23.9
1981	38.2	53.7	43.1	33.5	44.5	37.9	48.5	41.0
1982	24.4	75.3	31.4	27.5	29.7	24.3	28.5	23.3
1983	24.9	40.8	34.1	19.4	28.6	26.7	30.8	24.9
1984	27.2	29.3	35.2	52.5	36.3	25.6	32.5	27.0
1985	23.7	30.4	40.5	90.0	48.8	21.2	25.8	21.2
1986	22.9	29.7	63.9	71.3	37.0	21.7	31.4	23.0
1987	27.6	29.7	81.0	97.5	31.2	28.2	33.8	27.1
1988	26.5	31.4	50.3	27.7	35.1	25.6	34.6	25.3
1989	21.0	58.4	57.0	23.5	32.2	20.9	27.9	19.9
1990	29.5	53.2	44.3	28.4	43.7	29.3	38.1	29.4
1991	32.1	46.8	42.6	33.0	43.7	26.5	34.5	28.5
1992	31.3	49.5	41.8	27.8	35.3	50.3	40.6	31.0
1993	21.2	56.0	80.0	25.7	34.8	51.6	27.3	20.7
1994	26.8	39.0	78.4	26.8	29.1	64.6	34.2	28.5
1995	23.1	50.1	67.3	26.4	30.2	75.3	29.5	22.4
1996	21.3	40.0	105.4	24.0	35.4	78.2	30.6	24.9
1997	37.6	48.4	72.3	36.1	55.6	57.6	46.0	35.5
1998	28.0	33.5	37.0	31.4	48.3	92.0	32.5	27.0
1999	25.6	28.9	36.3	64.1	35.6	47.9	33.8	25.8
2000	30.0	63.5	34.9	116.6	32.0	41.4	40.2	31.0
2001	24.8	63.0	26.9	55.1	35.3	26.0	29.1	22.3
2002	23.8	47.9	29.9	60.6	42.6	23.9	28.4	21.3
2003	36.2	69.0	47.0	103.0	37.8	32.1	46.1	35.5
2004	34.6	58.2	35.8	85.9	34.3	34.4	41.2	35.4
2005	25.3	58.5	85.4	46.5	28.4	27.4	35.4	23.9
2006	26.5	50.0	56.9	79.3	42.4	23.2	31.2	25.6
2007	25.8	83.5	89.0	43.0	44.4	25.8	29.0	23.4
2008	27.7	63.0	71.6	99.0	41.2	27.1	33.5	27.4
2009	27.5	58.5	58.3	74.0	36.8	28.6	34.0	27.1
2010	33.3	75.3	137.5	80.0	52.5	28.9	43.9	33.3
2011	24.5	53.5	74.0	60.2	38.0	22.1	29.5	21.9
2012	33.3	60.0	105.5	85.9	37.0	33.6	41.3	34.7

2013	32.5	77.5	59.2	82.4	43.7	26.9	35.0	29.0
2014	31.7	63.0	110.6	83.0	51.8	27.0	35.7	28.1
2015	69.0	63.0	62.6	47.1	69.0	40.5	50.5	40.7
Max	69.0	83.5	137.5	116.6	69.0	92.0	50.5	41.0

Table A-4: pearson matrix correlation value for average monthly Rainfall of gauging stations (1980-2014)

Correlation matrix (Pearson):

Variables	Jimma	Bedele	Nekemte	Didesa	Gimbi	Nejo	Arjo	Shambu
Jimma	**1**	**0.935**	**0.963**	**0.922**	**0.980**	**0.965**	**0.996**	**0.997**
Bedele	**0.935**	**1**	**0.899**	**0.878**	**0.892**	**0.930**	**0.934**	**0.938**
Nekemte	**0.963**	**0.899**	**1**	**0.909**	**0.948**	**0.946**	**0.960**	**0.961**
Didesa	**0.922**	**0.878**	**0.909**	**1**	**0.881**	**0.905**	**0.919**	**0.920**
Gimbi	**0.980**	**0.892**	**0.948**	**0.881**	**1**	**0.933**	**0.973**	**0.974**
Nejo	**0.965**	**0.930**	**0.946**	**0.905**	**0.933**	**1**	**0.965**	**0.965**
Arjo	**0.996**	**0.934**	**0.960**	**0.919**	**0.973**	**0.965**	**1**	**0.996**
Shambu	**0.997**	**0.938**	**0.961**	**0.920**	**0.974**	**0.965**	**0.996**	**1**

Table A-5: Peak flow is estimated for each watershed at a given points shown on map.

Year	Lower Didesa	Angar	Arjo@	Dembi	dabana	wama
1982	643.1	646.3	366.9	347.4	713.1	160.4
1983	823.4	604.5	517.6	434.5	264	189.2
1984	758.8	1070	421.5	305.1	359.1	184
1985	946.5	1666	523.2	356.1	603.3	234.4
1986	641.1	873.9	435.4	284.5	205.9	288.1
1987	867.9	1688	451.8	326.2	307.5	222.8
1988	936.4	996.8	659	389.1	462.1	277.5
1989	718.2	678.1	399.1	306	332.6	197.6
1990	1009	971.5	671.9	482.7	584	218.2
1991	1051	1013	652	378	400.3	295.6
1992	991.8	943.6	678.2	407.9	505.3	255.3
1993	1309	1359	775.6	450.5	540.7	383.7
1994	978.1	1097	657.1	318.4	338.5	237.5
1995	1105	960.1	750.3	358.5	333.5	254.5

1996	980.2	1458	677.3	311.9	261.9	318.8
1997	1071	1079	683.7	355.4	648.1	239.9
1998	960	970.3	674.3	331.9	544.2	203.3
1999	1121	1290	730.7	381.8	416.4	231.9
2000	1008	2501	680	363	507.2	191.9
2001	1122	1139	824.1	495.6	597.1	209.8
2002	728.4	544.4	474.4	282.6	343.5	189.5
2003	926.1	1691	665.9	304.6	396.6	217.9
2004	988.4	1807	674.5	415.1	411.3	244.5
2005	1719	1185	1046	603.2	559.9	262.6
2006	1208	1499	779.6	401.7	589	250.1
2007	1163	1389	794.1	548.2	1006	239.2
2008	1440	2398	904	479.8	592.6	266.3
2009	1000	1380	679.6	383	592.5	247.8
2010	1605	1932	982.6	617.7	641.3	321.3
2011	1144	1076	756	366.5	455.3	206.3
2012	1442	2941	873.4	431.3	450.4	326.3
2013	1182	1425	747.4	557.9	698.4	196.4
2014	1698	1542	1046	400.6	622.4	375.3
$\bar{x}$	**1069.255**	**1327.712**	**686.4606**	**399.2939**	**493.4545**	**246.603**
S	**273.8392**	**544.3485**	**173.8669**	**89.02481**	**163.8651**	**53.56021**
Cs	**0.802658**	**1.164175**	**0.123522**	**0.963241**	**0.711344**	**0.932511**

Table A-6: Log of annual peak flow

Year	Lower Didesa	Angar	Arjo	Dembi	dabana	wama
1982	2.808	2.808	2.565	2.541	2.853	2.205
1983	2.916	2.916	2.714	2.638	2.422	2.277
1984	2.880	2.880	2.625	2.484	2.555	2.265
1985	2.976	2.976	2.719	2.552	2.781	2.370
1986	2.807	2.807	2.639	2.454	2.314	2.460
1987	2.938	2.938	2.655	2.513	2.488	2.348
1988	2.971	2.971	2.819	2.590	2.665	2.443
1989	2.856	2.856	2.601	2.486	2.522	2.296
1990	3.004	3.004	2.827	2.684	2.766	2.339
1991	3.022	3.022	2.814	2.577	2.602	2.471
1992	2.996	2.996	2.831	2.611	2.704	2.407
1993	3.117	3.117	2.890	2.654	2.733	2.584
1994	2.990	2.990	2.818	2.503	2.530	2.376

1995	3.043	3.043	2.875	2.554	2.523	2.406
1996	2.991	2.991	2.831	2.494	2.418	2.504
1997	3.030	3.030	2.835	2.551	2.812	2.380
1998	2.982	2.982	2.829	2.521	2.736	2.308
1999	3.050	3.050	2.864	2.582	2.620	2.365
2000	3.003	3.003	2.833	2.560	2.705	2.283
2001	3.050	3.050	2.916	2.695	2.776	2.322
2002	2.862	2.862	2.676	2.451	2.536	2.278
2003	2.967	2.967	2.823	2.484	2.598	2.338
2004	2.995	2.995	2.829	2.618	2.614	2.388
2005	3.235	3.235	3.020	2.780	2.748	2.419
2006	3.082	3.082	2.892	2.604	2.770	2.398
2007	3.066	3.066	2.900	2.739	3.003	2.379
2008	3.158	3.158	2.956	2.681	2.773	2.425
2009	3.000	3.000	2.832	2.583	2.773	2.394
2010	3.205	3.205	2.992	2.791	2.807	2.507
2011	3.058	3.058	2.879	2.564	2.658	2.314
2012	3.159	3.159	2.941	2.635	2.654	2.514
2013	3.073	3.073	2.874	2.747	2.844	2.293
2014	3.230	3.230	2.816	2.603	2.794	2.574
$\bar{x}$	3.016	3.016	0.113	2.592	2.670	2.383
σ	0.108	0.108	0.113	0.092	0.148	0.090
Skew	0.108	0.108	2.565	0.552	-0.330	0.434

Table A-7: Estimated annual average flow from Didesa sub basin watersheds

DATE	**ANGAR**	DEMBI	ARJO	DABANA	WAMA	Lower DIDESA
1982	82.8	71.3	122.1	46.4	60.5	218.1
1983	96.2	81.2	144.6	46.0	72.5	234.6
1984	118.9	77.5	147.5	60.4	76.1	253.2
1985	161.6	102.2	178.4	85.9	89.9	326.7
1986	102.7	60.1	123.6	44.6	68.0	209.6
1987	144.8	94.8	168.2	68.4	81.4	292.5
1988	143.5	110.2	198.1	82.8	93.3	330.5
1989	134.0	106.3	176.3	79.0	87.2	304.7
1990	138.9	93.9	180.4	66.0	87.1	303.9
1991	137.7	90.1	172.9	56.2	86.5	299.9
1992	159.2	96.3	192.0	62.3	91.2	343.0

1993	201.6	105.5	243.4	79.4	113.1	421.1
1994	140.4	64.4	186.6	46.1	86.7	289.6
1995	119.0	91.3	192.8	52.0	77.6	305.0
1996	160.6	89.8	229.7	62.6	96.1	355.6
1997	147.9	107.2	234.3	78.0	92.3	369.0
1998	151.8	98.8	240.0	79.3	90.8	372.8
1999	147.2	89.1	212.2	67.7	85.4	336.1
2000	168.7	106.4	232.6	71.5	82.6	368.2
2001	129.5	114.2	229.7	75.8	78.7	349.6
2002	75.7	58.4	136.9	41.5	59.4	222.1
2003	134.7	62.8	170.3	35.5	74.1	273.8
2004	145.8	99.3	203.6	59.5	76.3	336.8
2005	150.0	126.8	248.9	80.1	85.3	396.9
2006	171.1	135.3	278.2	84.7	93.9	425.7
2007	165.1	121.1	272.8	94.2	93.5	428.8
2008	215.2	119.1	282.7	84.8	103.2	454.5
2009	139.5	91.4	198.3	61.0	79.2	326.7
2010	201.8	110.4	277.5	76.1	102.9	432.2
2011	142.7	104.5	228.3	74.8	82.3	359.6
2012	140.7	98.4	207.8	58.0	80.4	331.0
2013	149.4	104.6	227.9	68.9	81.6	359.5
2014	239.5	142.2	366.9	116.2	130.6	576.5
AVERAGE (m^3/s)	**147.2**	**97.7**	**209.3**	**68.1**	**86.1**	**339.6**
(Km^3/Year)	**4.64**	**3.08**	**6.60**	**2.15**	**2.71**	**10.71**